43559

National Library of Canada / Bibliothèque nationale du Canada

CANADIAN THESES ON MICROFICHE / THÈSES CANADIENNES SUR MICROFICHE

NAME OF AUTHOR/*NOM DE L'AUTEUR* MICHAEL JOHN STALKER.

TITLE OF THESIS/*TITRE DE LA THÈSE* CIRCULAR WALL JETS IN CO-FLOWING CHANNELS

UNIVERSITY/*UNIVERSITÉ* UNIVERSITY OF ALBERTA

DEGREE FOR WHICH THESIS WAS PRESENTED/ *GRADE POUR LEQUEL CETTE THÈSE FUT PRÉSENTÉE* Master of Science

YEAR THIS DEGREE CONFERRED/*ANNÉE D'OBTENTION DE CE GRADE* 1979

NAME OF SUPERVISOR/*NOM DU DIRECTEUR DE THÈSE* DR. N. RAJARATNAM

Permission is hereby granted to the NATIONAL LIBRARY OF CANADA to microfilm this thesis and to lend or sell copies of the film.

The author reserves other publication rights, and neither the thesis nor extensive extracts from it may be printed or otherwise reproduced without the author's written permission.

L'autorisation est, par la présente, accordée à la BIBLIOTHÈQUE NATIONALE DU CANADA de microfilmer cette thèse et de prêter ou de vendre des exemplaires du film.

L'auteur se réserve les autres droits de publication; ni la thèse ni de longs extraits de celle-ci ne doivent être imprimés ou autrement reproduits sans l'autorisation écrite de l'auteur.

DATED/*DATÉ* 8/6/79 SIGNED/*SIGNÉ* Michael J Stalker

PERMANENT ADDRESS/*RÉSIDENCE FIXÉ* 119, NORTH ROAD
BELFAST BT5 5NG
N. IRELAND.

NL-91 (3-74)

National Library of Canada

Cataloguing Branch
Canadian Theses Division

Ottawa, Canada
K1A 0N4

Bibliothèque nationale du Canada

Direction du catalogage
Division des thèses canadiennes

NOTICE

The quality of this microfiche is heavily dependent upon the quality of the original thesis submitted for microfilming. Every effort has been made to ensure the highest quality of reproduction possible.

If pages are missing, contact the university which granted the degree.

Some pages may have indistinct print especially if the original pages were typed with a poor typewriter ribbon or if the university sent us a poor photocopy.

Previously copyrighted materials (journal articles, published tests, etc.) are not filmed.

Reproduction in full or in part of this film is governed by the Canadian Copyright Act, R.S.C. 1970, c. C-30. Please read the authorization forms which accompany this thesis.

THIS DISSERTATION
HAS BEEN MICROFILMED
EXACTLY AS RECEIVED

AVIS

La qualité de cette microfiche dépend grandement de la qualité de la thèse soumise au microfilmage. Nous avons tout fait pour assurer une qualité supérieure de reproduction.

S'il manque des pages, veuillez communiquer avec l'université qui a conféré le grade.

La qualité d'impression de certaines pages peut laisser à désirer, surtout si les pages originales ont été dactylographiées à l'aide d'un ruban usé ou si l'université nous a fait parvenir une photocopie de mauvaise qualité.

Les documents qui font déjà l'objet d'un droit d'auteur (articles de revue, examens publiés, etc.) ne sont pas microfilmés.

La reproduction, même partielle, de ce microfilm est soumise à la Loi canadienne sur le droit d'auteur, SRC 1970, c. C-30. Veuillez prendre connaissance des formules d'autorisation qui accompagnent cette thèse.

LA THÈSE A ÉTÉ
MICROFILMÉE TELLE QUE
NOUS L'AVONS REÇUE

NL-339 (3/77)

THE UNIVERSITY OF ALBERTA

CIRCULAR WALL JETS IN CO-FLOWING CHANNELS

by

© Michael John Stalker

A THESIS

SUBMITTED TO THE FACULTY OF GRADUATE STUDIES AND RESEARCH

IN PARTIAL FULFILMENT OF THE REQUIREMENTS FOR THE DEGREE

OF MASTER OF SCIENCE

Department of Civil Engineering

EDMONTON, ALBERTA

FALL 1979

THE UNIVERSITY OF ALBERTA

FACULTY OF GRADUATE STUDIES AND RESEARCH

The undersigned certify that they have read, and recommend to the Faculty of Graduate Studies and Research, for acceptance, a thesis entitled CIRCULAR WALL JETS IN CO-FLOWING CHANNELS

submitted by Michael John Stalker

in partial fulfilment of the requirements for the degree of MASTER OF SCIENCE

.....

Supervisor

.....

.....

Date..... 1 June 79.....

Abstract

The situation of a circular wall jet injecting water into a channel flowing in the same direction is important in that it directly parallels some of the methods used for effluent disposal in marine and river environments.

Research was conducted into the extent and the pattern of downstream spread of the jet to give some methods for the prediction of its velocity at any point in the flow.

Since previous research has shown that the velocity patterns produced by jets of various nozzle shapes were similar, a circular jet was chosen for simplicity. The downstream velocity profiles were found to be similar as had been predicted for free jets and wall jets issuing into a stagnant environment.

Relationships between downstream velocities and an excess momentum thickness θ that the jet posesses were shown to be similar for the various velocity ratios investigated and the theoretical justification for the use of this term is shown in the analytical section.

The correspondence between the velocity at any point and the concentration that results from an injection of pollutant at some position upstream is also shown so that these results can be used for the prediction of that concentration at any downstream section.

Agreement between these results and the relations for their theoretical prediction was extremely good.

Acknowledgements

The author would like to express his sincere gratitude to Professor N. Rajaratnam for his original suggestion of this topic and his guidance throughout the research.

The assistance provided by the staff of the T. Blench Hydraulics Laboratory during design, construction and installation of all apparatus is gratefully acknowledged.

The author is also grateful to the Department of Civil Engineering for the financial assistance provided during the course of study and to the Natural Sciences and Engineering Research Council of Canada for partial financial support through a grant to N. Rajaratnam.

Finally, thanks are due to Miss Sue Boyetchko for the typing of a large part of this thesis.

Table of Contents

Introduction.....1

Theoretical Considerations.....11

Effect of the wall on jet growth.....19

Effect of boundary roughness.....21

Calculation of dilution from velocity distribution.....23

Decrease of Momentum Efflux in the downstream direction.....25

Experimental Arrangement and Experimental Results.....27

Injection nozzle.....27

Constant head arrangement.....29

Velocity Measurement.....31

Shear Stress evaluation.....32

Instrumentation.....36

Experimental procedure and results.....40

Effect of depth alteration.....44

Analysis of experimental results.....45

Conclusions and Recommendations.....66

List of References.....71

Appendix A. List of symbols.

Appendix B. Results from Runs 1 to 7.

I. Introduction

The problem of effluent disposal in marine and river environments greatly concerns engineers and ecologists in the present day. With the rapid expansion of cities, towns and small communities the disposal of associated domestic and industrial sewage requires considerable thought and planning so as not to either instigate or increase harmful pollution in the receiving waters.

Large bodies of water have the ability to absorb relatively small amounts of wastewater, containing suspended solids and biodegradable products, and purify it with no detrimental effects. It is when relatively large quantities of wastewater are introduced to a water body that severe local and global pollution may result.

It is therefore clear that the most serious effects of this pollution will be experienced in inland waterways which must carry the effluents of large cities. As these rivers and lakes often provide recreation, and also water supply for the city, it is all the more important that they should be kept as free from any serious pollution as is reasonbly possible.

The main criterion when judging the possible effects of wastewater introduction is the dilution that wastewater experiences a short distance from the point of injection. It is generally accepted that a dilution of one part of wastewater to one hundred parts of receiving water (1:100)

will give adequate protection against serious pollution. It is therefore up to the engineer to present a design for a sewage outfall that will meet or exceed this requirement while staying within the limits of his budget.

Each different sewage disposal situation must be examined separately as it is a rare occurrence when a method applicable to one site can be used at a different one. The parameters that affect the final choice of outfall design will be the size of the receiving body of water, the relative density of the wastewater and receiving water, the relative flow velocity and the presence of surrounding fish life.

The disposal of wastewater in coastal areas usually presents much less of a problem than for its inland counterpart. Vast volumes of water are available to dilute the wastewater of even large cities and large depths also exist enabling the outfall to be placed as far below the water surface as possible. The most desirable situation would be if the effluent never reached the water surface, however with the density difference between salt water and fresh wastewater the effluent possesses buoyancy and will naturally rise towards the water surface unless suitable density gradients exist.

In river situations the density difference is less pronounced leading to effluent plumes and jets that rise to the surface of the water much more slowly. Illustrated in Fig. 1-01 is a passive plume of dyed fresh water entering a

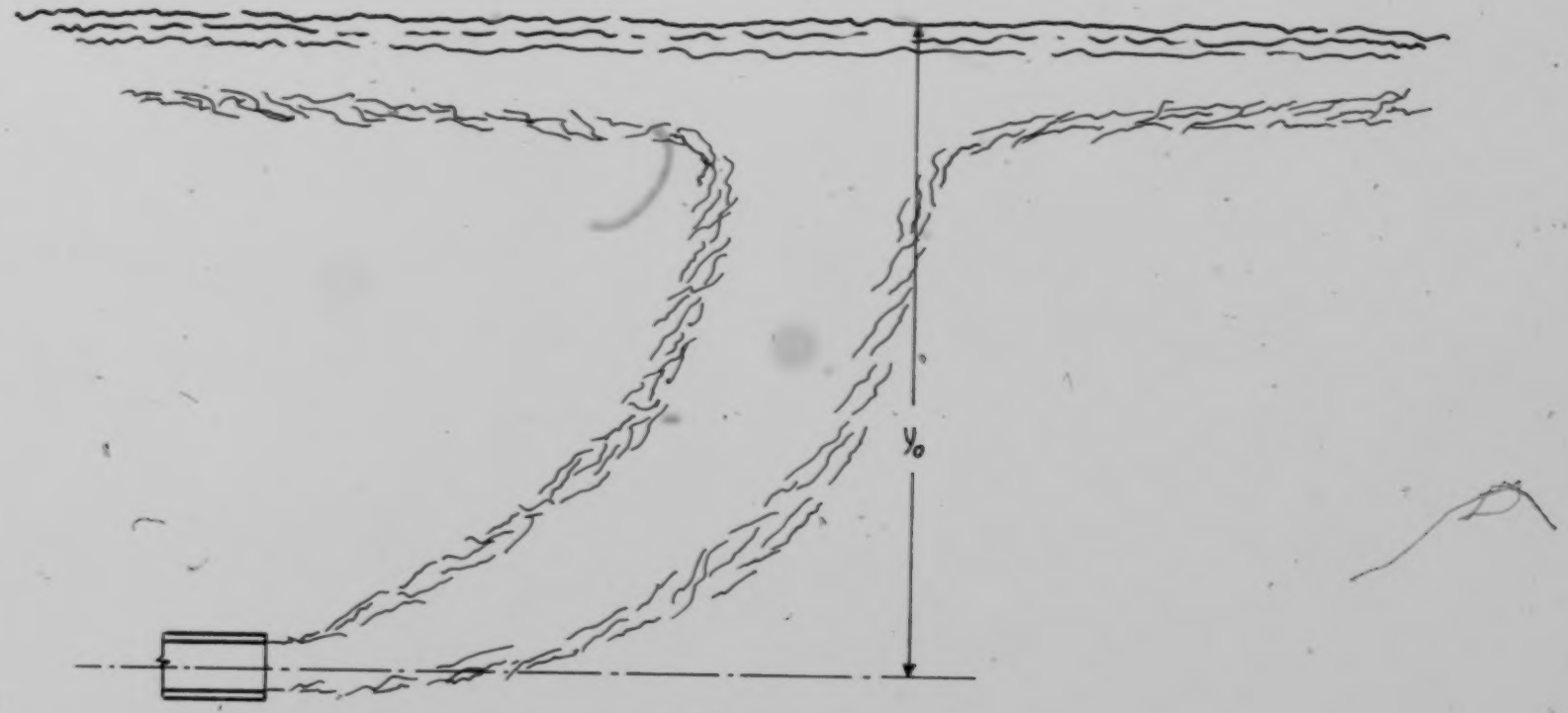

FIG. 1-01. SKETCH OF SINGLE RISING PLUME OF FRESH WATER IN A STAGNANT SALT WATER ENVIRONMENT.

stagnant salt water environment. The fresh water is passed through a horizontal outlet where immediately buoyancy forces cause it to rise to the surface and spread out in a layer. Rawn et al (1960) analysed the dilution that occurred and found it to be a function of the ratio of water depth to nozzle diameter and Froude number at the outlet. Below a Reynolds number of 5000 this parameter also becomes important; however almost all flows will be well above this value.

It is reasonable to assume that effluent disposed of into rivers will also rise similarly as there will be a certain amount of buoyancy due to the excess heat of the wastewater. This is approximately the situation that occurs in the disposal of effluent through an outfall pipe into the ocean. It does not, however, usually produce high initial dilutions and is only used if the water is deep, and away from any sites of recreational activity as it takes longer for the wastewater to become purified.

One commonly used method for obtaining high initial dilutions is to have a series of ports in a diffuser pipe which will attach to the end of the outfall. These ports ensure that the effluent is discharged over a wide area thus ensuring that as much of the receiving water as is practically possible will be used to dilute and render harmless the waste. A typical diffuser arrangement is shown in Fig. 1-02. In certain cases diffusers can provide initial dilutions ten or more times greater than with merely an open

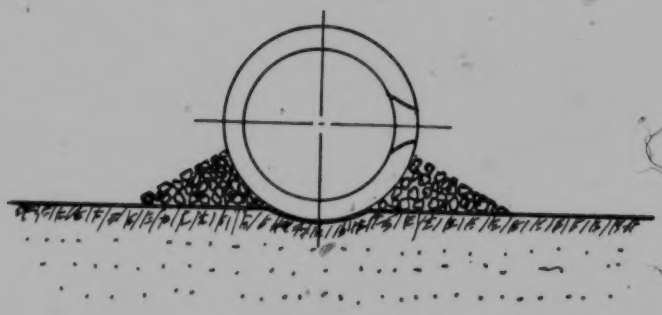

TYPICAL DIFFUSER SECTION.

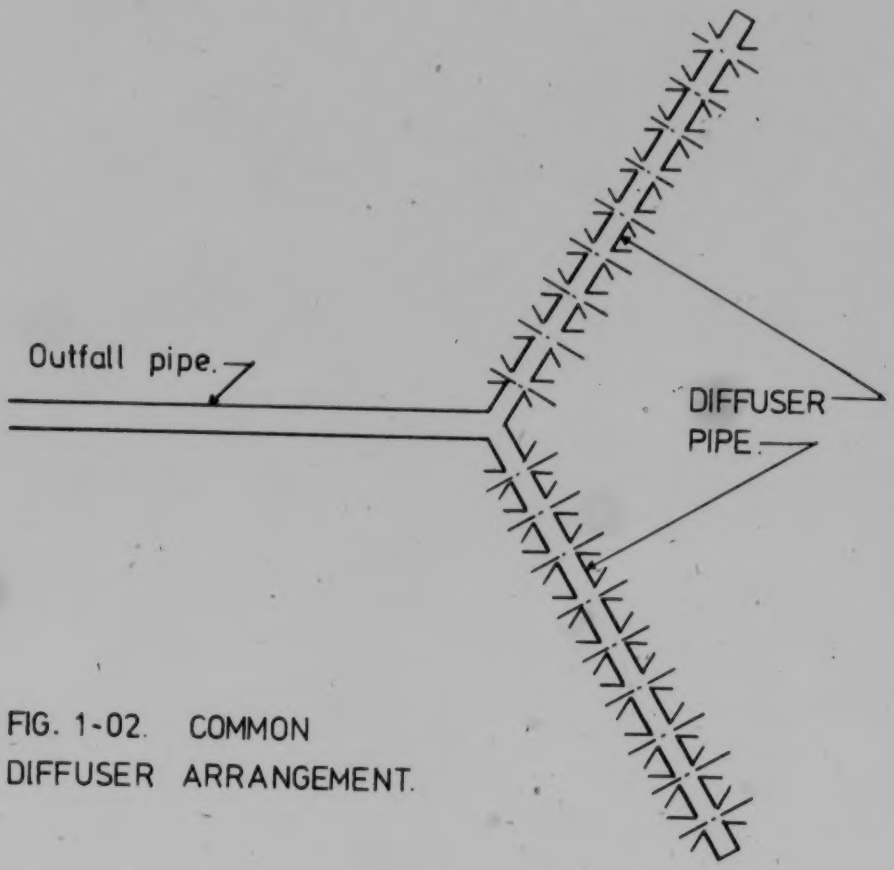

FIG. 1-02. COMMON
DIFFUSER ARRANGEMENT.

ended outfall (Rawn et al, 1960). Thus nowadays for almost all wastewater disposal schemes, some sort of diffuser is recommended.

Another common type is shown in Fig. 1-03. It consists of a buried outfall pipe with a series of vertical risers on its top surface. This may be used when clearance is a problem, for instance in a shallow river, as the main body of the diffuser is buried below bed level. Any excess velocity that an effluent jet may initially possess will eventually be reduced to zero and if it has buoyancy, it will then tend to rise to the surface. In the case of a co-flowing channel where the effluent and the receiving water are moving in the same direction, a plume will not usually manifest itself. However, the effluent may still rise to form a surface layer for some distance downstream of the point of injection.

If diffuser ports are spaced closely together, interference will result thus diminishing the dilution capability of the surrounding water. Almost all diffusers are designed with the aid of hydraulic models which would indicate whether this was going to be a severe problem. It is advantageous to have equal discharges flowing from each nozzle so that the total wastewater load may be spread along the whole length of the diffuser pipe. This entails careful design of both the exit nozzles and the pipe itself. One method is to have a tapering pipe getting smaller towards its end. This ensures a constant velocity inside the pipe

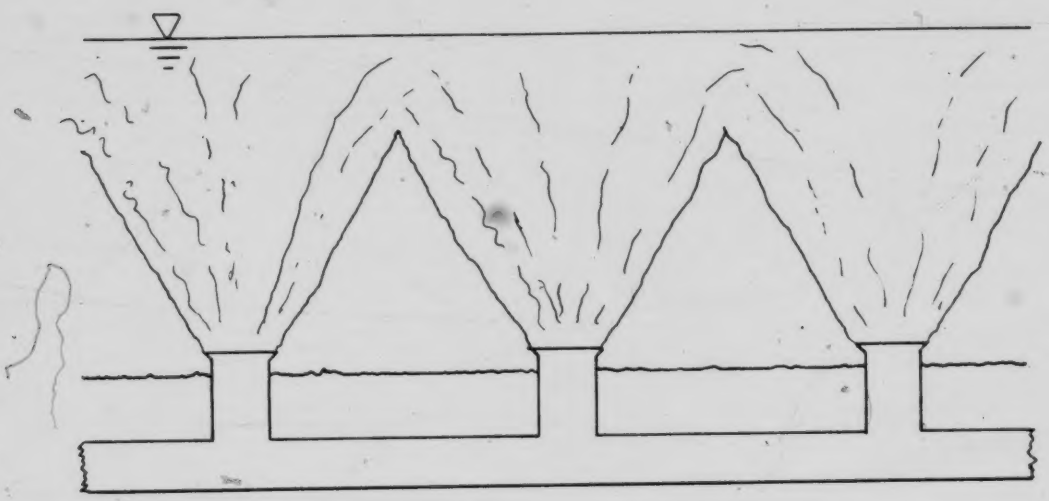

FIG. 1-03 DIFFUSER WITH RISER PIPES

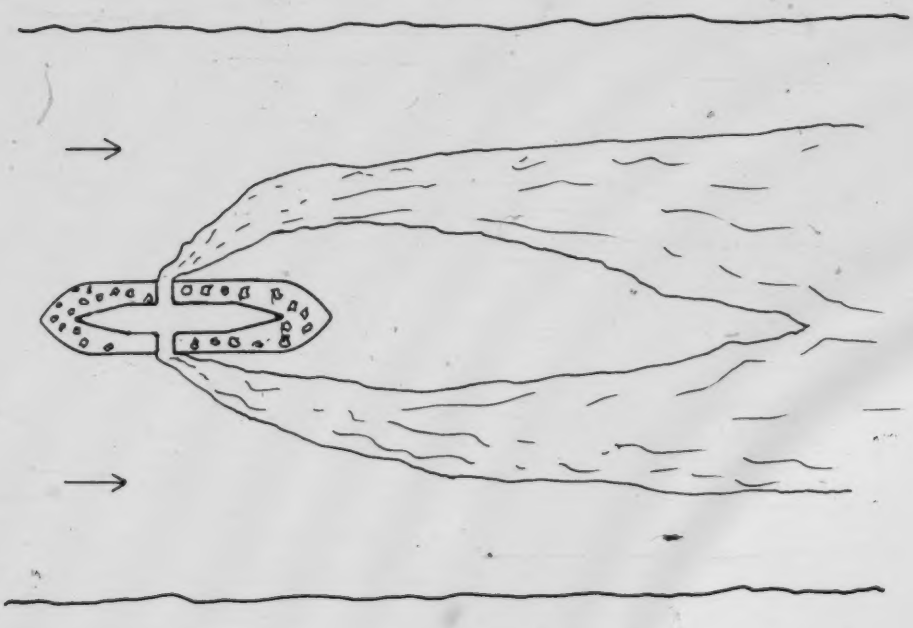

FIG 1-04 BRIDGE PIER DISPOSAL

and means that all port diameters may be kept the same. Conversely port diameters may be increased towards the end of the pipe for the same effect. Grace (1978) gives a method for calculating the discharge from each port which is of a step-by-step nature and ideally suited to computer application.

Another disposal technique is to use an outfall similar to a bridge-pier, shown in Fig. 1-04, with outlets on either side which point the effluent flow across the path of the river flow. This produces two distinct trails flowing with the river which will eventually meet at some point downstream.

A modification of one of the previous systems gives an underground pipe with risers which curve through forty-five degrees to lie on the bed of the channel and point downstream thus issuing their flow in the same direction as the receiving water flow. Clay and Gordon (1965) describe just such an outfall which was designed for a pulp and paper mill in the city of Kamloops, B.C. and is shown in Fig. 1-05. It was to handle a discharge of 0.65 cumecs of effluent to the Thomson River, a salmon-producing tributary of the Fraser River. Thus it was extremely important that the effluent be rendered completely harmless to the fish life as soon as possible after entering the river. A large amount of pre-treatment was already applied to the wastewater before it was passed to the river, but this would not normally have been sufficient were it not for the very

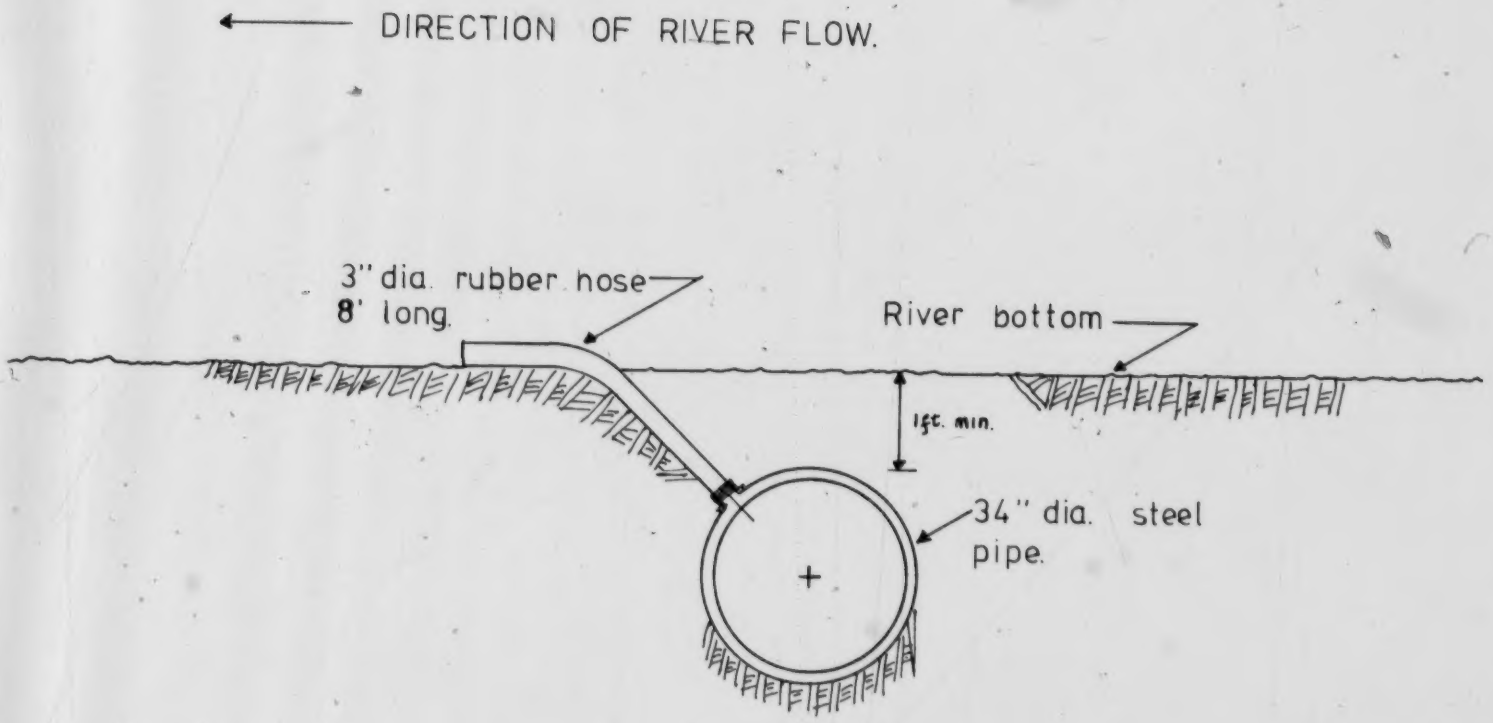

FIG. 1-05 CROSS-SECTION THROUGH THE KAMLOOPS DIFFUSER, SHOWING A TYPICAL NOZZLE ARRANGEMENT.

efficient diffuser through which it was passed. This diffuser provided initial dilutions of 1:100 from which no pollution hazzard would arise.

The diffuser itself consisted of a 183 m. length of 86 cm. diameter pipe lying perpendicular to the direction of the river flow buried to a depth of 30 cm. To this pipe are connected 110, 6.3 cm. nozzles each joined to a 7.6 cm. diameter rubber hose, 2.45 m. long. Each of these hoses emits a 3-D jet of effluent into the river which will spread in the lateral direction towards the adjacent jets and also in the vertical direction towards the water surface.

The practical work for this thesis consists of research into the velocity distributions at different vertical sections downstream of one nozzle of similar design. Vertical velocity profiles along the centre of the jet were measured as were lateral profiles which indicate effluent spread towards adjacent diffuser ports. In a practical case, at some distance downstream adjacent flows will interfere with each other and the situation will be reduced to that of a two dimensional slot jet.

Dilution of wastewater that occurs downstream of the injection nozzle is a direct function of velocity distribution and analysis of jet scales shows growth of the jet in the vertical and horizontal directions due to mixing.

II. Theoretical Considerations.

Analysis of a three-dimensional jet in a co-flowing channel may be approached by first considering the case of a circular jet with an efflux velocity of U_0 in an infinite fluid moving with a velocity of U_1. The definition sketch for this situation is shown in Fig. 2-01.

This diagram shows two distinct regions of flow. Close to the nozzle there is a potential core or flow development region followed by a region of fully developed flow. In the fully developed flow region, the velocity profiles are shown and these are found to be of a similar nature at every section downstream of the nozzle. Scales for the analysis of the profiles are now introduced. Um is the excess velocity of the jet over the surrounding flow and is defined by Eq. 2-01, um is the absolute maximum at any section, U_1 is the average surrounding flow velocity, the x-axis is in the downstream direction of flow and the r-axis is perpendicular to this.

$$Um = um - U_1 \qquad 2\text{-}01$$

A length scale b is now introduced where b is the distance from the point of maximum velocity to a point where the relative velocity is half the maximum. This is described in Eq. 2-02.

$$b = r(Um) - r(Um/2) \qquad 2\text{-}02$$

The equations of motion and the continuity equation for this jet can be written as (Rajaratnam)

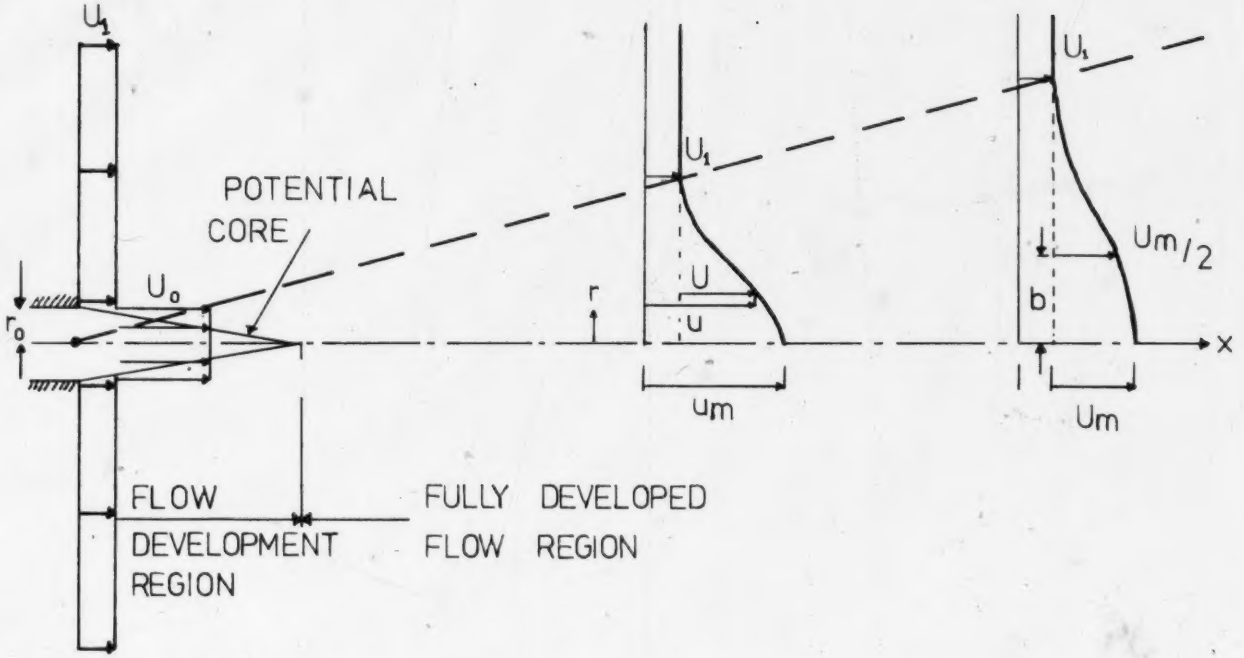

FIG. 2-01 DEFINITION SKETCH FOR CIRCULAR COMPOUND JETS.

$$u\frac{\partial u}{\partial x} + v\frac{\partial u}{\partial r} = \frac{1}{\rho}\cdot\frac{1}{r}\frac{\partial r\tau}{\partial r} \qquad 2\text{-}03$$

$$\frac{\partial ru}{\partial x} + \frac{\partial rv}{\partial r} = 0 \qquad 2\text{-}04$$

where u and v are the time averaged velocities in the x (or axial) and in the r (or radial) directions respectively, ρ is the fluid density and τ is the turbulent shear stress.

By integrating Eq. 2-03 with respect to r from r=0 to r= ∞ we could arrive at (Rajaratnam, 1976)

$$\int_0^\infty \rho ur\frac{\partial u}{\partial x}.dr + \int_0^\infty \rho vr\frac{\partial u}{\partial r}.dr = \frac{1}{2\pi}\frac{d}{dx}\int_0^\infty 2\pi rdr\rho u^2 - \frac{1}{2\pi}\frac{d}{dx}\int_0^\infty 2\pi rdr\rho uU_1$$

$$= \frac{1}{2\pi}\frac{d}{dx}\int_0^\infty 2\pi rdr\rho u(u - U_1)$$

and $$\int_0^\infty \frac{\partial r\tau}{\partial r}.dr = \{ r\tau \}_0^\infty = 0$$

So Eq. 2-03 becomes

$$\frac{1}{2\pi}\frac{d}{dx}\int_0^\infty 2\pi rdr\rho u(u - U_1) = 0 \qquad 2\text{-}05$$

which says that the rate of change of excess momentum flux in the x or downstream direction is zero; ie. the excess momentum flux of the jet in the axial direction is preserved.

The similarity between velocity profiles at different sections downstream of the nozzle can be expressed as

$$\frac{u - U_1}{um - U_1} = \frac{U}{Um} = f\left(\frac{r}{b}\right) = f(\eta) \qquad 2\text{-}06$$

Using this relation along with Eq. 2-05 we get

$$\frac{d}{dx}\int_0^\infty b^2\eta\left(\frac{Umf}{U_1} + \left(\frac{Um}{U_1}\right)^2 f^2\right)d\eta = 0 \qquad 2\text{-}07$$

In the case of a jet issuing into a fluid that is travelling very much slower, then Um/U_1 close to the nozzle in the fully developed flow region will be large. This situation where the jet is dominant is known as the strong jet case. Further downstream the jet effects will diminish until Um is of the same order as U_1 and still further $Um \ll U_1$. The latter case is known as the weak jet case.

The two extreme cases could now be considered separately along with dimensional analysis.

For the strong jet where $Um \gg U_1$ Eq. 2-07 becomes

$$\frac{d}{dx}\int_0^\infty b^2\eta\left(\frac{Um}{U_1}\right)^2 f^2 d\eta = 0$$

or

$$\frac{d}{dx}\left(b^2Um^2\right)\int_0^\infty \eta^2 f^2 d\eta = 0 \qquad 2\text{-}08$$

The integral in Eq. 2-08 will be a constant, therefore

$$\frac{d}{dx}\left(b^2Um^2\right)=0 \qquad 2\text{-}09$$

We may now assume that both the terms within the brackets in Eq. 2-09 are some function of x, namely

$$Um \propto x^p \quad \text{and} \quad b \propto x^q$$

Therefore $2p+2q=0$ or $p+q=0$ 2-10

For the weak jet case $Um \ll U_1$ and Eq. 2-07 becomes;

$$\frac{d}{dx}\int_0^\infty b^2\eta\frac{Umf}{U_1}d\eta = 0$$

or $$\frac{d}{dx}\int_0^\infty b^2\eta Umf\,d\eta = 0$$

Simplifying, this gives

$$\frac{d}{dx}(b^2Um)\int_0^\infty \eta Umf\,d\eta = 0$$

and $$\frac{d(b^2Um)}{dx}=0 \qquad 2\text{-}12$$

and therefore $$2q+p=0 \qquad 2\text{-}13$$

When Um is of the same order as U_1 this analysis is not applicable and other methods must be found.

Now using the similarity of the equations of motion, we have firstly;

$$u = U_1 + Um(f)$$

and $$u\frac{\partial u}{\partial x} = Um'f + UmUm'f^2 - U_1Umb'\eta f' - Um^2\frac{b'}{b}\eta ff'$$

where primes denote differentiation with respect to x.

Integrating the continuity equation 2-04 we get

$$v = Umb'\frac{1}{\eta}\int_0^\eta \eta^2 f'd\eta - bUm'\frac{1}{\eta}\int_0^\eta \eta f d\eta \qquad 2\text{-}14$$

and $$\frac{\partial u}{\partial r} = \frac{Umf'}{b}$$

If $$\tau/(\rho Um^2) = g(\eta)$$

then $$\frac{\partial r\tau}{\partial r} = \frac{\partial}{\partial r}(\rho Um^2 rg) = \rho Um^2(g + rg'/b)$$

$$\frac{1}{\rho}\frac{1}{r}\frac{\partial r\tau}{\partial r} = \frac{Um^2}{b}\left(\frac{g}{\eta} + g'\right) \qquad 2\text{-}15$$

Using these expressions along with Eq. 2-03 and simplifying

$$\frac{bU_1}{Um^2}Um'\eta f + \frac{b}{Um}Um'(\eta f^2 - f'\int_0^\eta \eta f d\eta) - \frac{U_1}{Um}b'\eta^2 f'$$

$$- b'(\eta^2 ff' - f'\int_0^\eta \eta^2 f' d\eta) = g + \eta g' \qquad 2\text{-}16$$

If we now assume that in Eq. 2-16 all terms in η, or functions thereof are the same order of magnitude, then the first term reduces to,

$$\frac{U_1}{Um} x^q \frac{x^{p-1}}{x^p}$$

and the third term to

$$\frac{U_1}{Um} x^{q-1}$$

ie. both are proportional to $\frac{U_1}{Um} x^{q-1}$.

For the strong jet case when $Um >> U_1$ the second and fourth terms in the equation will be dominant,

$$\frac{b}{Um}Um'(\eta f^2 - f'\int_0^\eta \eta f d\eta) - b'(\eta^2 ff' - f'\int_0^\eta \eta f' d\eta) = g + \eta g'$$

from which we get

$$\frac{bUm'}{Um} \alpha\ x^0 \text{ and } b' \alpha\ x^0.$$

This gives the result that $q-1=0$ or $q=1$. Using this along with Eq. 2-10 we get

$$q=1 \text{ and } p=-1$$

This means that for a strong jet $Um \alpha 1/x$

and $b \alpha x$.

For the weak jet the second and fourth terms drop out and we are left with

$$\frac{bU_1Um'}{Um^2}\eta f - \frac{U_1 b'}{Um}\eta^2 f' = g + \eta g'$$

giving,

$$\frac{bUm'}{Um^2} \alpha x^0 \text{ and } \frac{b'}{Um} \alpha x^0$$

or $$q-p-1=0$$

Using this result along with Eq. 2-13 we get

$$q=1/3 \text{ and } p=-2/3$$

or $$Um \alpha 1/x^{2/3} \text{ and } b \alpha x^{1/3}.$$

We have already demonstrated that excess momentum M_0 is conserved in the axial direction. Now using dimensional analysis we can first say that

$$Um = f_1(M_0, \rho, x)$$

wherein the viscous effects are neglected, which is valid if the jet Reynolds number is greater than a few thousand and it has been further assumed that the channel is wide enough for the effects of the side walls to be negligible and that the flow is so deep that the presence of the free surface does not affect the process of jet diffusion. Using the Pi-theorem we get

$$\frac{Um}{\sqrt{(M_0/\rho x^2)}} = \text{Const.} \quad \text{or} \quad \frac{Um}{\sqrt{(U_0(U_0-U_1))}} = \frac{C_1}{(x/r_0)}$$

or

$$\frac{Um}{U_1} = \frac{C_1}{(x/\theta)}$$

where θ is the so-called momentum thickness term used in the analysis of scales in the axial direction and is defined by the equation;

$$M_0 = \pi r_0^2 . \rho U_0 (U_0 - U_1) = \pi \theta^2 . \rho U_1^2$$

or

$$\theta = \sqrt{\left(\frac{M_0}{\pi \rho U_1^2}\right)} = r_0 \sqrt{(\alpha(\alpha-1))}$$

where α is the initial ratio of velocities between the jet and the surrounding fluid ($=U_0/U_1$). If U_1 is also included in the initial list of independent parameters it can be shown that

$$Um/U_1 = f\ (x/\theta).$$

Experimental research in this area has been conducted by Forstall and Shapiro (1950), Tani and Kobashi (1951) and Antonia and Bilger (1973) among others. These observers, in trying to supply a formula that will fit their data, have chosen a variety of solutions. Squire and Trouncer (1944) proposed that a relation involving the cosine of (r/b) be used to predict velocity in the fully developed region, while Bradbury and others indicate a power relation between all the relevant terms. Rajaratnam (1976) and Pande and Rajaratnam (1976) present a study of the data gathered by some of the observers along with various empirical relations

for their prediction. While each observer has usually derived a relation that is applicable to his data, discrepancies appear when all the data is correlated together and plotted. Pande and Rajaratnam have developed a method of analysis using both the integral momentum equation and the integral energy equation that predicts U_1/Um for values of x/θ for both strong and weak jets. When used with the results by Antonia and Bilger this equation provides good agreement. It is also used in the analysis in Chapter 3 of this thesis.

Effect of the wall on jet growth

In the case of a three dimensional jet issuing tangentially onto a wall the situation will be somewhat different to that described in the previous section. The definition sketch for this is shown in Fig. 2-02. The growth of the jet on one side is now restricted by the presence of the wall bringing the velocity to zero.

The variation of velocity in the outer or free mixing region is similar to that for the free jet, however a different analysis must be applied to the inner region where the velocity rises from zero to maximum.

Rajaratnam (1976) again analysed the scales and found the relations for jet growth and velocity decay to be of the same type as those derived for the free jet. Experimental observations indicate that the lateral spread, parallel to

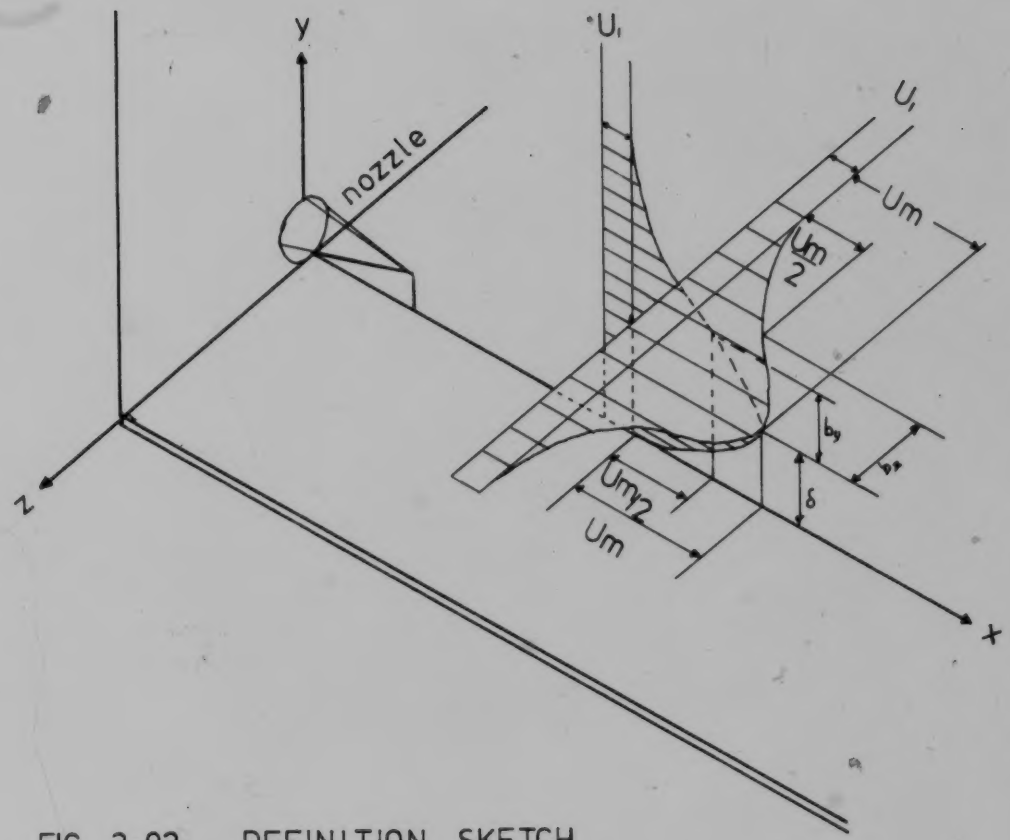

FIG. 2-02. DEFINITION SKETCH FOR BLUFF CIRCULAR WALL JETS.

the wall and formerly the same as the vertical spread, now increases at a rate approximately four to five times as fast.

The velocity variation in the inner region may be approximated by a power law distribution of the form,

$$\frac{U}{Um} = \left(\frac{y}{\delta}\right)^{1/4} \text{ to } \left(\frac{y}{\delta}\right)^{1/10}$$

These two power values cover the extremes of an envelope within which all boundary layer results would generally lie.

Fig. 3-12 shows these two curves drawn on the graph of inner region velocity variation and it can be seen that almost all results lie inside these two.

Effect of boundary roughness

During all the data collection, the flume had an artificial roughness on the bed caused by a strip of sandpaper, which is described in more detail in Chapter 3. Pani (1972) studied the effect of boundary roughness on a wall jet in a stagnant receiving environment. He compared measurements obtained for jet velocities over a smooth aluminum bed with those for the same nozzle over a bed of identical sandpaper to that used in this research.

He concluded that the presence of a rough boundary does not affect the maximum velocity decay along the centre line of the jet to any appreciable extent. Plotting his rough and smooth wall data together in a Um_0/U_0 vs. $x/\sqrt{A}$ form, where A is the nozzle area produced remarkably close agreement for

d/ks= 1, where ks is the equivalent sand roughness of the sandpaper. He considered two distinct regions of flow, the first being the inner or boundary layer where the velocity increases to its maximum value and the second being the outer or free mixing region where the velocity decays from maximum to zero.

Analysis showed that the presence of roughness caused the boundary layer to increase in size and thus the maximum velocity to occur further from the wall. However the free mixing region remains unaffected by the presence of boundary roughness. Pani also found that the roughness had most effect on the inner region close to the nozzle. This is to be expected as here the boundary layer is thin and the ratio of roughness height to boundary layer size is much larger than for sections further downstream. He concluded that the presence of boundary roughness has no effect on the lateral spread of the jet.

As most real situations such as dicharge through a diffuser into a river include the presence of boundary roughness and as, according to the work of Pani, that roughness did not significantly affect the analysis, it was felt justified in including the roughness during all measurements.

Calculation of dilution from velocity distribution

If we consider the case of a pollutant added to a moving flow then its concentration will diminish as it spreads out in all directions downstream due to turbulent mixing, entrainment and ambient turbulence.

An analysis similar to that performed on the jet in the first section yields the result that for a 3-D pollutant source, pollutant concentration at any point can be expressed in terms of the maximum along the diffuser centreline and its distance from the centreline. This situation is entirely analagous to the spreading of the jet and we can say that

$$\frac{C}{Cm} = f\left(\frac{z}{b}\right) = f(\eta)$$

and $Cm \propto x^{s}$, $b \propto x^{q}$,

where Cm is the maximum concentration at any section downstream of the source, C is the concentration at any point, z is the distance from the centreline and b is the distance to half the maximum concentration.

We may again say that Cm and b are both functions of x and using the pollutant conservation equation we can show that the variation of Cm in the downstream direction is the same function of x as the velocity scale Um. From these considerations, we could indicate that for the strong as well as weak jet cases the concentration will vary in the same manner as the velocity scale. Of course these proportionalities do not contain any constants and this is

where the relations will differ. This is comparable to the case of a passive plume where a jet is injected into a channel with zero excess momentum. The equation

$$f(\eta) = e^{-0.693\eta^2}$$

can be used to describe the profiles of a pollutant in both the outer region and the transverse direction, spreading downstream of a source.

It has been found by experimentation that the concentration spreading from a circular turbulent jet is 15 to 20 percent greater than the velocity spread. That is the length scale b is greater by that amount at every downstream section for the pollutant. Various researchers have conducted experiments into the exact value of this difference and among them the value of 17 percent by Hinze & Zijnen(1949) appears to be the best.

If we include this factor in the equation it becomes

$$\frac{C}{Cm} = e^{-0.693\mu\eta^2}$$

where

$$\mu = \frac{1}{k^2} = \frac{1}{1.17^2}$$

k being the ratio of the growth rate of the pollutant and velocity profiles respectively. Thus it can be seen that from the velocity variations collected in this research, knowing the original concentration, the concentration of pollutant at any section downstream could also be obtained.

So the rate at which a pollutant is diluted can be determined for a particular situation and from the guidelines that have been proposed for effluent disposal it may also be determined whether the propsed installation will prevent pollution of the receiving water.

Decrease of Momentum Efflux in the downstream direction

In the original analysis it was shown that the momentum efflux in the downstream direction was preserved. This is not, in fact, strictly true as the shear stress on the bed will cause the efflux to diminish.

If the momentum efflux is decreased by an appreciable amount, say more than 25 percent, then the analysis is no longer applicable to sections downstream of this area. The actual decrease was therefore computed for runs 5 and 7 which have two different nozzle diameters.

The procedure used was an approximate one but was assumed to be reasonably accurate. Instead of an exponential variation of velocity in the lateral direction, a straight line was assumed and although it has been shown that the actual spread of the jet is about 2.25bz a value of 2bz was used as the jet is an elliptical shape and its width would tend to diminish as it approached the bed.

Drag force was computed by splitting the downstream area into twelve sections. For each section an average shear stress was calculated along the centreline and this was again averaged along with the free stream shear stress. The

area of the trapezoidal section on one side of the jet was determined and the two values multiplied together to give the average shear force for one side of a section.

The drag force at each other section was found and all these were summed together and doubled to give the total drag force on both sides of the jet. The percentage of the total momentum excess was then determined at the end of each section.

It was found that the figure of 25 percent was exceeded in both cases at the last downstream section. With the small nozzle and α = 19.89, the momentum reduction was 35 percent at the last section and for run 7 with the large nozzle and α = 3.54 it was 40 percent.

However for the first case the reduction was within limits up to the eleventh section and for the second case was within limits up to the tenth section.

It was therefore felt that although a reduction occured it was not significantly large in the main research area to cause any modification of the analytical technique.

III. Experimental Arrangement and Experimental Results.

The apparatus used in this study consisted of a flume approximately 50 metres in length and just under one metre in width. The slope of the flume can be varied by use of a motor and screw jacks at 10 metre intervals but for all experiments the slope was kept at a constant value of 0.03%. A tail gate was used to control water level in the flume and a valve on the water supply line altered the discharge from 0 to 2.5 c.f.s.

Along the bed of the flume for a distance of 15 metres cloth sandpaper was glued to give an artificial roughness. This sandpaper is described in greater detail in the section on shear stress.

Injection nozzle

The method chosen for water injection was by two different diameters of nozzles. The first had an exit diameter of 1/4 inch and was used for Runs 1 through 6 and a large nozzle of 3/4 inch diameter was used for Runs 7 and 8. The alternatives in the placement of the nozzle consisted of either cutting a hole in the bottom of the flume and have the water supply come in through the bed or else suspend the nozzle from some point above the bed in order to avoid drilling holes in the flume. The latter alernative was rejected as it was felt that a supply pipe to the nozzle coming down through the flow would seriously upset

downstream velocity distributions by causing turbulent eddies behind the pipe. It was therefore necessary to cut a hole 2.5 inches in diameter in the bottom of the flume to accomodate the nozzle as shown in Fig. 3-01.

In order to minimize flow disturbance as the water is pointed downstream, the angle of the elbow upstream of the nozzle was made 45 degrees. This entailed a larger cut out in the flume bed but was considered to be worth the extra trouble to avoid irregular velocity patterns in the flow created by a right angled bend.

Constant head arrangement

A simple constant head tank was constructed to maintain a steady flow of water into the nozzle at a constant velocity. This tank was mounted on the side of the flume as shown in Fig. 3-02 and had a fine adjustment that enabled accurate heads to be maintained. The head difference between the water level in the flume and that in the constant head tank was measured by a point guage with a vernier scale.

Originally the water supply to the nozzle came direct from the city fresh water supply. This was found to be satisfactory for the first and third runs but inconsistencies were observed in the second run. It was found, while measuring velocities at various sections downstream of the nozzle, that the jet would apparently disappear and just as suddenly then reappear.

The cause of this problem remained a mystery for a long

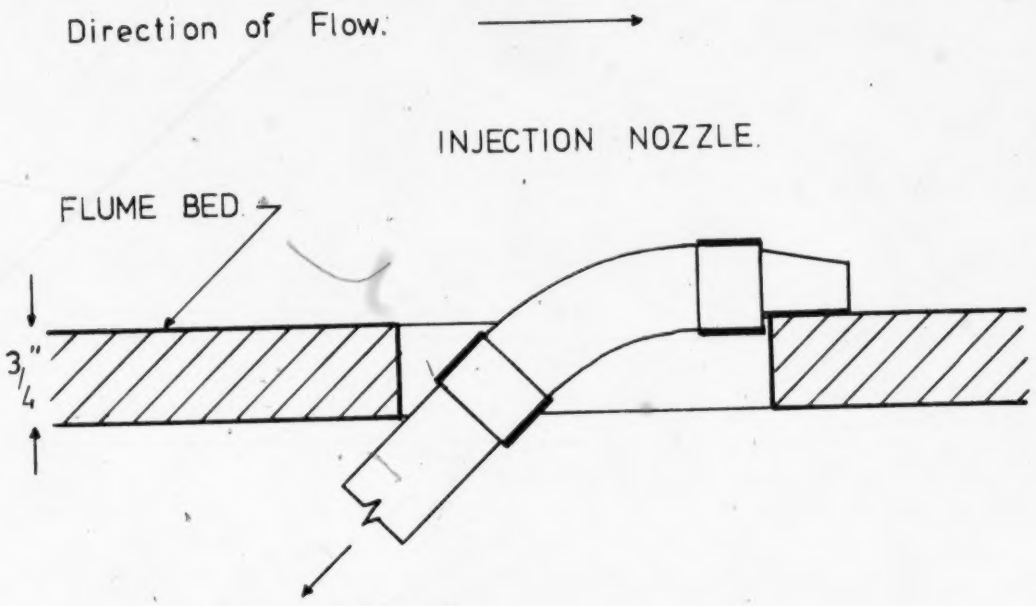

FIG. 3-01.

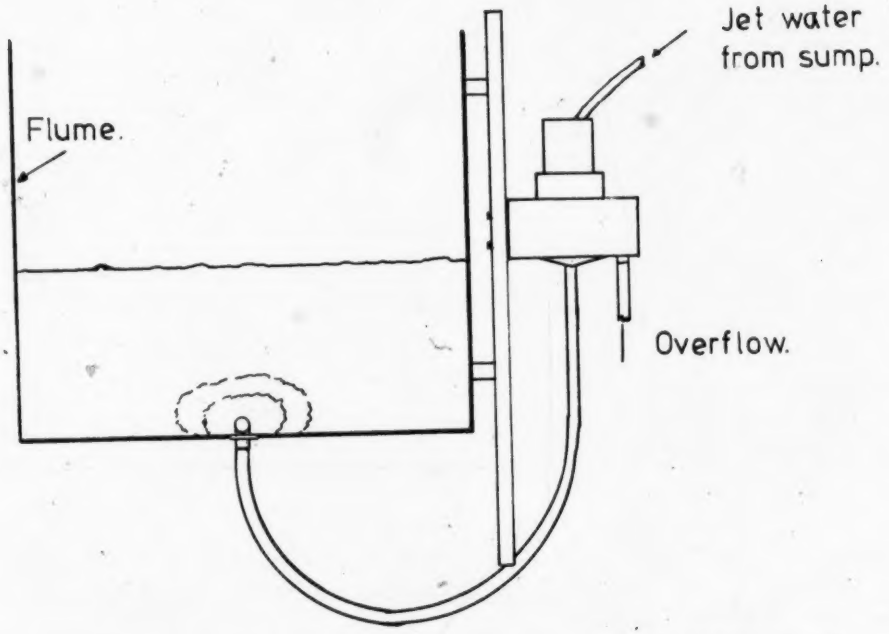

FIG. 3-02 CONSTANT HEAD ARRANGEMENT.

time until it was noticed that an air lock would appear in the nozzle supply line on occasions. Further investigation revealed that as the city water came into the the warm laboratory, air bubbles would form and these would eventually join together to form one large air lock at the beginning of the nozzle supply line thus interrupting flow to the jet. The reason for this problem not arising in the other runs was that, in the first case, the jet discharge was sufficiently high to carry air bubbles into the flume through the nozzle while in the third run the discharge was sufficiently low to allow the bubbles to rise to the surface under their own buoyancy.

After the cause was discovered, the city supply was discontinued and instead a submersible pump was placed in the water sump to supply the constant head tank. This appears to be a better solution as temperature and density differences between the flume water and jet water would cause only negligible buoyancy effects. No further problems with the appearance of air bubbles were experienced as the sump water had become de-aired over a long period of time.

Velocity Measurement.

All velocity measurements were made with a pitot-static tube 1/16 inch in diameter. It was considered that this tube was of small enough size so as not to cause severe disturbance to the flow. The two outlets from the pitot tube were connected to either side of a pressure transducer which sensed the magnitude of the differential pressure at any point in the flow. This pressure is entirely due to the velocity at that point.

The transducer consists of a magnetic pressure plate which is moved towards one side of the transducer body by the excess head corresponding to the velocity at a certain point. This magnetic signal is interpreted by a transducer meter and output as a voltage.

The calibration of the transducer was accomplished by two water supply pots. By the use of a valve board, the pressure supply can be switched between the calibration pots and the pitot tube itself. The transducer is first zeroed by having identical heads in both calibration pots and then a differential head of 1 inch is applied to the transducer and the meter adjusted till this corresponds to an output of one volt. Thus a voltmeter would indicate velocity head directly in inches of water.

It is extremely important that no traces of air remain in the lines. For this purpose de-aired water was used. Any air bubbles that exist in the lines cause non-linearity of head measurements as the air bubbles become compressed.

After calibration, the supply pots are switched out and the transducer is connected to the pitot tube which has also been carefully de-aired.

Shear Stress evaluation

The measurement of dynamic head on the bed of the flume at various distances downstream of the injection nozzle was made at the time of the general velocity distribution measurement and from this head the shear stress was later calculated.

This method was suggested by Preston in 1954. Preston assumed that the total pressure P indicated by a total head tube resting on the wall and facing the flow minus the static pressure at the wall P_0 is a function of only the shear stress at the wall τ_0, diameter of the tube d, the mass density ρ and the kinematic viscosity of the fluid ν.

Using the Pi-theorem, the above statement could be reduced to,

$$\frac{(P-P_0)d^2}{\rho\nu^2} = F\left(\frac{d^2\tau_0}{\rho\nu^2}\right) \qquad 3\text{-}01$$

Patel (1965) found Preston's original equations to be somewhat in error and suggested three new relations connecting

$$\Delta p^* = \frac{\Delta p d^2}{4\rho\nu^2} \qquad 3\text{-}02$$

and

$$\tau_0^* = \frac{\tau_0 d^2}{4\rho\nu^2} \qquad 3\text{-}03$$

for smooth boundaries. Hwang and Laursen (1963) applied Preston's work to rough boundaries and found that, with some modification, the technique was applicable there also.

In the case of rough boundary flow, further parameters must be introduced, these being u*, the friction velocity and k the roughness height of the bed. For completeness the internal diameter of the tube opening, a, could be introduced but it was demonstrated by Hsu (1955) that the effect of including this parameter was small.

Again using dimensional analysis these groups can be obtained,

$$\frac{\Delta p}{\rho u^{*2}} = f\left(\frac{u^* k}{\nu} , \frac{d}{k}\right) \qquad 3\text{-}04$$

or

$$\frac{\Delta p}{\tau_0} = f\left(\frac{u^* k}{\nu} , \frac{d}{k}\right) \qquad 3\text{-}05$$

In the fully rough flow region, viscosity is no longer important and the ratio of dynamic pressure to shear stress becomes a function of tube diameter to roughness size alone. Furthermore, if one tube is used along with constant roughness, d/k itself becomes a constant.

Hollingshead (1972) produced a graph of

$$\frac{\Delta p}{\tau_0} = f\left(\frac{\Delta p d^2}{4\rho\nu} , \frac{d}{ks}\right) \qquad 3\text{-}06$$

where ks is Nikuradse's equivalent sand grain roughness, using the equations of Patel and Nikuradse and his experimental measurements. This curve is shown in Fig 3-03.

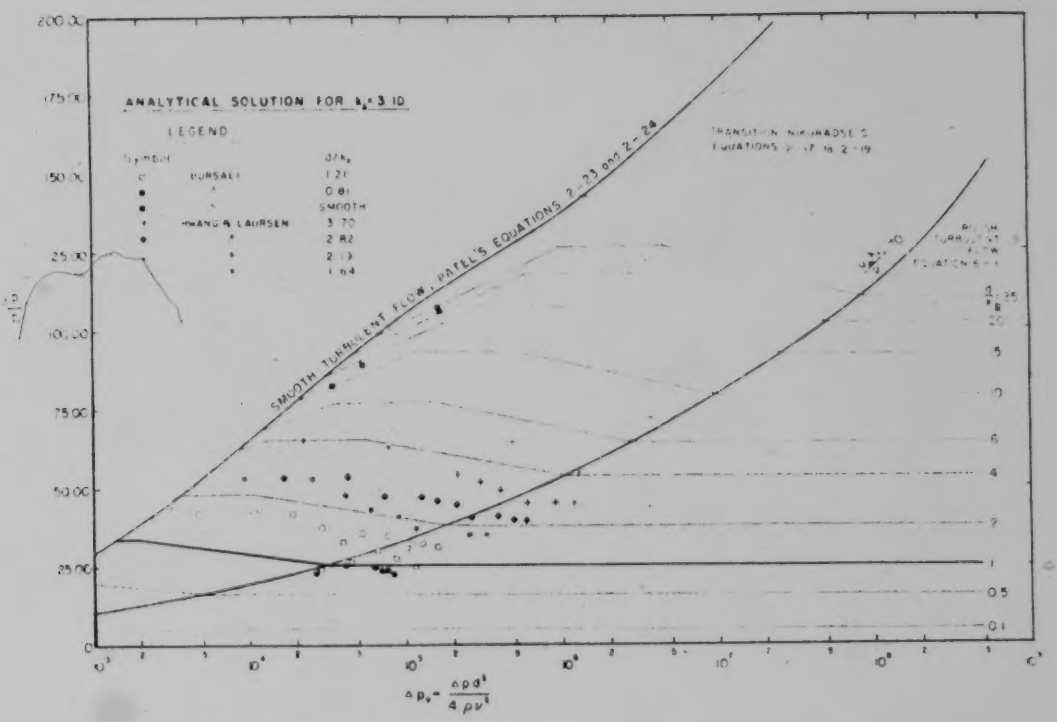
ANALYTICAL SOLUTION FOR $k_s = 3.10$
LEGEND
SMOOTH TURBULENT FLOW : PATEL'S EQUATIONS 2-23 and 2-24
TRANSITION NIKURADSE'S EQUATIONS 2-17 to 2-19
PURSALL
SMOOTH
HWANG & LAURSEN
$\Delta p_s = \frac{\Delta p d^2}{4 \rho \nu^2}$

PRESTON TUBE CALIBRATION ANALYTICAL SOLUTION
WITH OTHER EXPERIMENTAL DATA

FIG. 3-03 GRAPH FOR SHEAR STRESS PREDICTION.

The roughness used throughout the testing was a length of No. 36 aluminum oxide wet or dry cloth shown in Plate 3-01. It was placed on the bed of the flume at a sufficient distance upstream of the measurement area to insure a fully developed rough wall boundary layer. Hollingshead (1972) found that the grain size was 0.00183 feet which gave an equivalent roughness ks of 0.00607 feet. The curve used for shear stress prediction was the one for a d/ks value of 0.0067/0.00607 or approximately 1.

Hollingshead's graph gives a very complete treatment of shear stress determination in the smooth turbulent flow, transition and rough turbulent flow regions and provides a relatively simple method of finding the wall shear stress from easily measureable parameters. All shear stress points for this research lay on the constant part of the curve for fully developed rough turbulent flow.

Instrumentation

Data collection was by means of a system originally developed to study 3-dimensional flow around a cantilevered obstruction. It consisted of a control unit, traverse unit and logging and recording unit. The control unit was a microprocessor activated 3-D traverse positioner containing a computer program written in basic language. This program allowed various modes of operation from numerical point entry to coordinate editing to locating the bed of the flume at various measurement sections. All information entry was

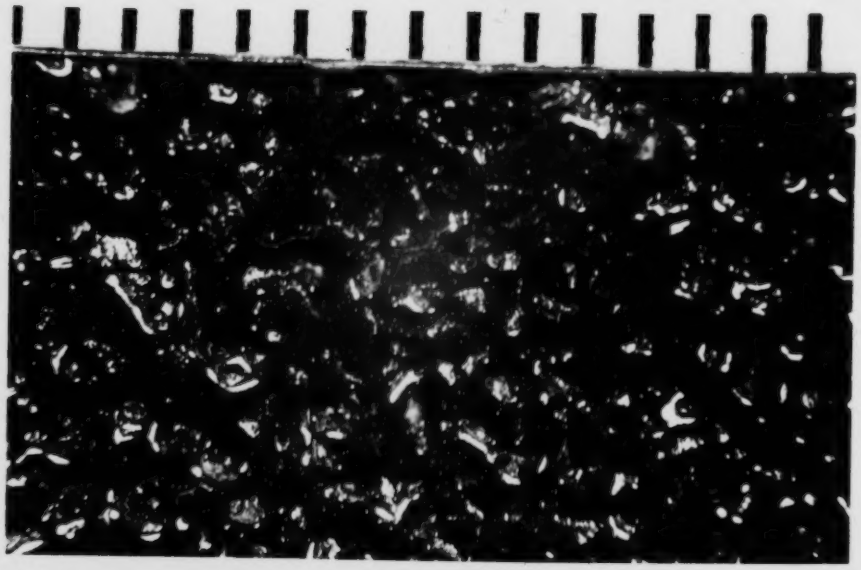

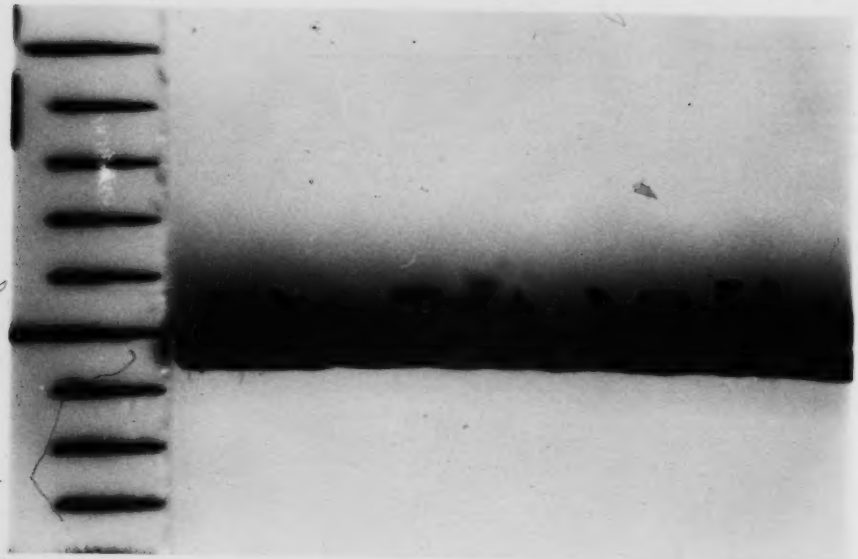

All divisions are in millimetres.

Plate 3-01. BED ROUGHNESS.

via a teletype and usually in the form of punched paper tape for hard copy storage.

A typical run necessitated firstly loading the relevant program depending on whether a lateral or vertical scan was to be performed, then entering the coordinates that the pitot tube was to visit. After entering the run command, the microprocessor would issue signals to a motorized traverse whose exact location was measured by potentiometers.

The traverse unit contains a carriage for the pitot tube mounted on stainless steel rods and using linear bearings for motion in the vertical and lateral directions. Potentiometers on the non-slip driving cables ensure exact location of the tube in all directions every time the measurements are repeated. In the downstream direction the traverse unit rides on three aluminum wheels and tracks on the top of the flume.

Once the pitot tube and traverse unit have been positioned at a particular co-ordinate a delay of approximately forty-five seconds ensues in order to give conditions in and around the pitot tube time to settle down.

The coordinates and transducer values are scanned by a Fluke 2240A datalogger with 60 channels entered. The first four channels read are the y, x, and z coordinates and a water level reading and the remaining 56 channels are repeated readings of the pressure transducer for the pitot tube with periodic readings of the water level in between.

The whole process of datalogging takes about 35 seconds

for each coordinate, so it can be seen that an averaged value of the transducer readings will yield a very accurate result. All 60 channels are recorded on a digital cassette for each coordinate and once the run is started, the traverse unit will keep moving from point to point, logging its data each time, till either the cassette is full or all coordinates have been visited.

The traverse and control equipment are illustrated in Plate 3-02. Once the cassette has been filled, it is transferred to a PDP/8 computer which has a program, again in basic, to reduce the 60 channels to one line of 6 readings. Those 6 readings are the y, x, and z coordinates, the water level, the transducer pressure, averaged from 50 readings, and the corresponding velocity at that point.

Once again a typical run consists of 12 sections downstream of the nozzle with usually 21 measured coordinates in either the vertical or horizontal direction, so altogether 454 points were visited for each run and a velocity measured at all of them.

All the data from the PDP/8 was then transferred to the main university system for subsequent plotting and further analysis.

Plate 3-02. Traverse and data aquisition system.

Experimental procedure and results

The practical work for this thesis was mainly composed of eight separate series of velocity distribution measurements. The first six experiments were performed with jet injection through a 0.25 inch nozzle and the last two through a nozzle of 0.75 inch diameter.

Various ratios of velocity between the jet and the surrounding channel flow were chosen to cover as broad a spectrum as possible and these are listed in Table 3-01. A suitable channel discharge was selected and with the flume width constant at 2.97 feet, a convenient depth was chosen. This depth was to be kept at 0.61 feet throughout the research as it was felt that this gave an adequate depth to nozzle size ratio so as not to cause any free surface effects on the jet.

The constant head tank was then adjusted to provide the chosen velocity ratio. The calculation of jet velocity was first taken as $\sqrt{2gh}$ where h is the difference in height between the water surface in the constant head tank and the free stream surface and g is the acceleration due to gravity. On measuring the actual velocity of flow from the nozzle with the pitot tube however, it was found to be considerably lower, due to the friction and fitting losses in the nozzle feed pipe. Therefore the actual velocity ratio was calculated using the measured velocity of the jet rather than the calculated value.

Sections at suitable distances downstream of the nozzle

Run no.	$\alpha (=U_0/U_1)$	d (in.)	y_0 (ft.)	U_0 (ft./s.)	U_1 (ft./s.)	B/d	y_0/d	M_0 (lbs.)	θ (ft.)	Re (nozzle)
1	12·62	0·25	0·61	9·82	0·778	142·6	29·3	0·0586	0·126	17 260
2	4·47	"	"	3·48	"	"	"	0·0062	0·041	6 119
3	2·21	"	"	1·72	"	"	"	0·00107	0·017	3 024
4	7·03	"	"	5·47	"	"	"	0·01697	0·068	9 617
5	19·89	"	"	6·92	0·348	"	"	0·0301	0·20	12 170
6	30·64	"	"	7·78	0·254	"	"	0·0390	0·315	13 680
7	3·54	0·75	"	3·25	0·916	47·52	9·76	0·0451	0·094	25 370
8	10·00	"	"	3·15	0·324	"	"	0·053	0·297	25 370

TABLE 3-01.

were chosen for velocity distribution measurement and these are shown in the graphs in Appendix B in an x/d form. The microprocessor deals not in absolute distances but rather in co-ordinates which translate into voltage measurements at the potentiometers located on the traverse lines. Thus the chosen distances were converted into their respective co-ordinates before entry into the computer. After selection of the points of velocity measurement, the next procedure was to locate the exact bed of the flume at these points. This is described in the section on instrumentation.

After a co-ordinate corresponding to the bed position was found, a choice had to be made of how many positions in the vertical direction were to be measured. For the first run a figure of 38 was chosen and the values of the co-ordinates that would be added to the bed value worked out. Because of the large velocity gradient in the lower region of the flow, the co-ordinates were naturally spaced more closely together near the bed.

After all values were selected, the run command was entered and the microprocessor took over. It first issued commands to move the traverse to the section closest to the nozzle and along its centreline, then dropped to the bed and after a suitable delay began scanning the data and recording it on cassette tape. On completion of measurement at the bed, it moved to another section above it and repeated the process. Because some of the vertical points of measurement were so close together, the movement of the pitot tube

carriage was in an up and down fashion enabling it to move and come to rest accurately at the proper location.

It was found that 38 points in the vertical direction were more than enough to obtain an accurate profile of velocity variation and this was subsequently reduced to 27 points and then again to 21 points.

Once the pitot tube had visited all vertical points at one section, it then moved downstream to the next one, while still remaining on the nozzle centreline and repeated the whole process. After 6 sections the cassette tape was usually full and had to be changed. The data on the tape was then analysed and reduced as described previously.

From this, the point of maximum velocity occurence could be easily found and this was the vertical position chosen for the lateral scan. The program in the microprocessor was modified slightly to scan in this new direction and suitable incremental co-ordinates were again chosen.

The lateral scan was started slightly to the left of centre, to check on symmetry of the jet as most measurements were confined to one side alone.

The procedure was repeated for the same 12 sections downstream of the nozzle and after all data had been collected it was known accurately how the jet decayed along the centreline of the nozzle and how it spread in the lateral direction.

Effect of depth alteration

Although the depth of flow was kept constant throughout the experiments two different depth to nozzle size ratios were investigated. It was decided that a study of the effect of flow depth alteration on the injected water would complete the research. Accordingly a standard velocity ratio of 10:1 was chosen for all tests and the depth was reduced step by step while photographs were taken for later comparison. When these photographs were studied together, it was noticed that little or no effect was exerted on the plume by the depth alteration. The actual reduction was from the usual depth of 0.61 ft. down to 0.22 ft. which corresponds to a depth to nozzle ratio of 3.25:1. At the lowest depth considerable rippling of the water about 1 ft. downstream of the nozzle was noticed indicating that the jet water had reached the surface. During the experiments conducted at the normal water depth the position where the jet water finally surfaced was not noticed till a large distance downstream. The scales layed on the bed of the flume indicated the lateral spread to be approximately the same for all depths. The depth to nozzle size ratio varied from about 10:1 down to 3:1. It is safe to say that there will be few installations where the above-mentioned ratio will approach or go below 10:1.

It should be mentioned, however, that this investigation was confined to a short distance downstream of the nozzle and with depth reduction the plume will naturally

reach the the water surface much sooner at some point downstream.

Analysis of experimental results.

Most analysis and reduction of the data was done on the main University computer. A listing of all co-ordinates and velocities for each point visited by the pitot tube was obtained and from this the maximum velocity (um) for each section was read, the height above the bed at which this occured was found and the surrounding velocity of flow calculated from averaging the last 6 or 7 readings near the surface. This average velocity was used in calculations rather than the one read from the orifice meter in case of any slight calibration errors in the transducer.

The co-ordinates first obtained from the datalogger were only voltages and so they had to be converted to a suitable length unit, in this case feet. Next the value of half the relative velocity was calculated and its point of occurence found by interpolation between two positions. Once this point was found the value of δ was subtracted from it and this then became the b value for length scale analysis.

This procedure was repeated for every downstream section and thus the four parameters used in the analysis, the maximum velocity um, the surrounding flow velocity U_1, the height of maximum velocity occurence δ and the distance to half the maximum velocity b, were obtained.

For the lateral spread the analysis was similar except

that the value of δ was not required and the average velocity used was the value of velocity measured at this height in the free stream.

All points were first plotted in dimensional form with velocity in ft/s vs. depth or width in feet. The plots from run no. 8 were selected as a typical example for illustration here. The rest of these plots are contained in Appendix B. Dimensional plots of the twelve vertical and lateral sections are shown in Figs. 3-04 to 3-07.

The variation of the length scales in the axial direction is now illustrated. Fig. 3-08 shows the growth of the boundary layer thickness and it can be seen that Runs 1 through 6, with the small nozzle all lie in approximately the same area while the values for the larger nozzle appear to decrease in the downstream direction. This is perhaps due to the nozzle being placed in a slightly downward attitude affecting the normal increase in boundary layer size.

Fig. 3-09 shows the growth of the vertical scale and this indicates the rise of the jet towards the surface in the downstream direction. As would be expected, the larger the velocity ratio the greater the jet growth.

Fig. 3-10 illustrates the transverse spread of the jet. This is shown to great effect in Plate 3-03 with photographs of the dyed jet being injected into the channel at velocity ratios varying from 2:1 to 30:1. The scales lying on the flume bed are in feet and tenths.

The flow area was divided into 3 regions for plotting

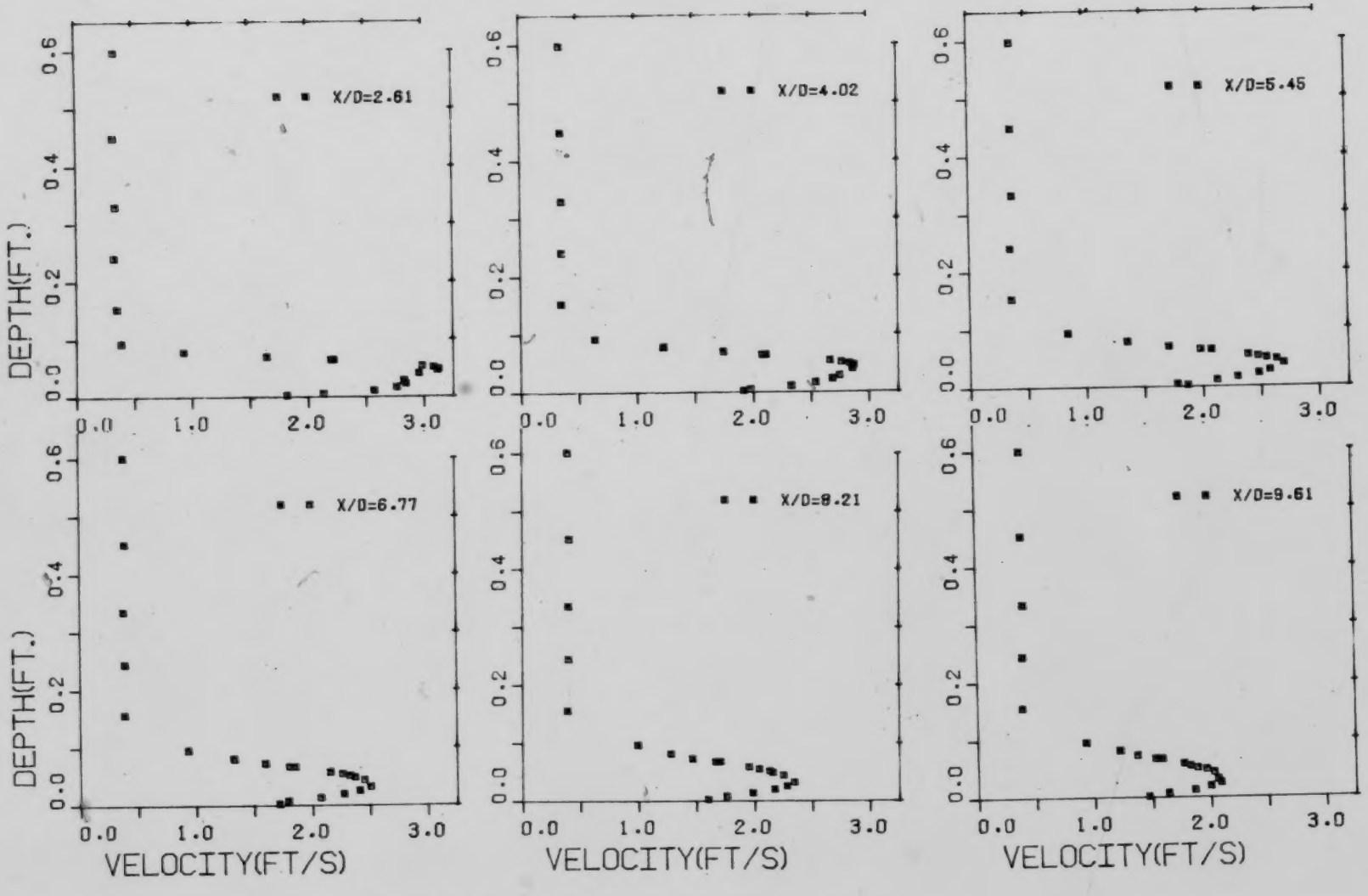

FIG. 3-04 EXPT. 8 ALPHA=10.0:1

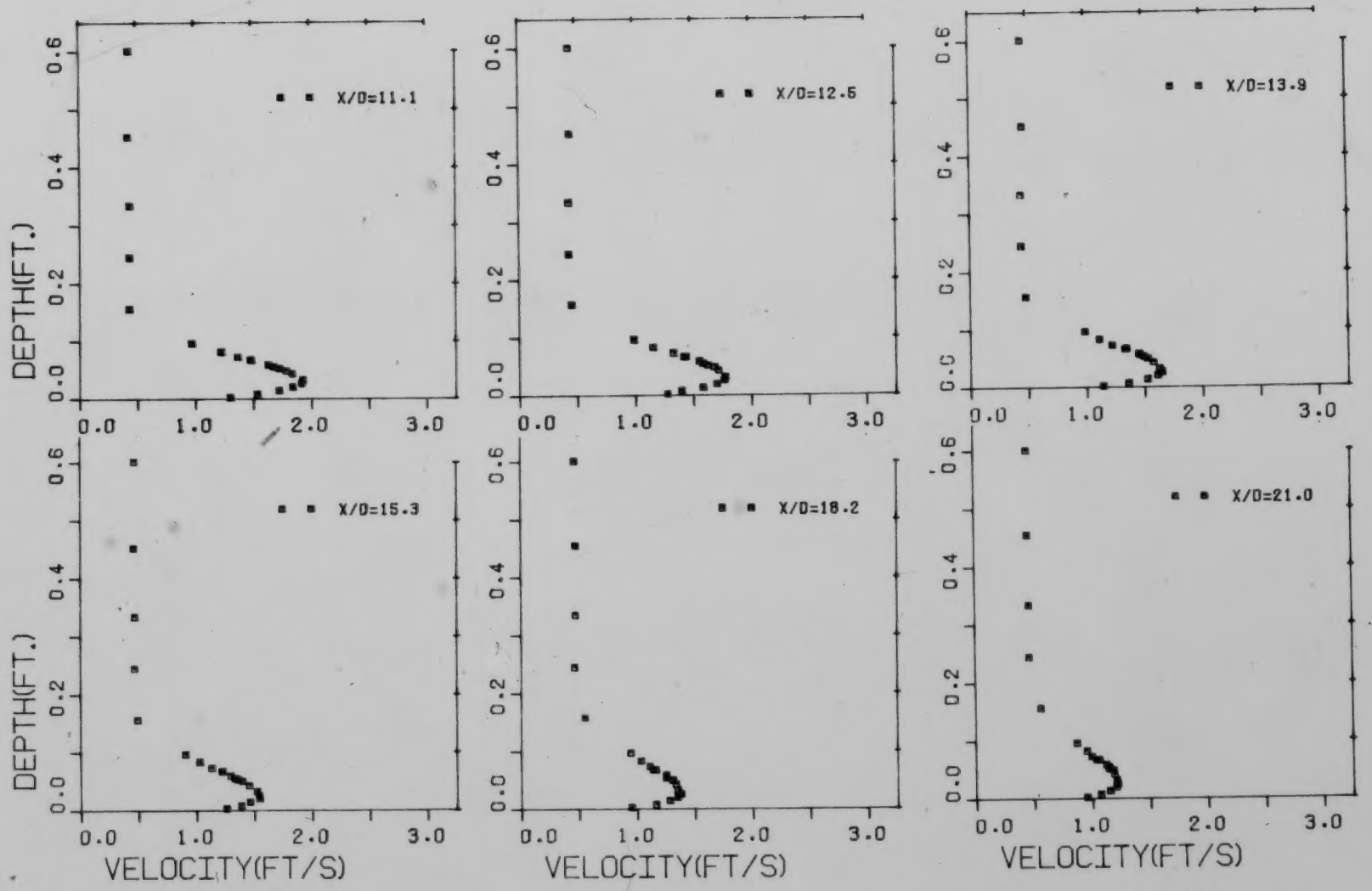

FIG. 3-05 EXPT. 8 ALPHA=10.0:1

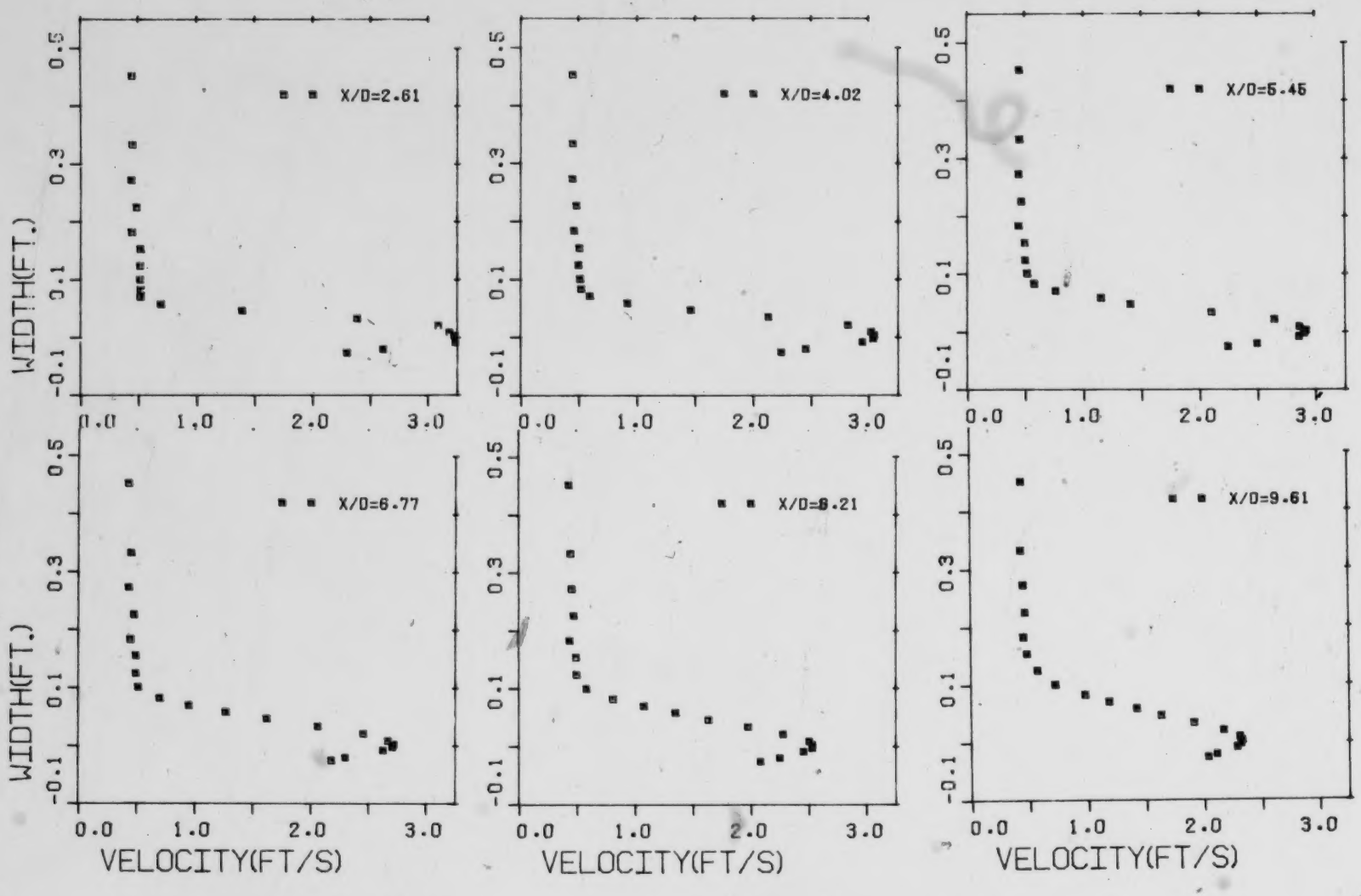

FIG. 3-06 EXPT. 8 ALPHA=10.0 :1

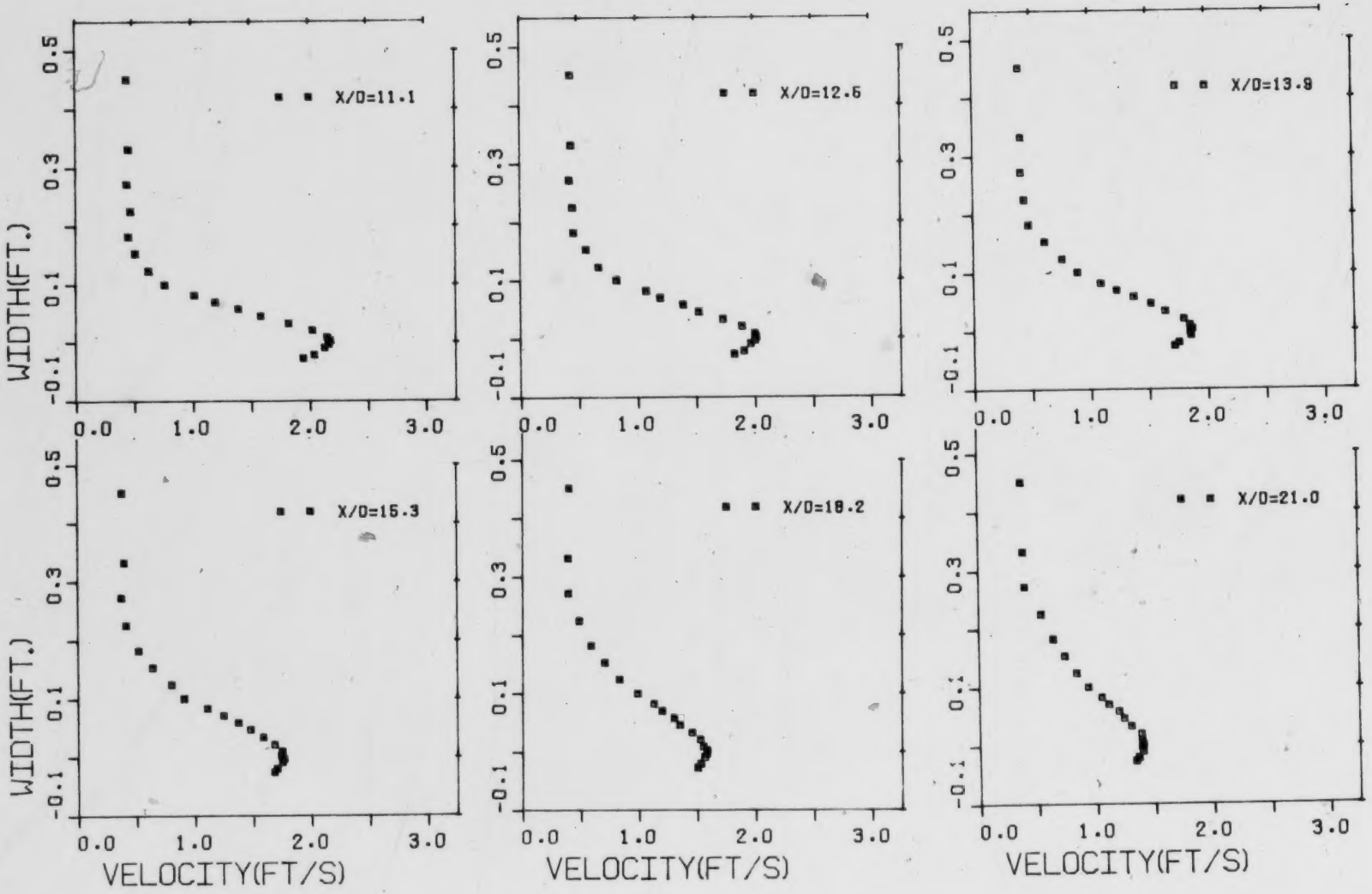

FIG. 3-07 EXPT. 8 ALPHA=10.0 :1

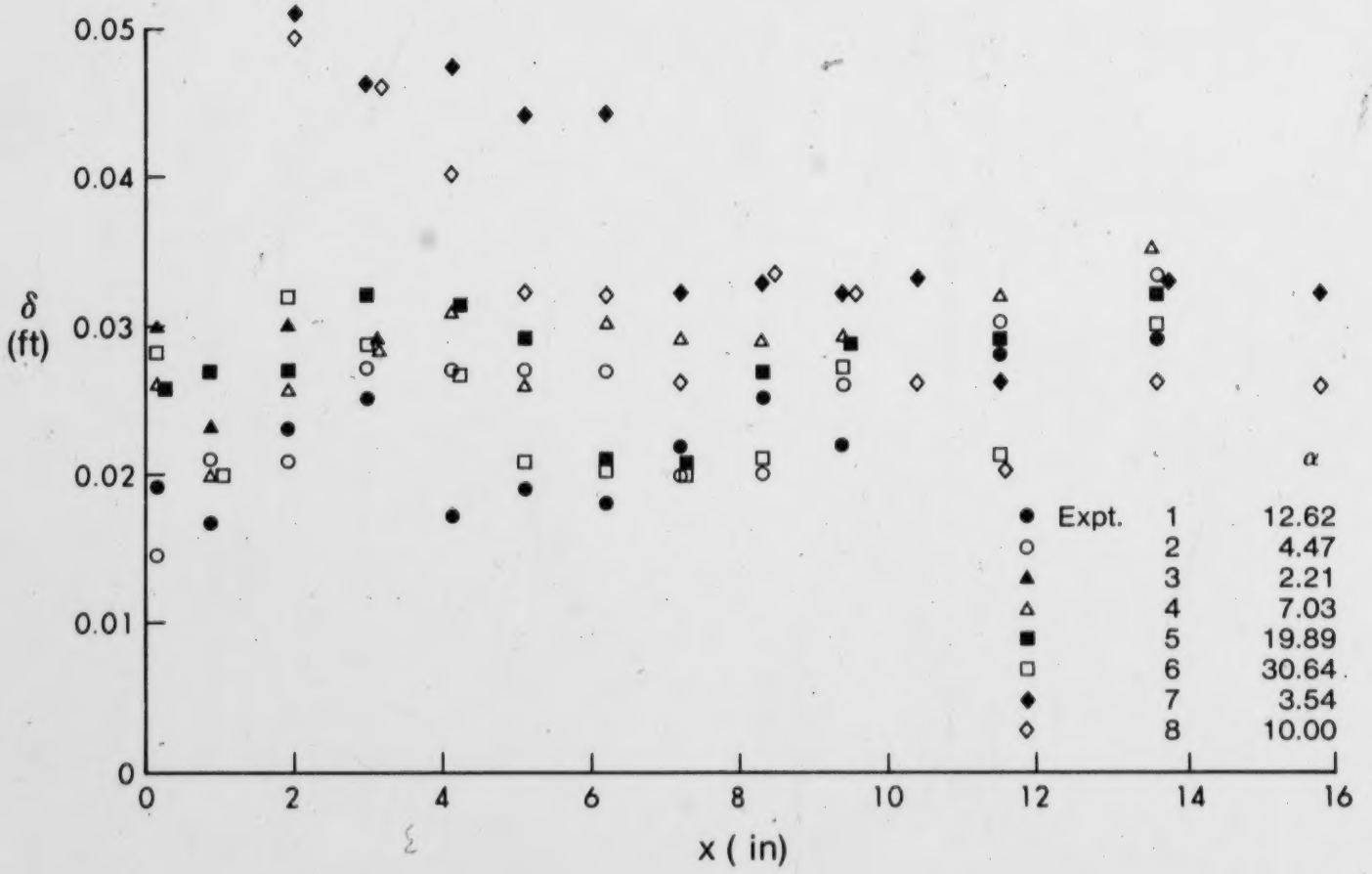

FIG. 3-08 Growth of boundary layer in the axial direction

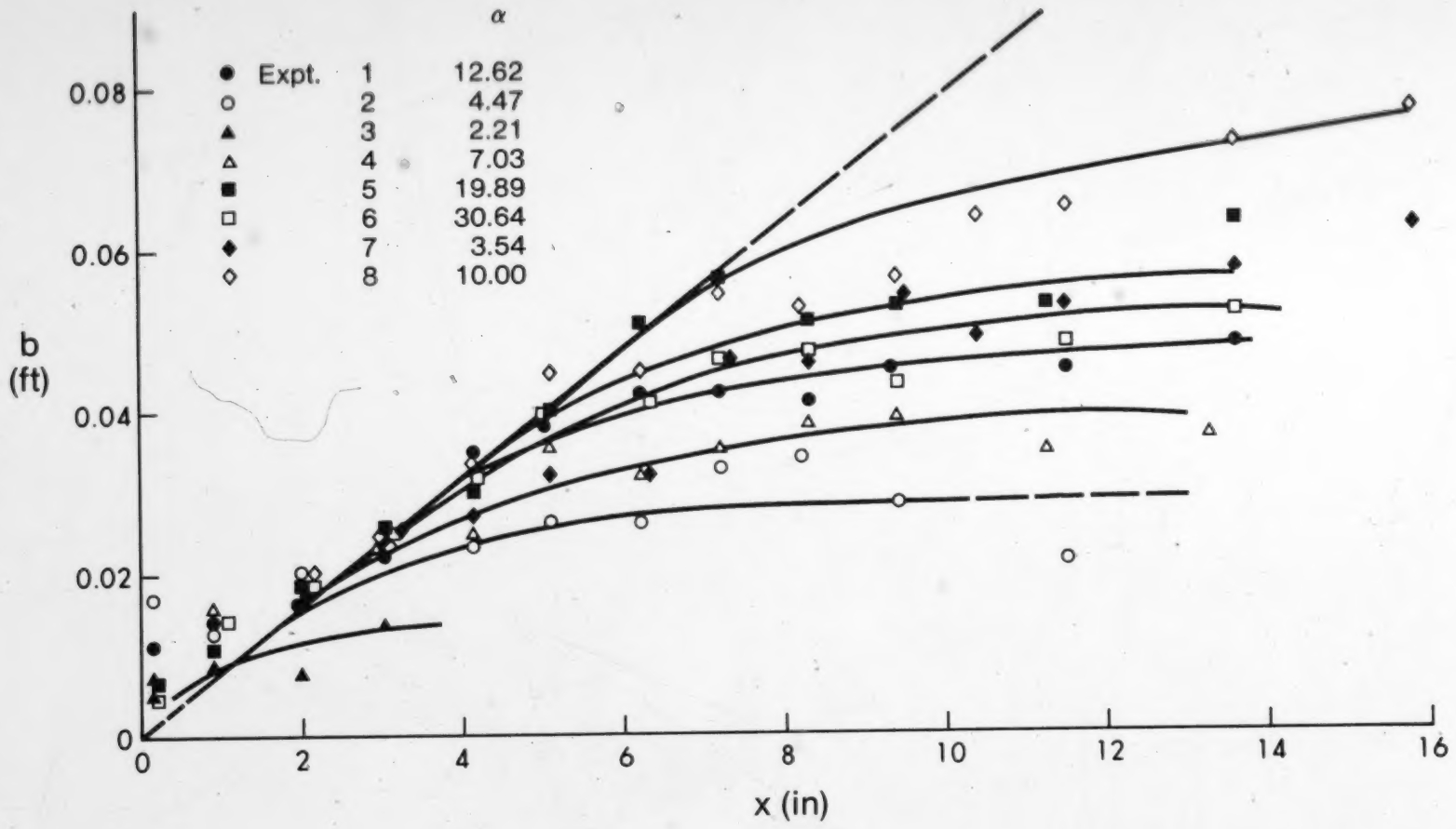

Figure 3-09 Growth of jet in the axial direction

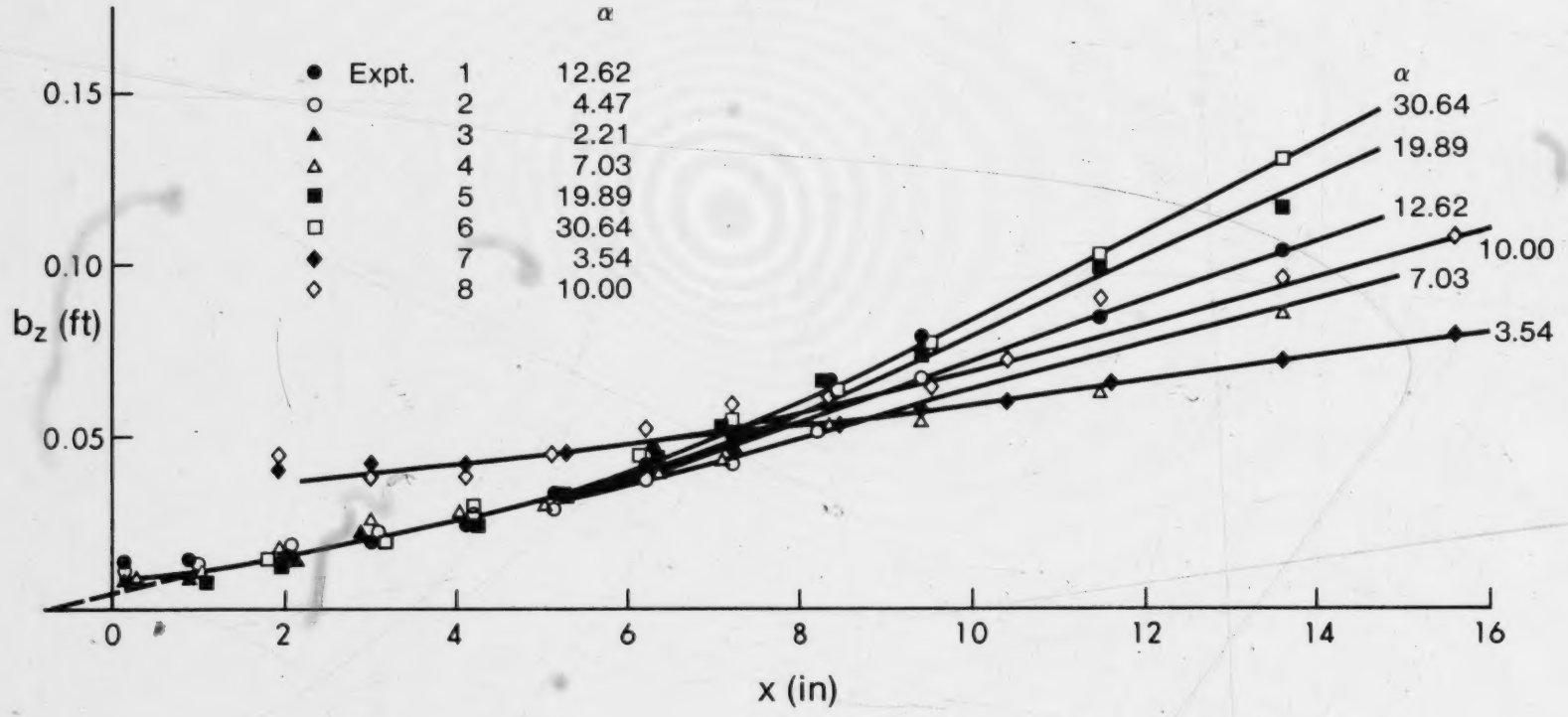

FIG. 3-10 Growth of transverse length scale in the axial direction

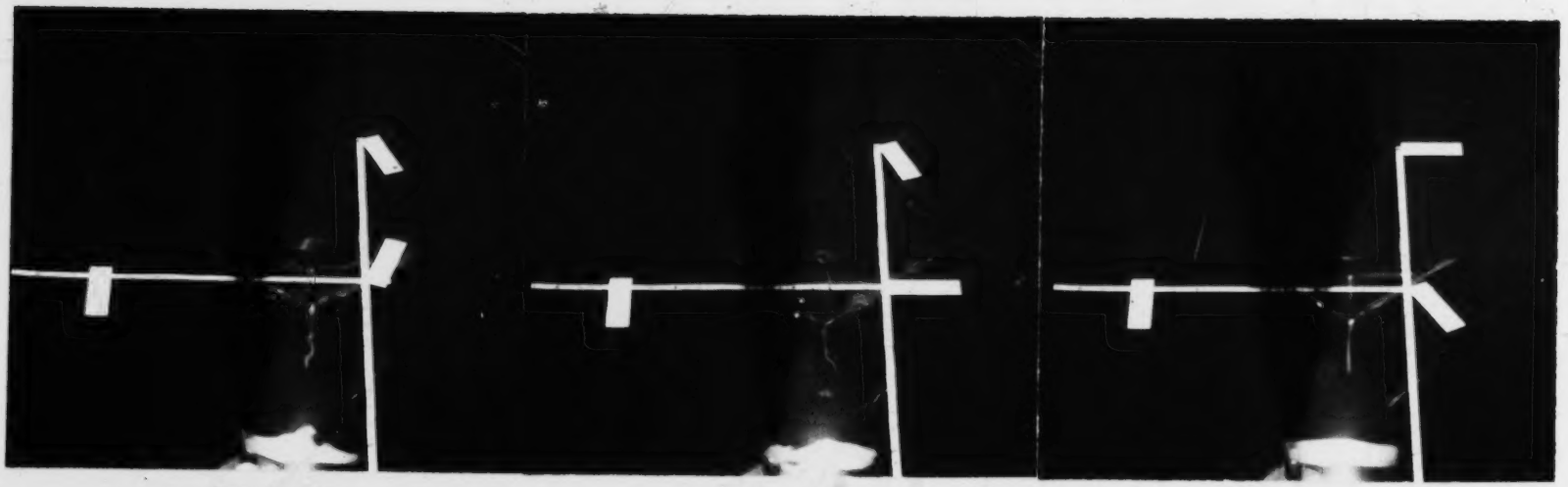

ALPHA = 2:1 ALPHA = 5:1 ALPHA = 10:1

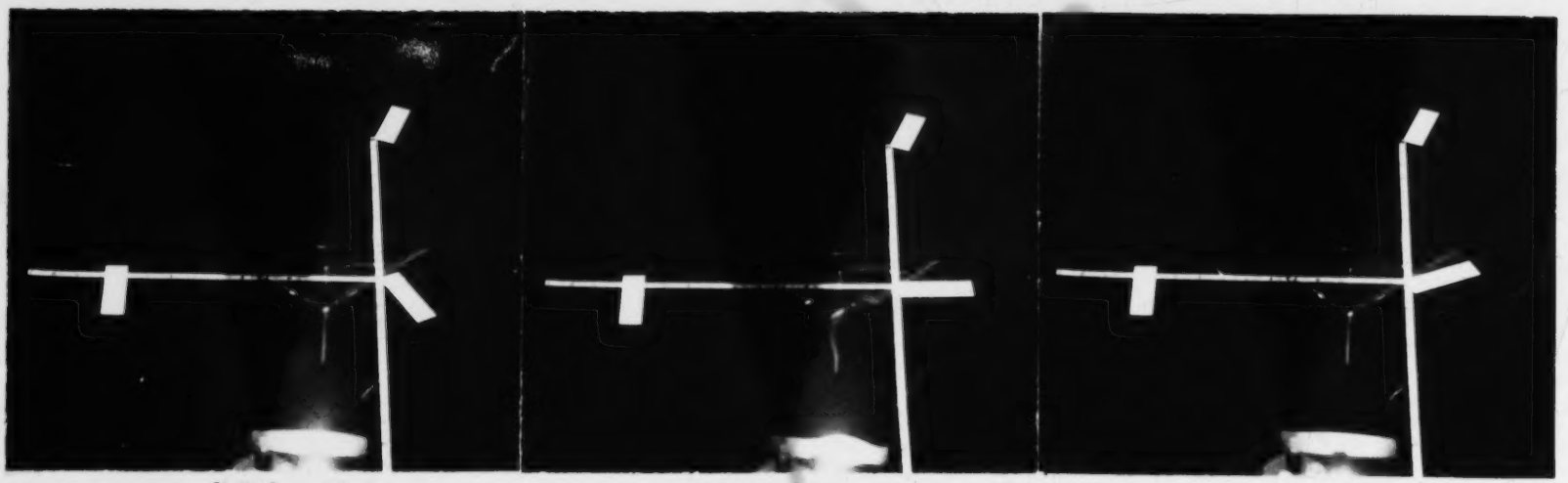

ALPHA = 15:1 ALPHA = 20:1 ALPHA = 34:1

Plate 3-03. Growth of jet for different velocity ratios.

the outer or free mixing region, the inner or boundary layer region and the transverse region. For the outer region a non-dimensional plot of $(y-\delta)/b$ vs. U/Um was produced, where the velocities are with respect to the free stream. Also plotted was the exponential curve and it was found that very close agreement exists between the data from this research and this curve. All data in the boundary layer and more than a $(y-\delta)/b$ value of about 3 was ignored in this plot which is shown in Fig. 3-11.

In the boundary layer y/δ was plotted against u/um where in this case the velocities are absolute. The data is found to lie within a power law envelope as described earlier and shown in Fig. 3-12.

In the case of Runs 1 through 6 the first two sections downstream of the nozzle were not included as these lay within the potential core region. When plotted up along with the other sections they displayed considerable inconsistency as the jet was not developed. In the runs of lower velocity ratio the jet effects had diminished a short distance downstream and some of the further sections were omitted.

The velocity variation in the lateral direction although different from that in the upper region can again be described by an exponential curve at each section. The lateral spread from the data of Run 8 is shown in Fig. 3-13. The remainder of these plots for the other velocity ratios appear in Appendix B also.

The scales used in non-dimensionalising the previous

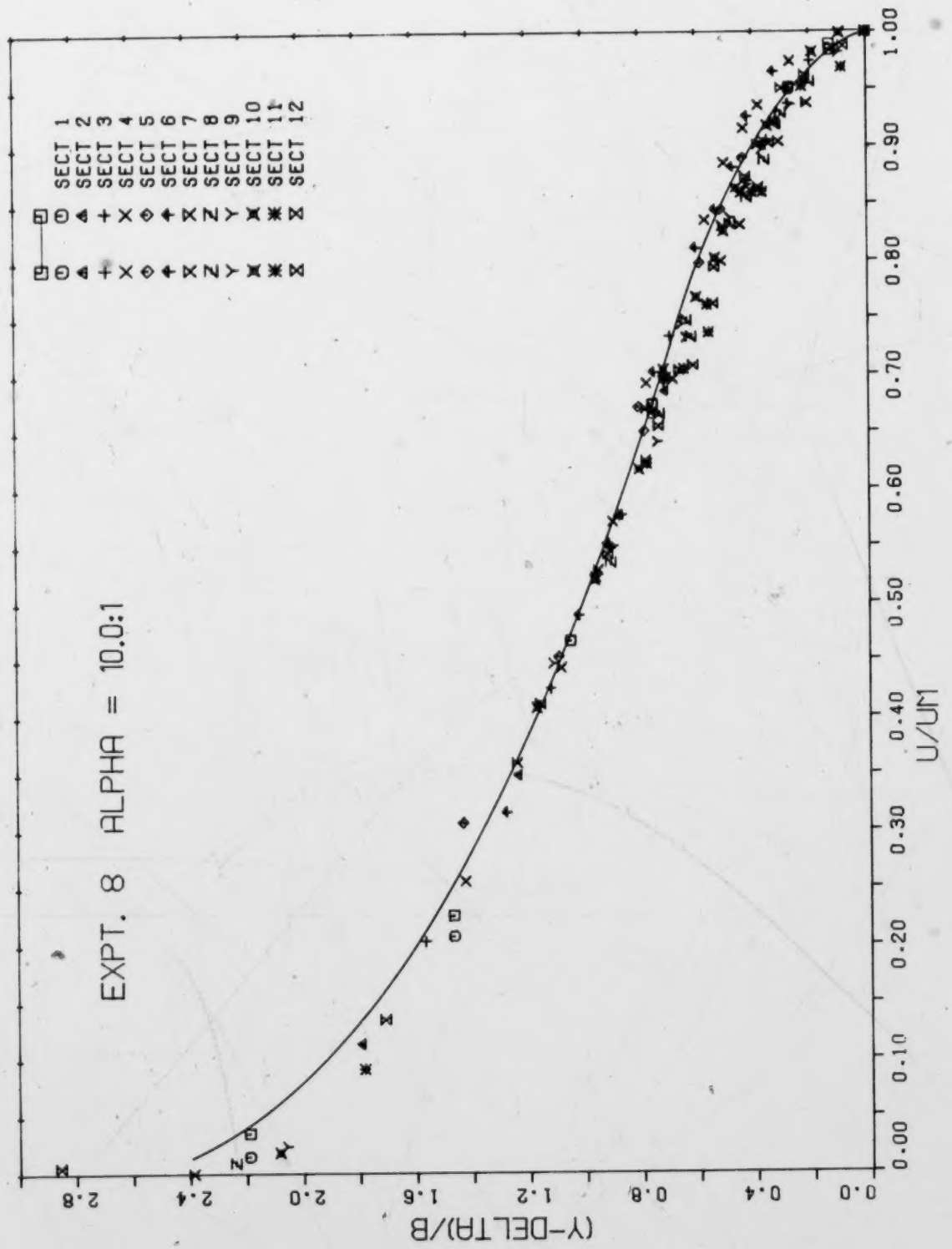
EXPT. 8 ALPHA = 10.0:1
SECT 1
SECT 2
SECT 3
SECT 4
SECT 5
SECT 6
SECT 7
SECT 8
SECT 9
SECT 10
SECT 11
SECT 12
(Y-DELTA)/B
U/UM
0.0
0.4
0.8
1.2
1.6
2.0
2.4
2.8
0.00
0.10
0.20
0.30
0.40
0.50
0.60
0.70
0.80
0.90
1.00

FIG. 3-11

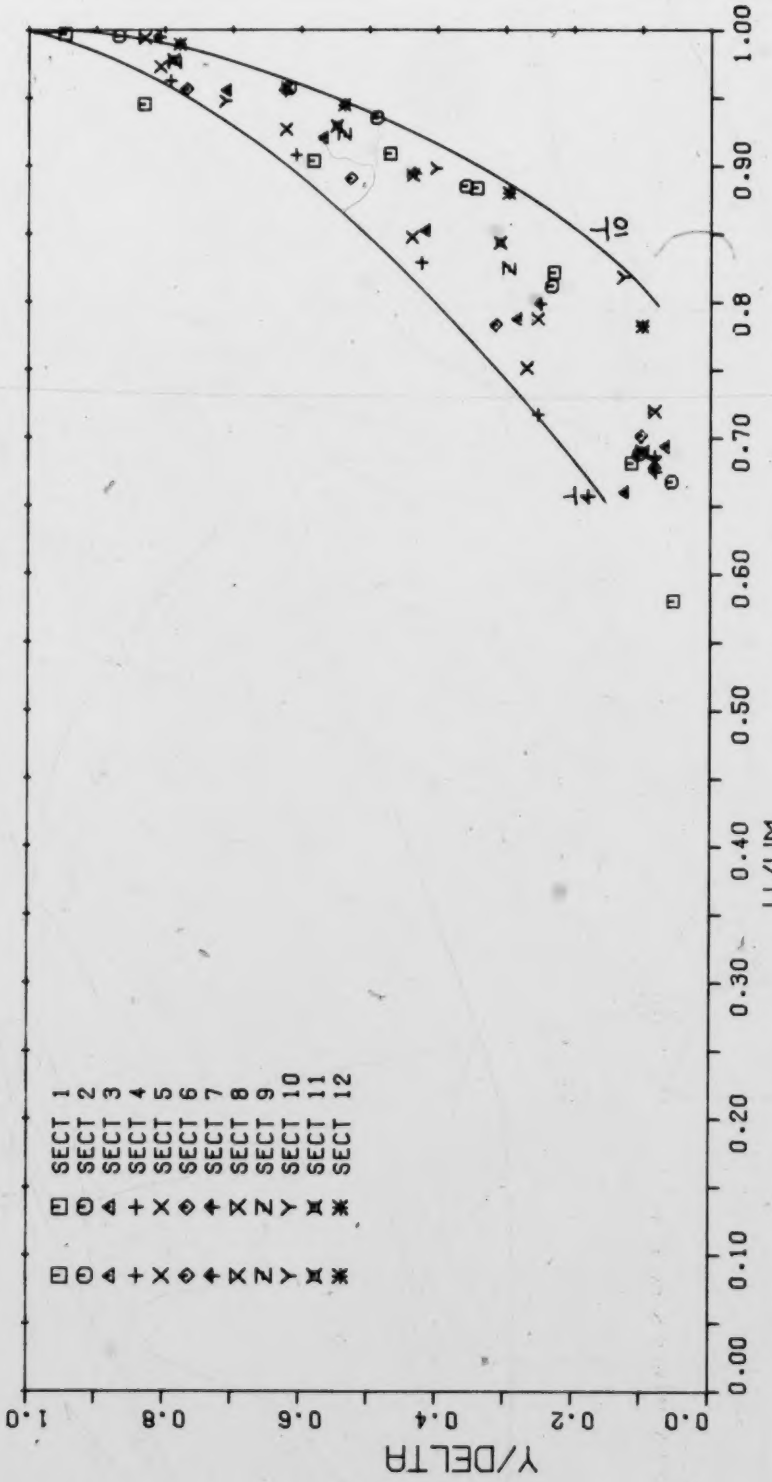
SECT 1
SECT 2
SECT 3
SECT 4
SECT 5
SECT 6
SECT 7
SECT 8
SECT 9
SECT 10
SECT 11
SECT 12
0.0
0.2
0.4
0.6
0.8
1.0
Y/DELTA
0.00
0.10
0.20
0.30
0.40
0.50
0.60
0.70
0.8
0.90
1.00
U/UM
EXPT. 8 ALPHA = 10.0:1

FIG. 3-12

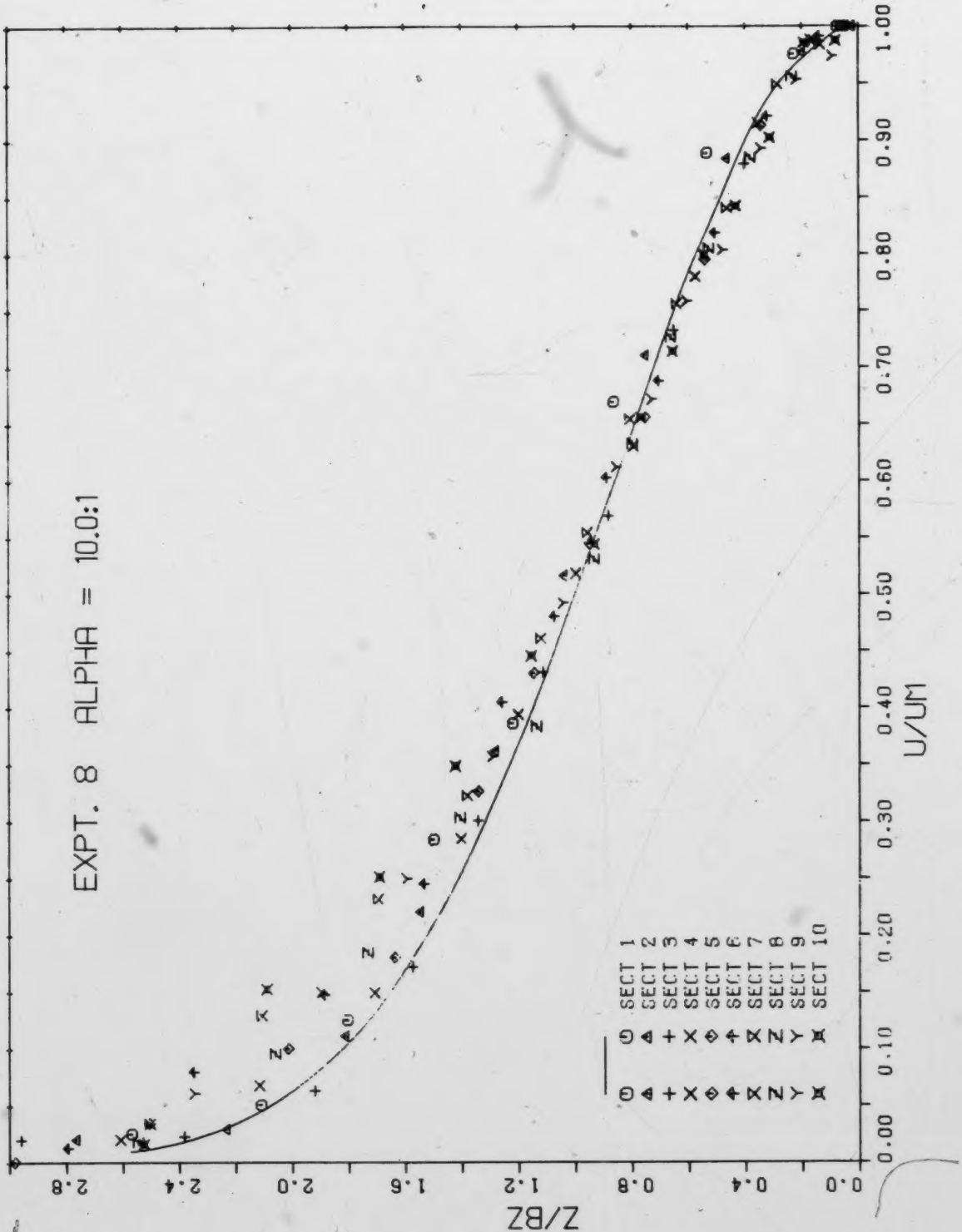
EXPT. 8 ALPHA = 10.0:1
U/UM
Z/BZ
0.00
0.10
0.20
0.30
0.40
0.50
0.60
0.70
0.80
0.90
1.00
0.0
0.4
0.8
1.2
1.6
2.0
2.4
2.8
SECT 1
SECT 2
SECT 3
SECT 4
SECT 5
SECT 6
SECT 7
SECT 8
SECT 9
SECT 10

FIG. 3-13

plots were then analysed along with other terms such as the momentum thickness θ, the shear velocity U* and the bed shear stress τ_0.

Shown in Fig. 3-14 is the non-dimensional variation of maximum centreline velocity Um in the x-direction. The momentum thickness term θ is used as the axial length scale and this then takes into account any large momentum effluxes so that data from large or small velocity ratios will plot along the same line. It can be seen that agreement is good in the lower areas and ignoring the data of Run 3, a mean line can be drawn. The results of Run 3 have caused problems before due to the very low velocity ratio and the difficulty of detecting any velocity variation far from the nozzle. It is therefore safe to say that the jet effects in this run have dissappeared a short distance downstream of the nozzle and it is valid to ignore points further away. The other two curves shown on this graph are the results of Rajaratnam for similar analysis applied to plane wall jets and circular jets, both in co-flowing channels. The agreement is good up to an x/θ value of about seven and after that the effect of the wall becomes significant and the maximum velocity Um decreases much more quickly.

Fig. 3-15 shows the variation of bed shear stress τ_0 in the axial direction. Some of the measurements were made very close to the nozzle before the jet had time to properly establish itself on the bed against the wake effects of the nozzle body and this is the reason for the low shear stress

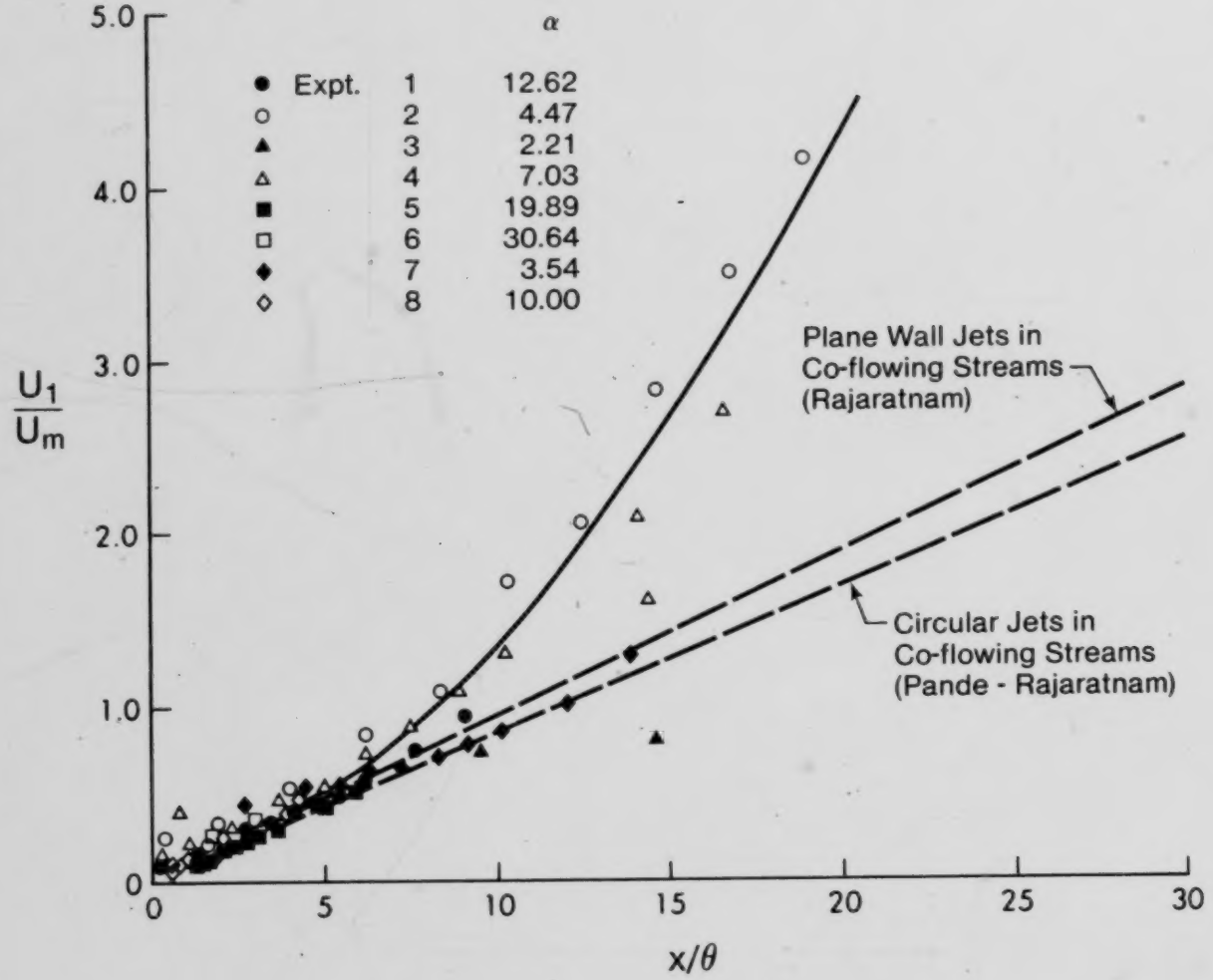

FIG. 3-14 Prediction of velocity scale at a downstream centreline section

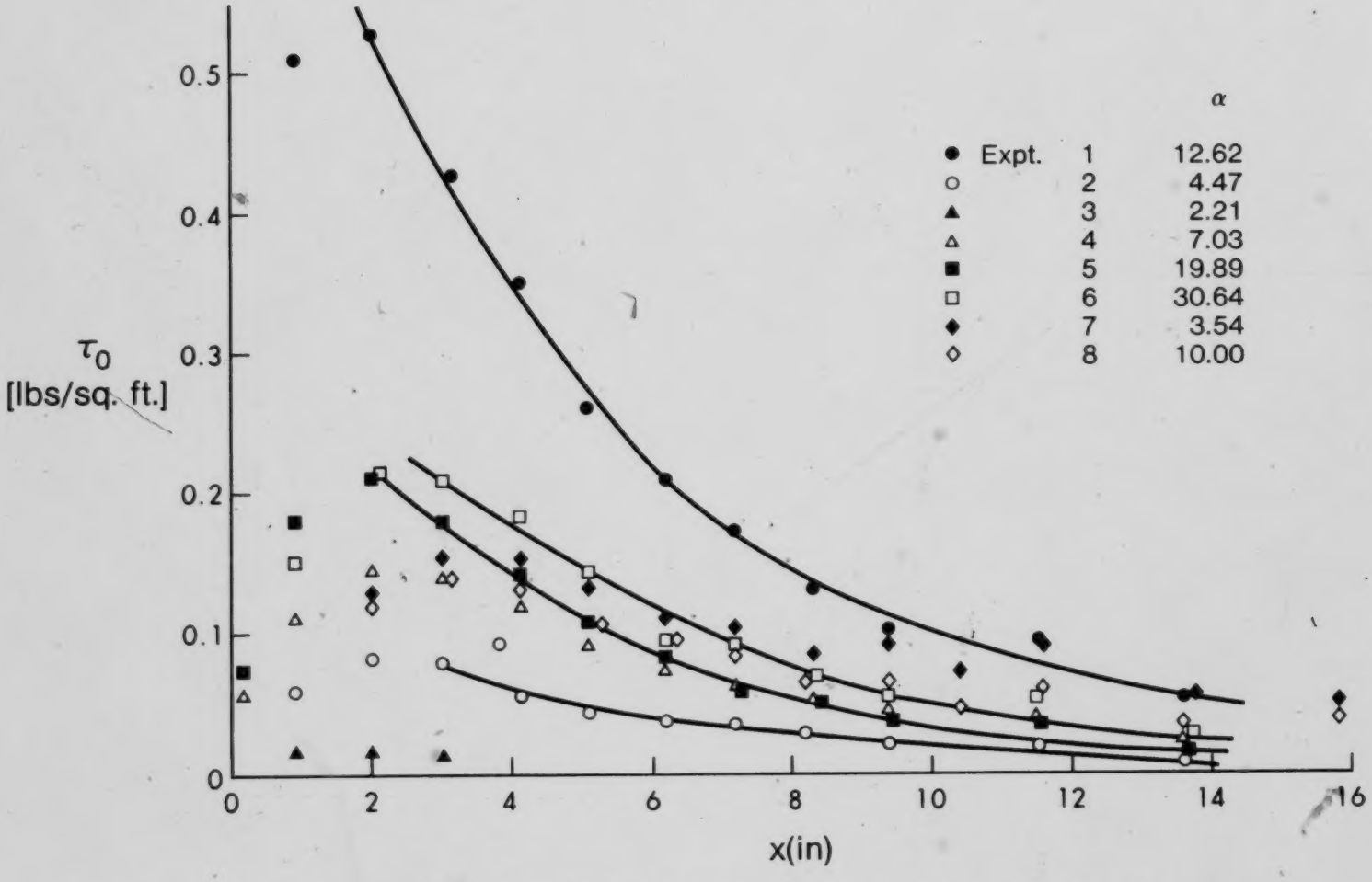

FIG. 3-15 Variation of bed shear stress in the axial direction

values near the nozzle.

Figs. 3-16 and 3-17 show the non-dimensional variation of the vertical and lateral length scales. It can be seen that the lateral scale grows significantly more slowly than its counterpart in a stagnant receiving environment. This is to be expected as the flow in the channel past the nozzle restricts its growth.

Fig. 3-18 describes the variation of shear velocity U* in the axial direction. Good agreement is found between the data for all runs but there is a significant difference between this curve and that for plane wall jets in co-flowing streams.

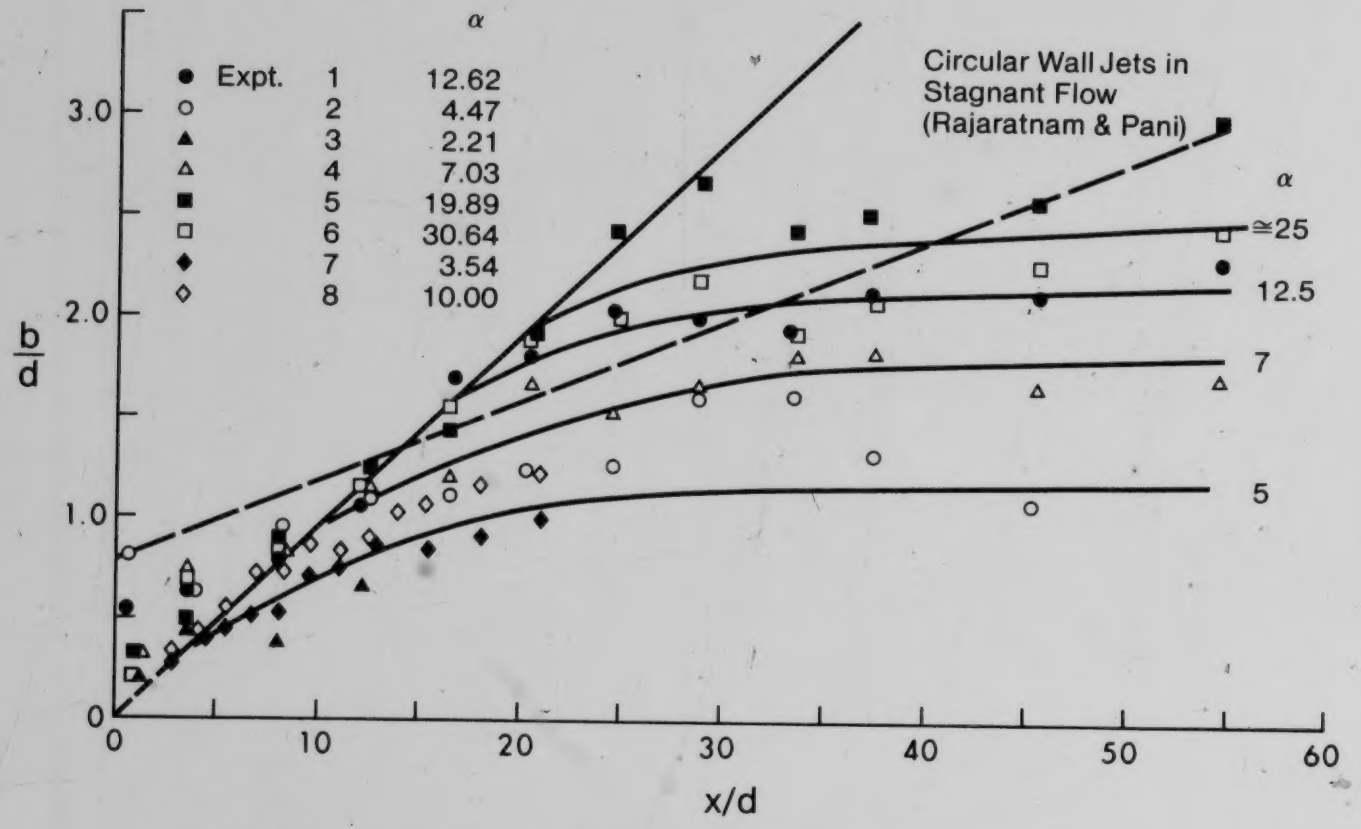

FIG. 3-16 Prediction of growth in the vertical direction

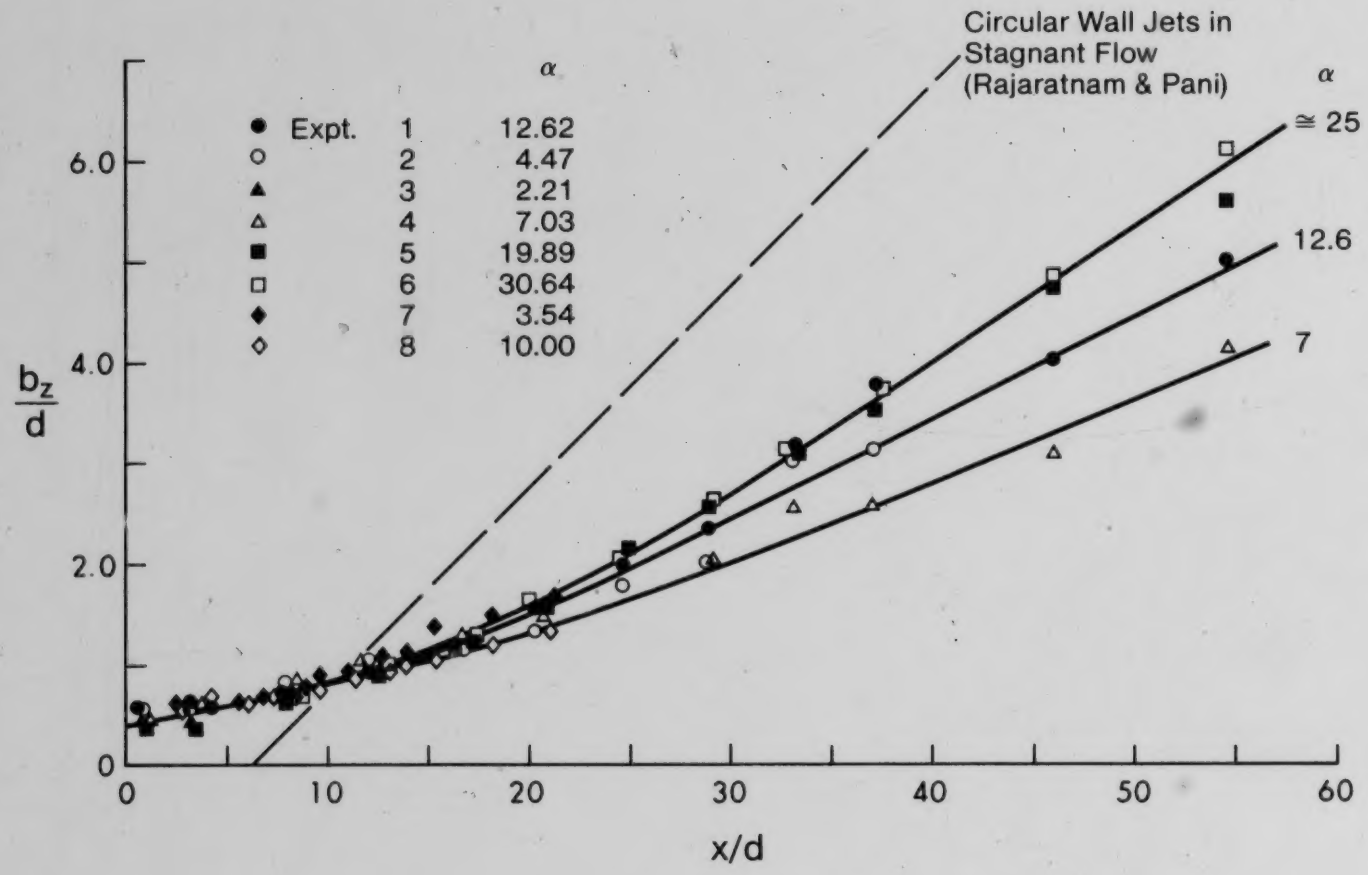

FIG. 3-17 Prediction of growth in the lateral direction

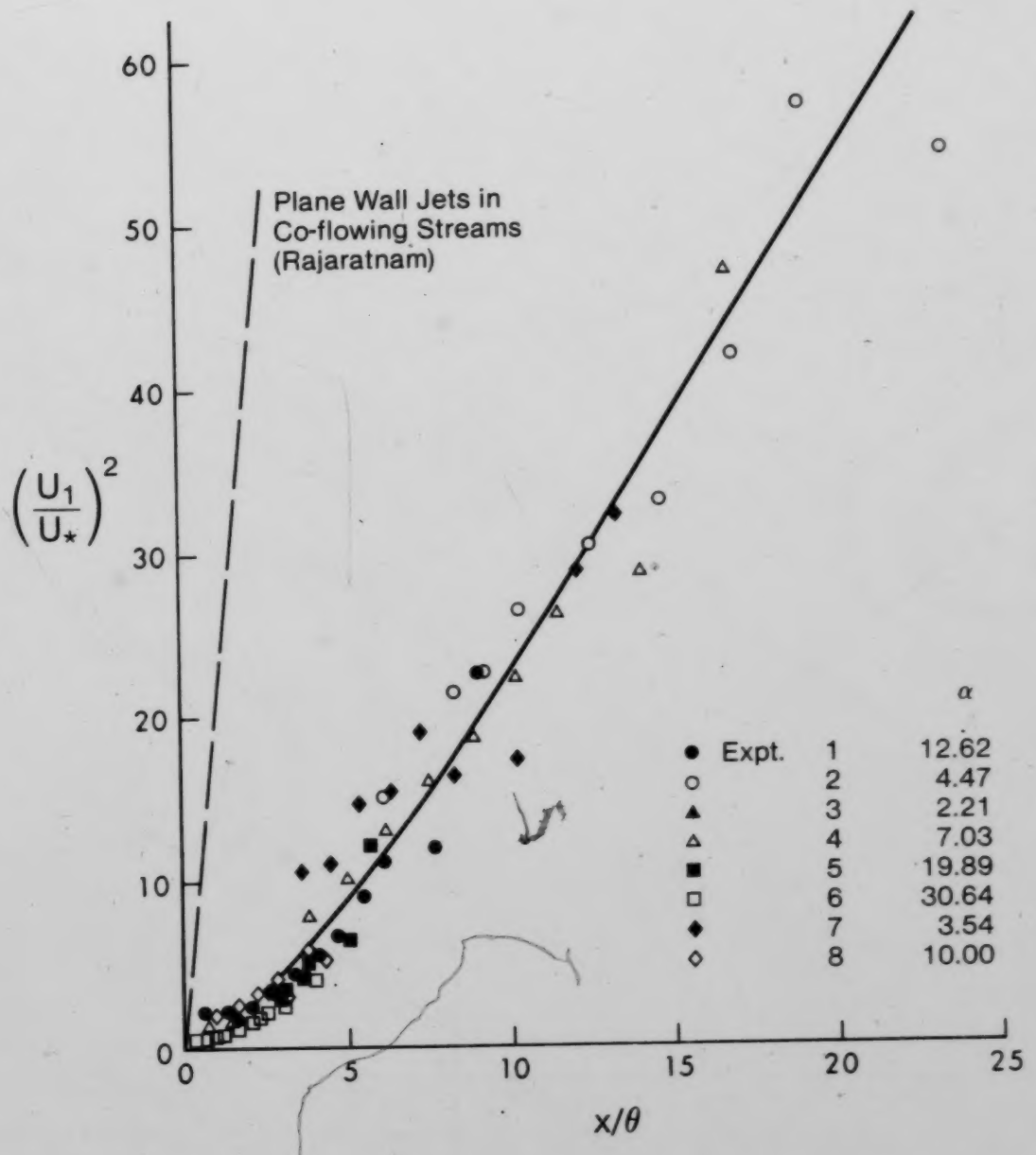

Prediction of shear velocity at a downstream centreline section

FIG. 3-18

IV. Conclusions and Recommendations

In this research, consideration has been made of its application to practical cases of effluent disposal in river environments. The case of one isolated diffuser nozzle is unlikely to be encountered for reasons explained earlier and, as previously shown, a common disposal technique is to use a series of identical nozzles with equal discharges flowing from each. Thus it can be seen that the situation investigated in this work will only exist for a short distance downstream of the nozzle before interaction with adjacent diffuser flows occurs.

The point of occurence of this overlap may be predicted from the graph of transverse length scale growth for a particular velocity ratio and the designer may then choose how far apart to space the injection nozzles such that he gets a sufficient reduction of concentration by the time overlapping occurs.

From then on the jet could be considered to act approximately as if it had been emitted from a long narrow slot, although exact interaction of this type has not been previously investigated.

The results gathered from this research and the analysis applied to them has shown that, as has been previously found for other jet types, all sections downstream of a jet have velocity profiles in the lateral and free mixing regions that are similar. These profiles can

be adequately described by an exponential relation given in Chapter 2.

This research has been restricted to the measurement of velocity profiles in the vertical direction along the centreline and in one lateral plane at the point of maximum velocity occurence. So the actual area of investigation, compared to the total size of the jet, is small. However Pani (1972), after studying 4 lateral sections at various heights above the bed, showed that all these profiles, no matter whereabouts in the outer region they are measured, can again be described by the exponential relation. Thus any point in the jet can be selected and its velocity predicted using this relation and knowing the centreline velocity from the vertical profile corresponding to its particular height above the bed.

It has also been shown that the concentration variation downstream of a pollutant injection is of the same form as the velocity variation, both spread and decay being corresponding functions of the distance downstream.

The justification for the scales used in producing non-dimensional profiles has been shown theoretically and the graphs produced using these scales have displayed good agreement with previous research.

As was seen from the graph of vertical jet growth a levelling out occurs indicating that after a certain point the jet and main channel flow have become one inhibiting it's further expansion. This was also noticed on comparison

of a series of photographs showing lateral spread. However, in this case, it was felt that the side walls of the flume were causing a certain amount of constriction to growth. It seems reasonable that after a certain time all the excess momentum of the jet will have diminished to zero and from then the only diffusion that will take place will be because of the ambient turbulence in the river.

The graph of lateral spread shows no indication of levelling off but it only covers a range of sixty diameters downstream whereas the aforementioned effects took place at least one hundred diameters away from the nozzle.

The actual amount of upward spread of a pollutant will depend greatly on the circumstances of its disposal. In most river situations the effluent will be somewhat warmer (and therefore less dense) but it will also contain a certain amount of dissolved and suspended solids.

One area of further research would be an investigation into the effects of buoyancy in the jet, due to either heat in the water or perhaps having the jet inject into a salt water environment. It would be anticipated that the vertical spreading would be significantly larger, however it is doubtful if the lateral spread would be much different.

An area that is not well suited to this type of data collection is the case of a jet that enters the surrounding channel flow with approximately the same velocity. Due to the nature of the apparatus it functions best when large velocity variations have to be detected. This means that it

is most suited to large velocity ratios.

It was noticed in Run no. 3 (alpha=2.21) that the jet effects diminished within such a short distance from the potential core that the data was for some purposes unusuable. Because of the boundary-layer shape of the background flow it was impossible to classify it as an infinite medium flowing past with a constant average velocity. The boundary-layer shape meant that the maximum velocity in some cases occured near the surface, rather than in the jet.

When water is injected at a ratio of between 1 and 2 its effects will diminish in such a short distance that diffusion by channel turbulence must be considered. It was proposed to investigate some spreads for a ratio of close to 1 using salt injection and a conductivity probe however time and other considerations precluded this.

The presence of river curvature would be another important factor and an investigation into the growth of jets in curved channels would reveal just how much effect a river bend would have in restricting or enhancing dilution of a pollutant.

The results gathered in this research agree very closely with the predictions made by previous observers on the variation of the jet as it as it gets further away from its point of injection. The prediction of velocity distributions downstream of uniform circular wall jets and, as shown by Pani (1972), regular bluff wall jets, in

co-flowing channels of large depth and width to nozzle size ratio can now be made accurately. From this a suitable value of pollutant concentration can be calculated that will enable the effectiveness of any similarily shaped effluent disposal system to be determined without resorting to expensive physical model studies.

List of References

Clay, C. H. and R. M. Gordon, "Experience with Industrial Effluent outfalls on the Pacific coast of Canada". I. A. H. R. 11th. International Congress, Vol. 2, Leningrad 1965.

Grace, R. A., "Marine Outfall Systems", Prentice-Hall, Toronto, 1978.

Hinze, J. O. and B. G. van der H. Zijnen, "Transfer of heat and matter in the Turbulent mixing zone of an axially symmetrical jet.", J. of Applied Scientific Research, A-1, 1949, pp. 435-461.

Hollingshead, A. B., "Boundary Shear Distribution in Open Channel Flow", Ph. D. Thesis, Deptartment of Civil Engineering, University of Alberta, Edmonton, Canada, 1972.

Hsu, E. Y., "The measurement of local turbulent skin friction by means of surface pitot tubes", David W. Taylor Model Basin Report, No. 951, August 1955.

Hwang, L. S. and E. M. Laursen, "Shear measurement technique for rough surfaces", J. of the Hydraulics Division, Proc. A.S.C.E., March 1963.

Nwachukwu, B. A., R. G. Gitzel and A. W. Peterson, "An application of microcomputers in the control, measurement and analysis of hydraulic testing.", Department of Civil Engineering, University of Alberta, Edmonton, Canada, 1978.

Patel, V. C., "Calibration of the Preston tube and limitations on its use in pressure gradients", J. of Fluid Mechanics, Vol. 23, 1965, pp. 185-208.

Preston, J. H., "The determination of turbulent skin friction by means of Pitot tubes", J. of the Royal Aero. Society, London, England. Vol. 58, Feb. 1954, pp. 109-208.

Rajaratnam, N., "Turbulent Jets", Elsevier Scientific Publishing Co., Amsterdam, 1976.

Rawn, A. M., F. R. Bowerman and N. H. Brooks, "Diffusers for disposal of sewage in sea water", J. of the Sanitary Engineering Division, A.S.C.E. March 1960, pp. 65-105.

Schlichting, H., "Boundary Layer Theory", McGraw-Hill, New York, 1960.

Appendix A.

List of symbols.

List of symbols

b	Length from position of maximum velocity to position of half the maximum velocity.
B	Channel width.
C	Concentration of a pollutant at any point downstream of its injection.
Cm	Maximum concentration of the pollutant.
d	Nozzle diameter.
k	Size of bed roughness projections.
ks	Nikuradse's equivalent sand grain roughness.
M_0	Excess momentum of the jet.
P	Total pressure recorded by the pitot tube.
P_0	Static pressure at the wall.
Re	Nozzle Reynolds number.
u	Absolute velocity at any point.
um	Absolute maximum velocity at any centreline section.
U	Velocity relative to the channel at any point.
Um	Relative maximum velocity at any section.
U_0	Initial velocity of the jet.
U_1	Average channel velocity.
x	Downstream or axial direction.
y	Direction perpendicular to the wall.
z	Transverse or lateral direction.

List of symbols(cont.)

α	Ratio of jet velocity to average channel velocity.
δ	Height from the wall to the point of maximum velocity occurence.
η	Dimensionless distance from the centreline of the jet.
ν	Kinematic viscosity of a fluid.
ρ	Fluid density.
θ	Momentum thickness.
τ	Shear stress.
τ_0	Shear stress at the wall.

Appendix B.

Results from Runs 1 to 7.

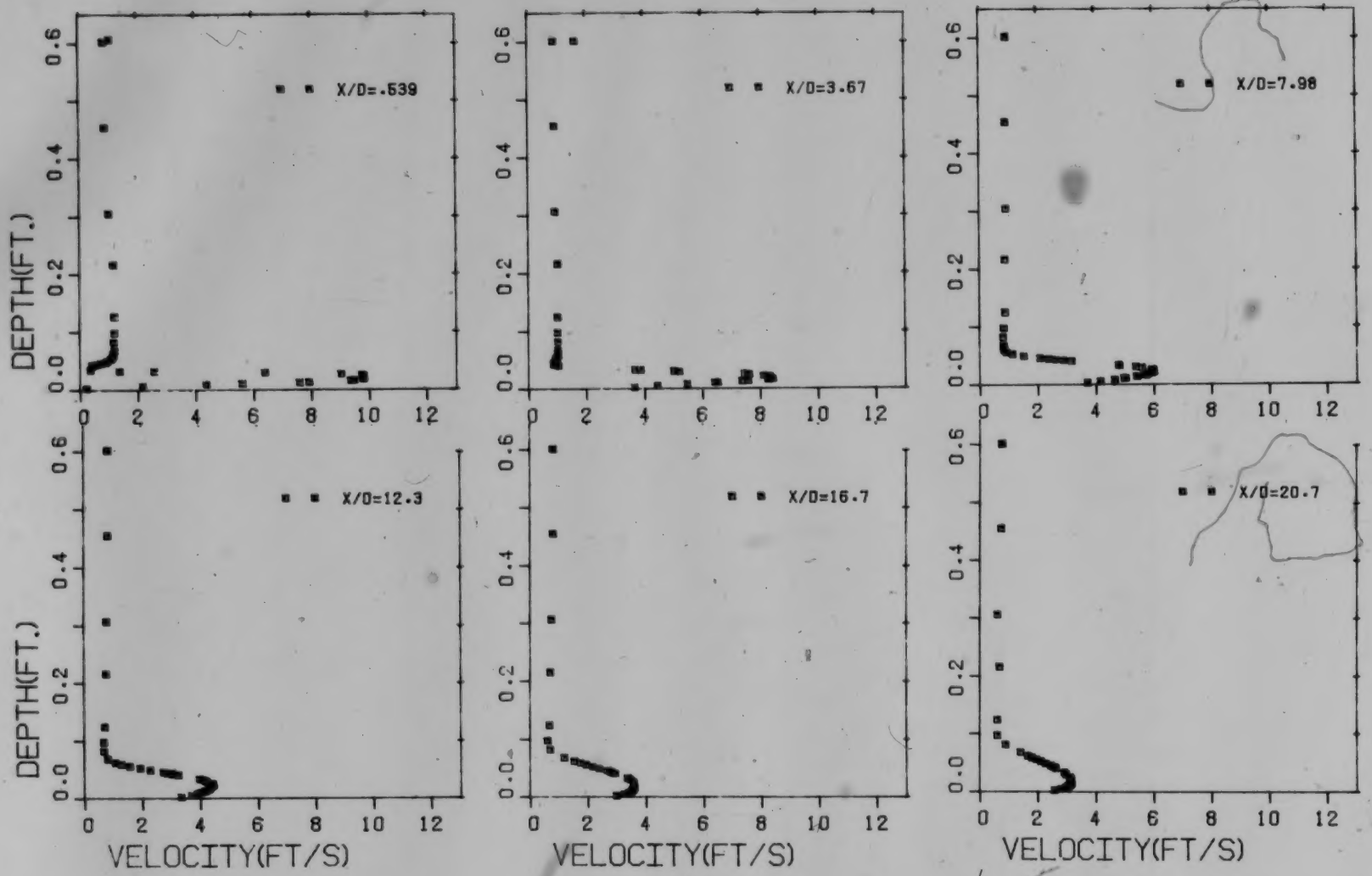

EXPT. 1 ALPHA=12.62:1

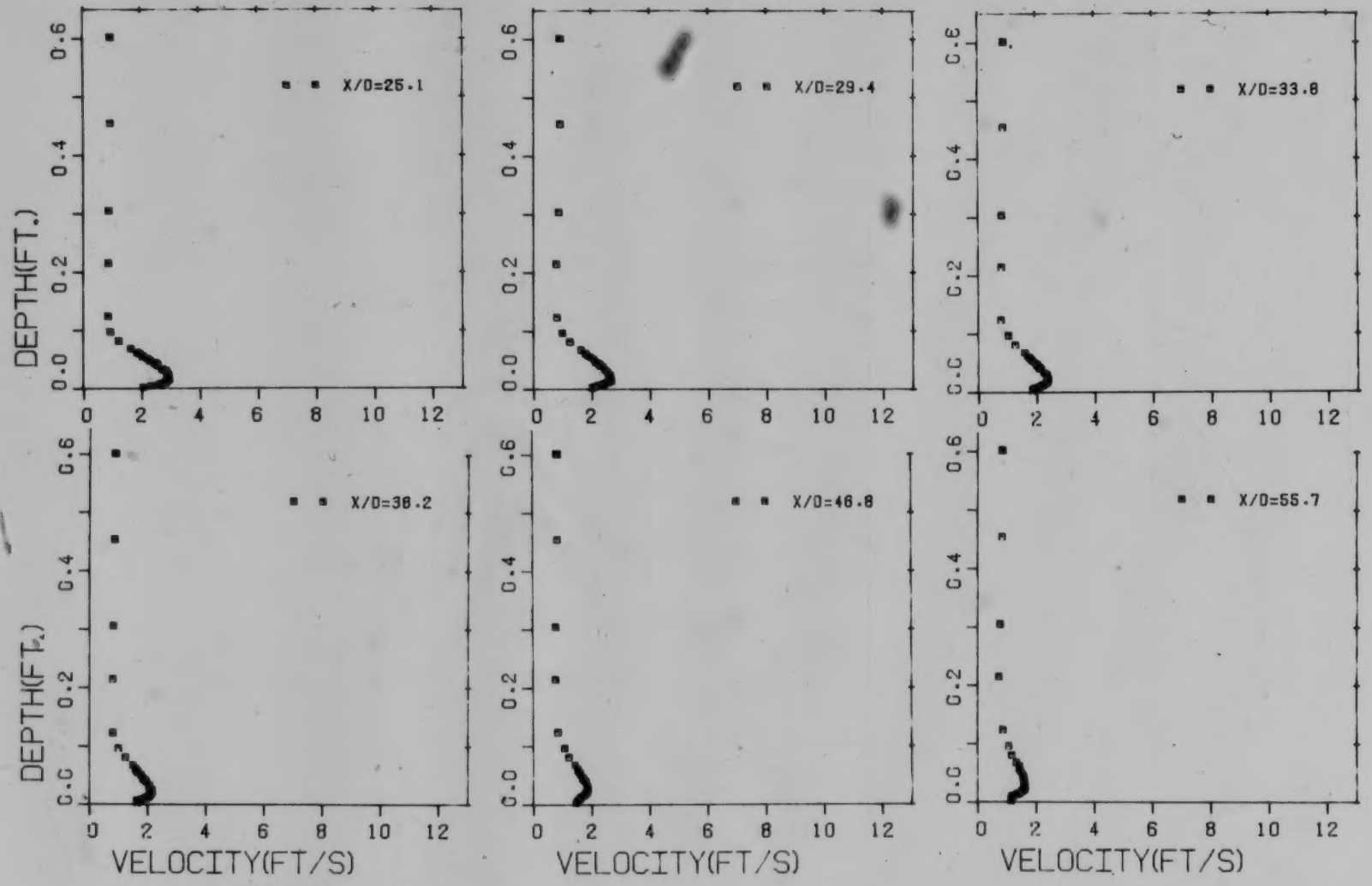

EXPT. 1 ALPHA=12.62:1

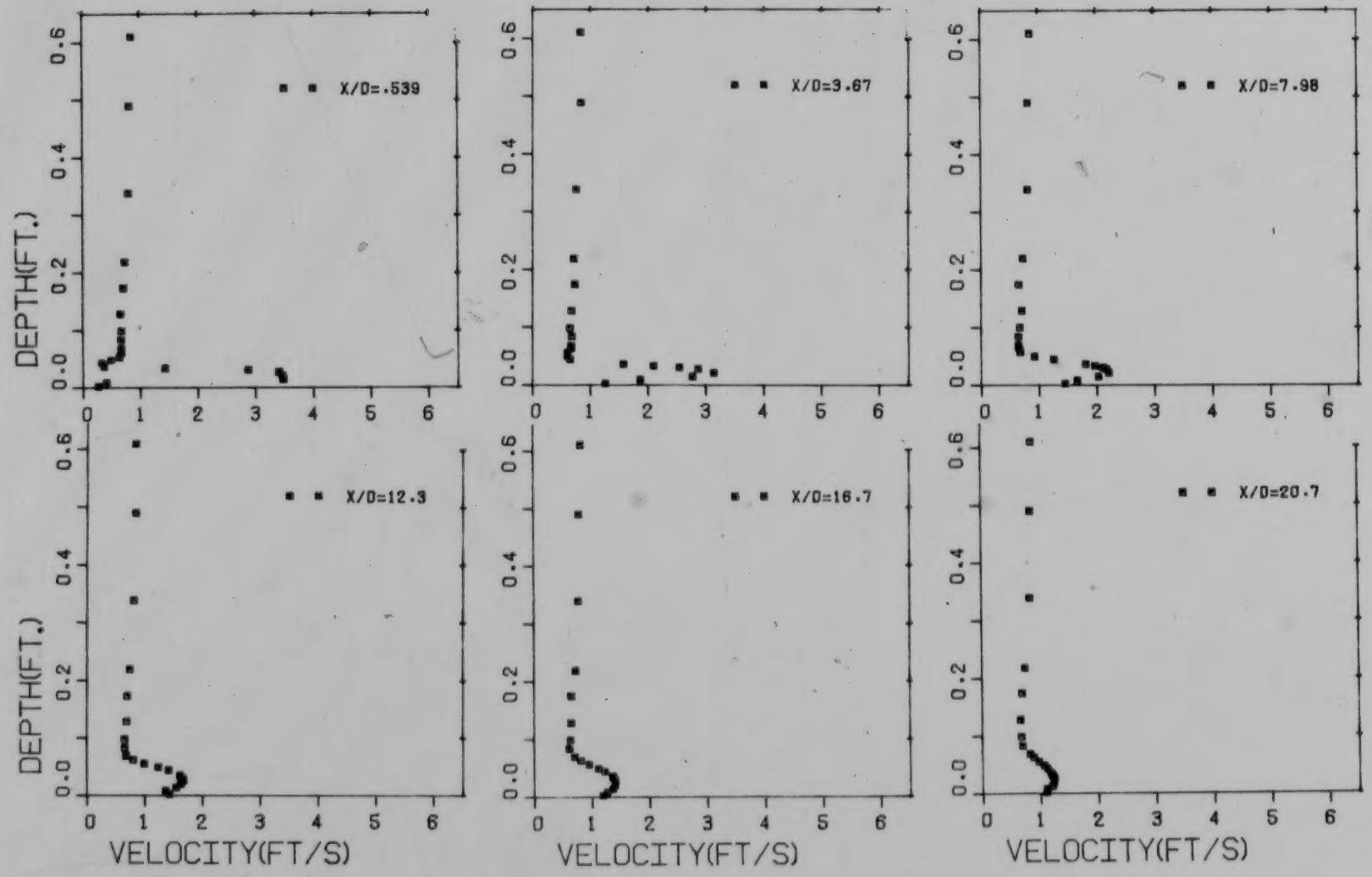

EXPT. 2 ALPHA=4.47:1

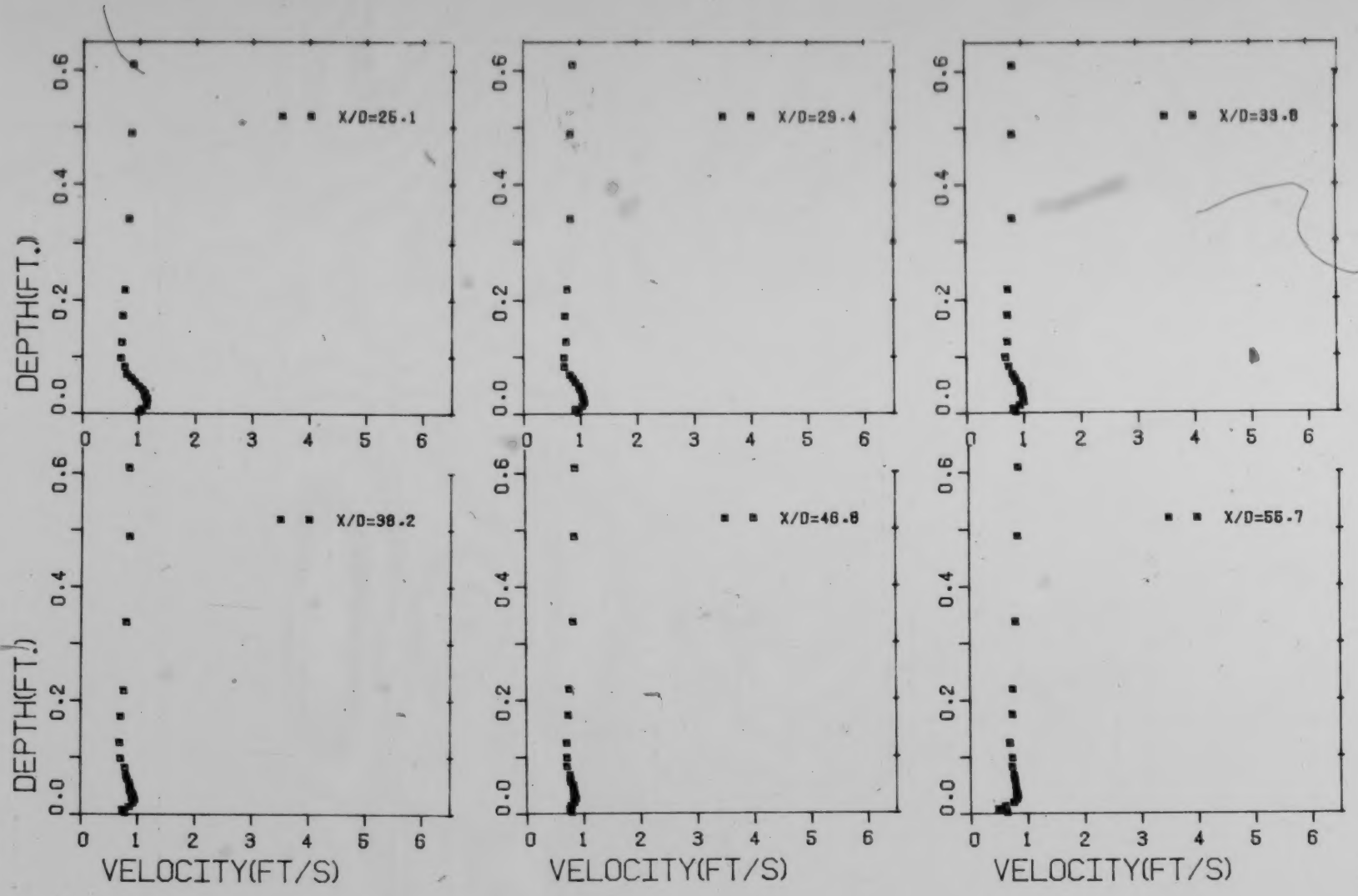

EXPT. 2 ALPHA=4.47:1

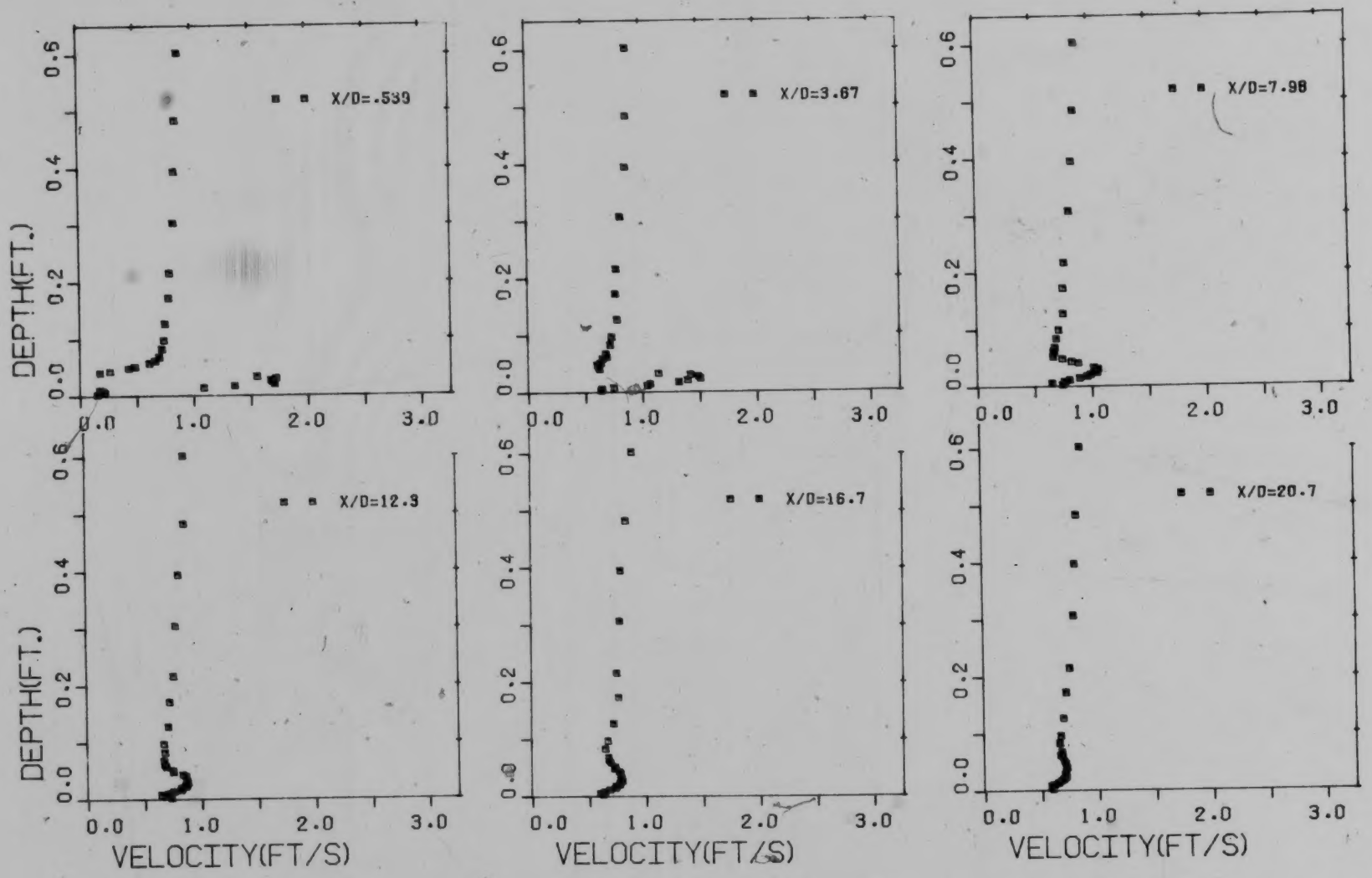

EXPT. 3 ALPHA=2.21:1

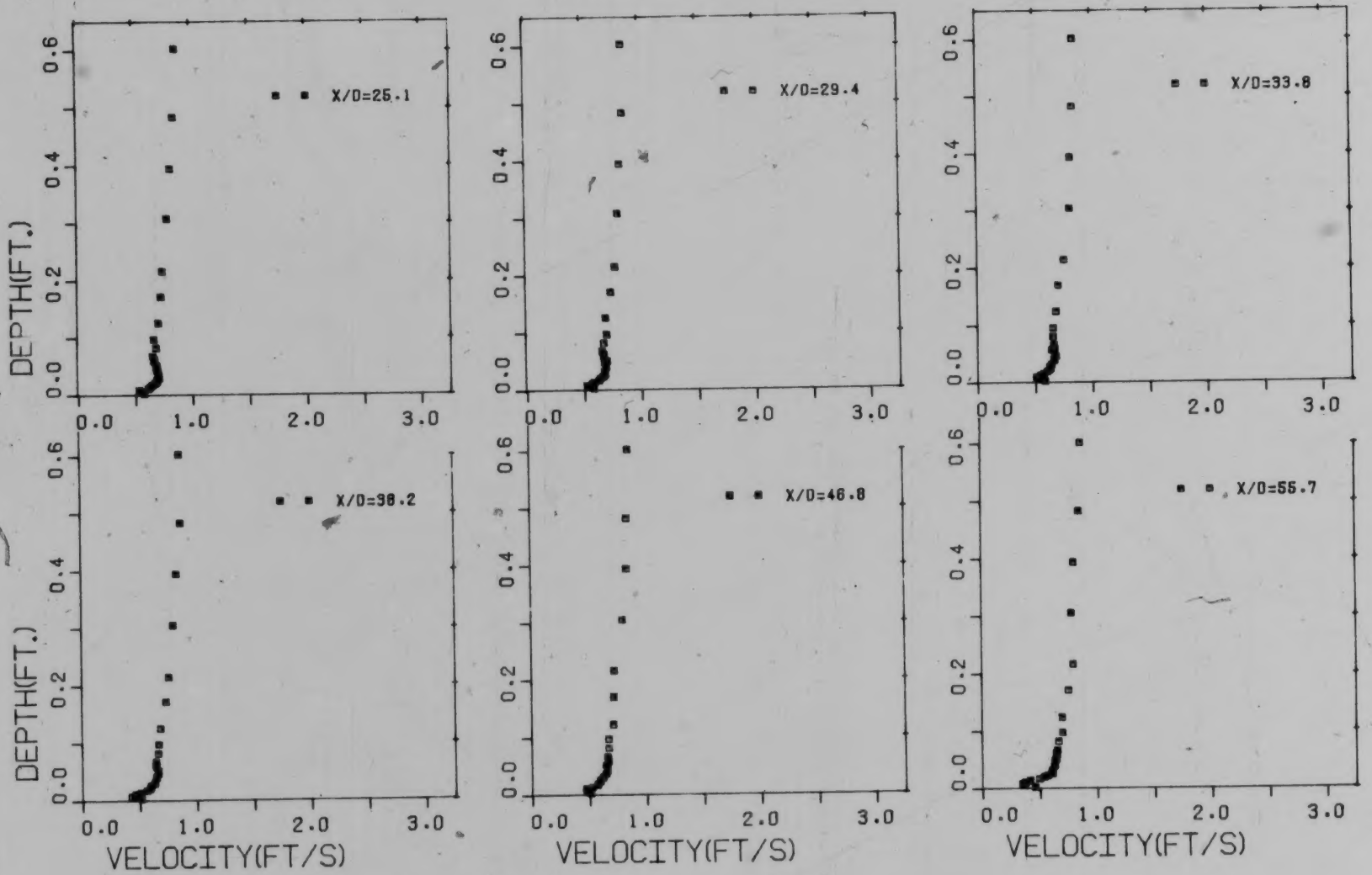

EXPT. 3 ALPHA=2.21:1

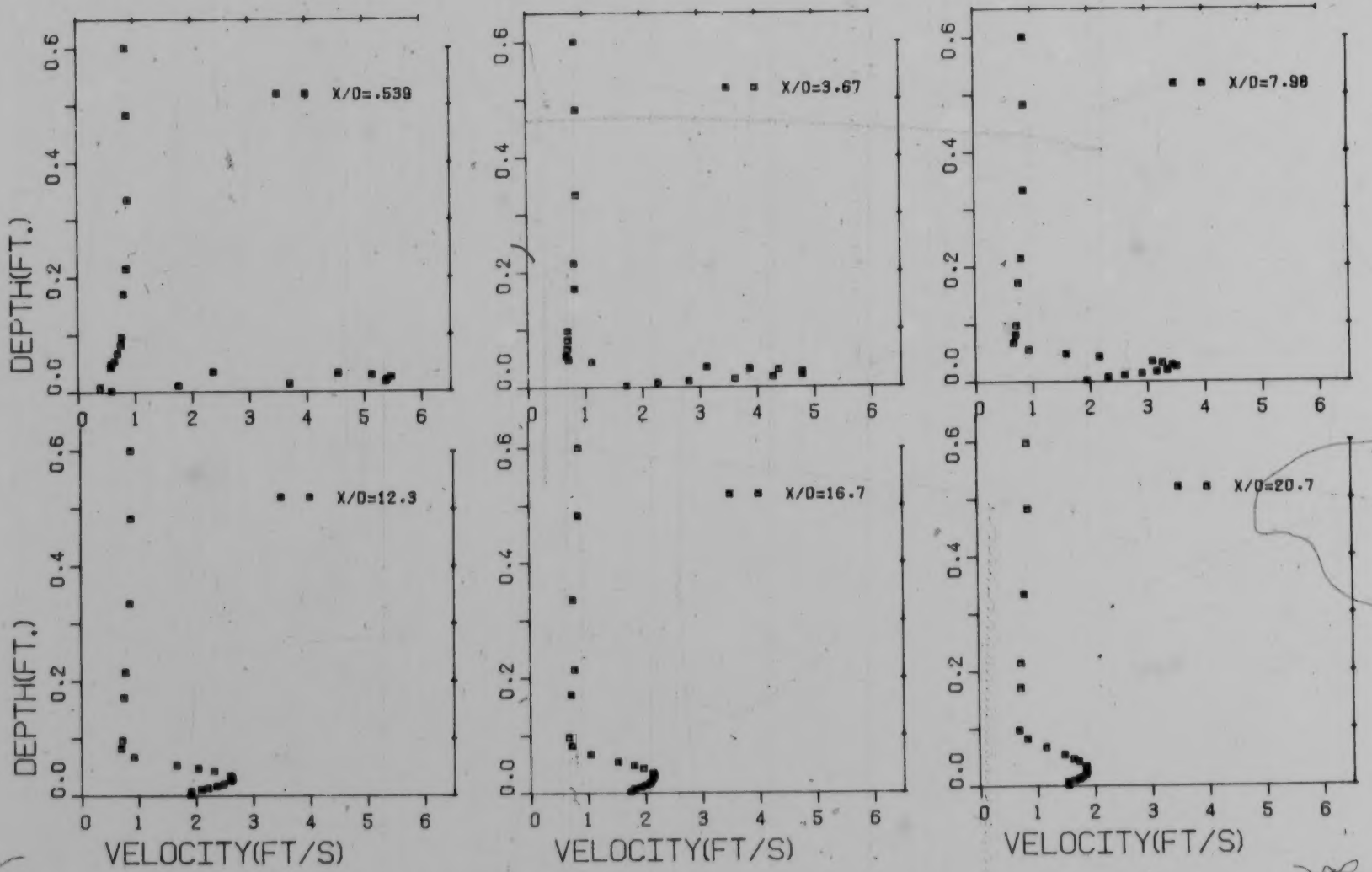

EXPT. 4 ALPHA=7.03:1

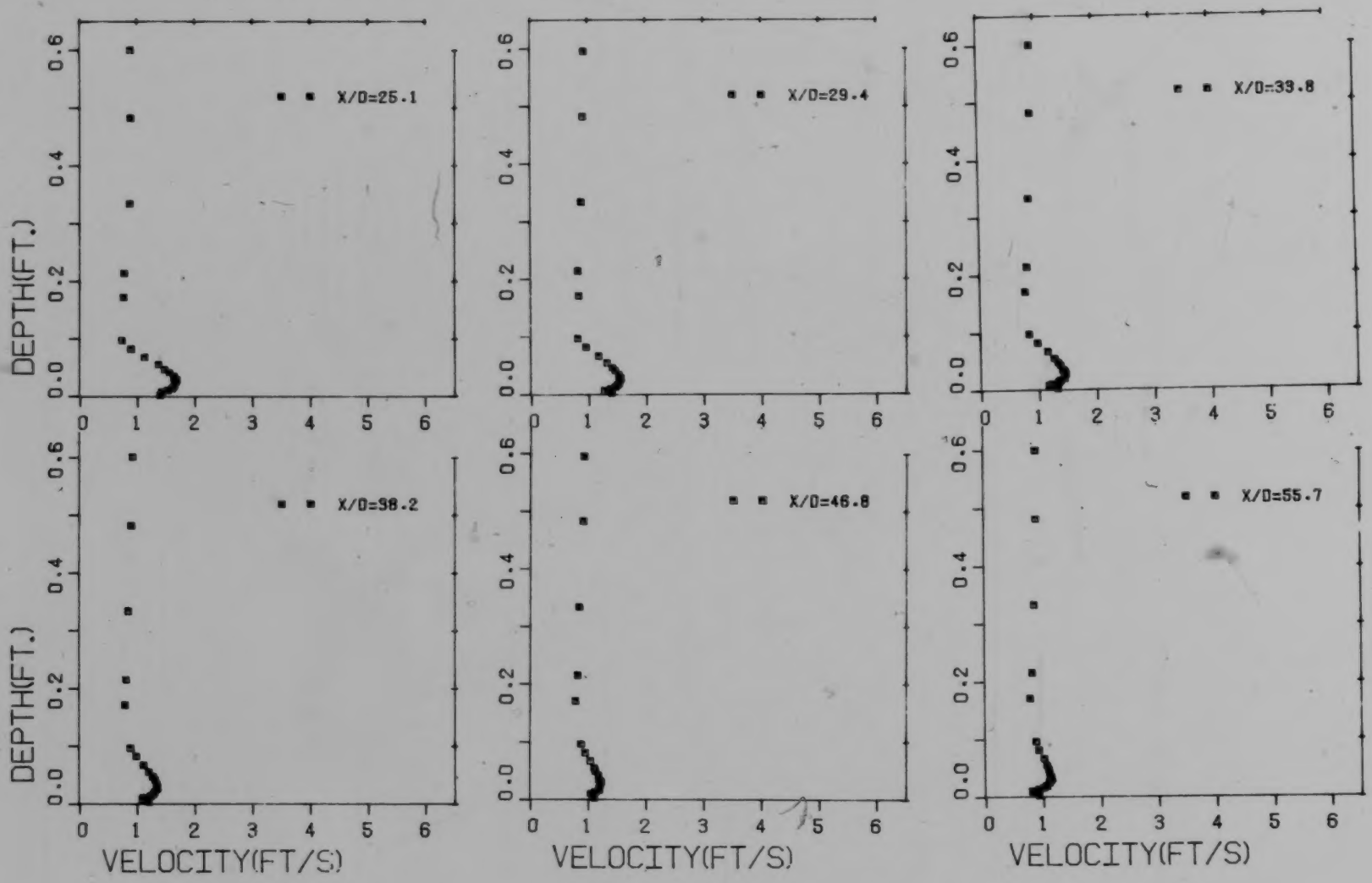

EXPT. 4 ALPHA=7.03:1

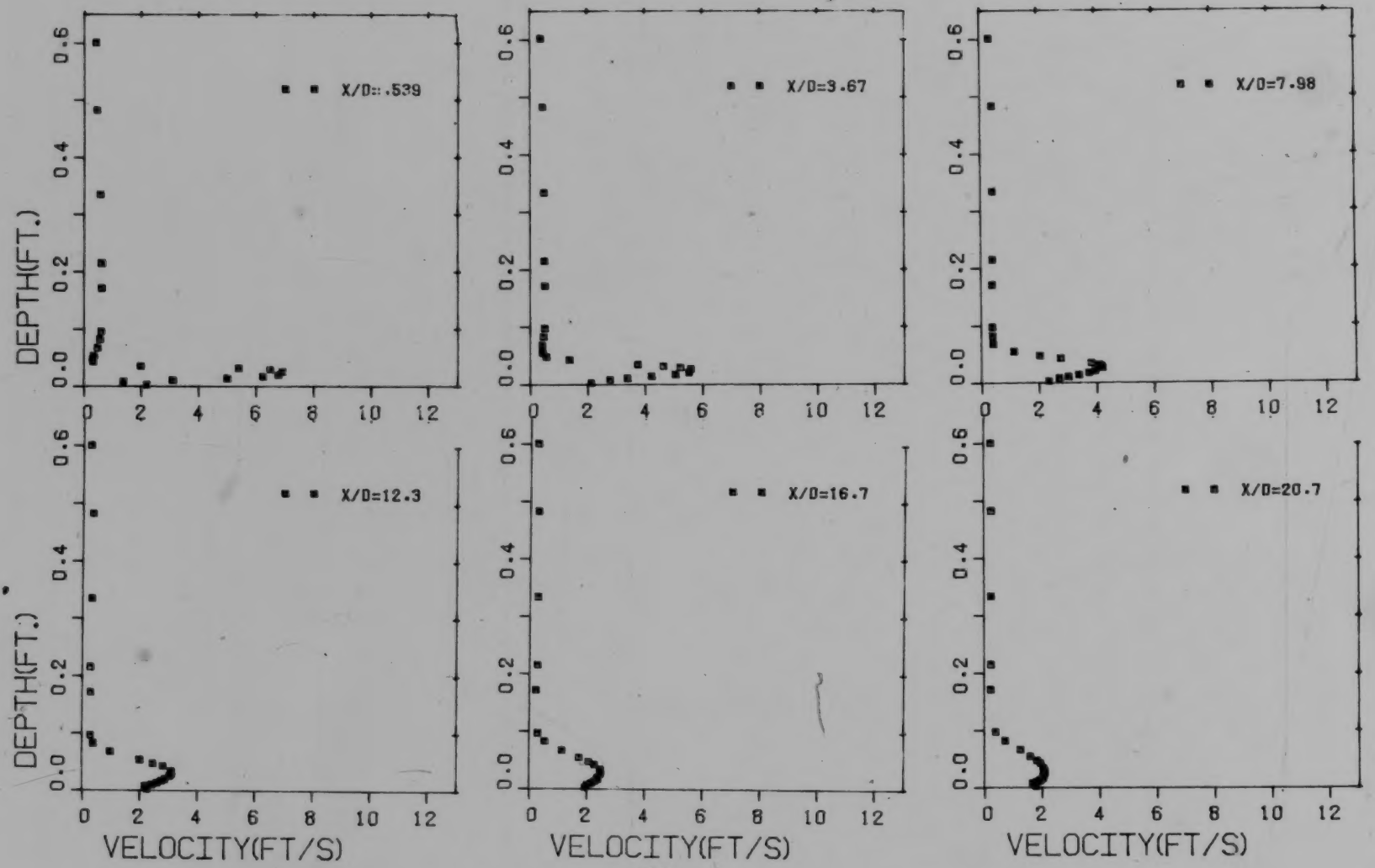

EXPT. 5 ALPHA=21.1:1

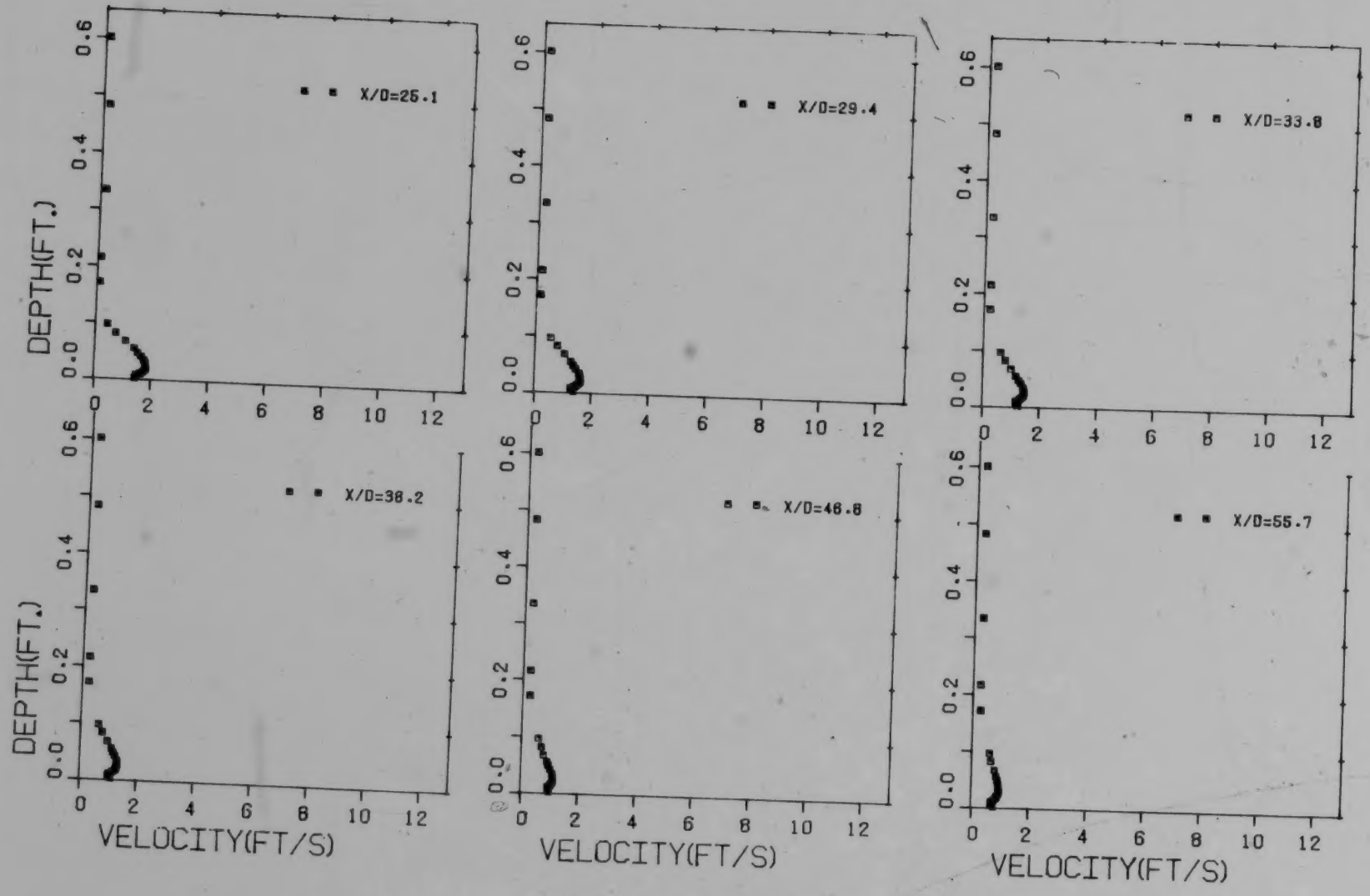

EXPT. 5 ALPHA=21.1:1

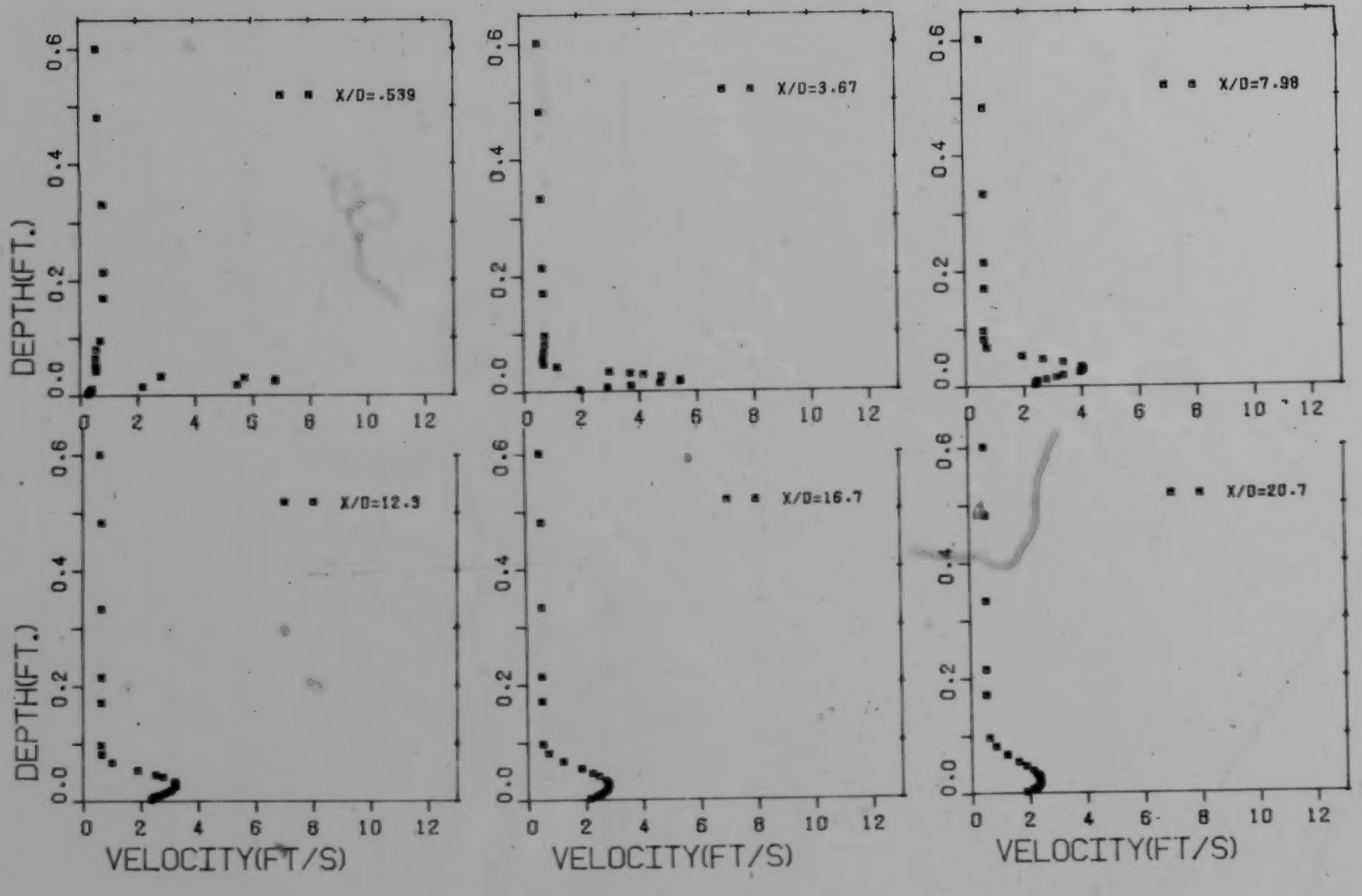

EXPT. 6 ALPHA=31.4:1

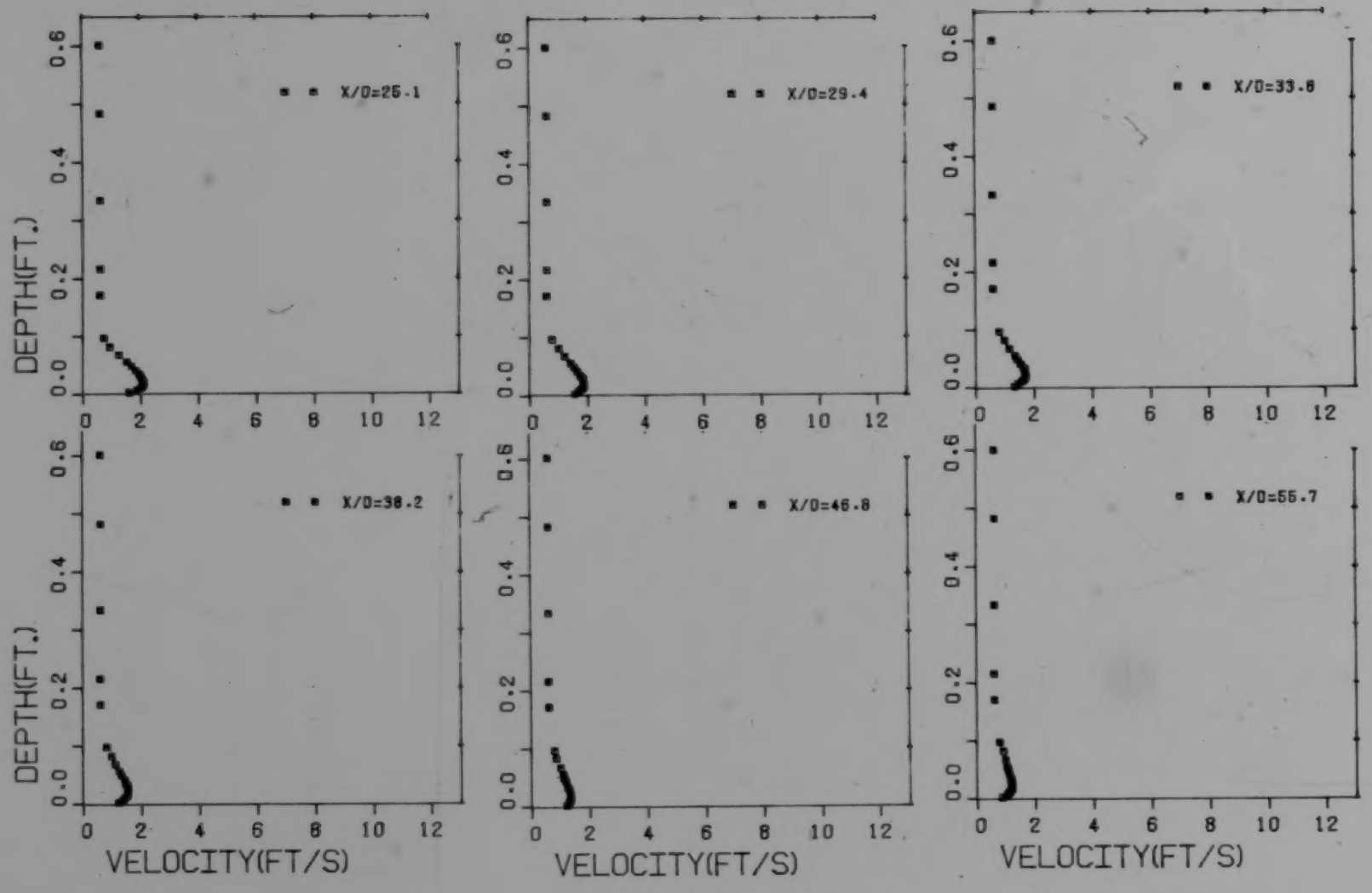

EXPT. 6 ALPHA=31.4:1

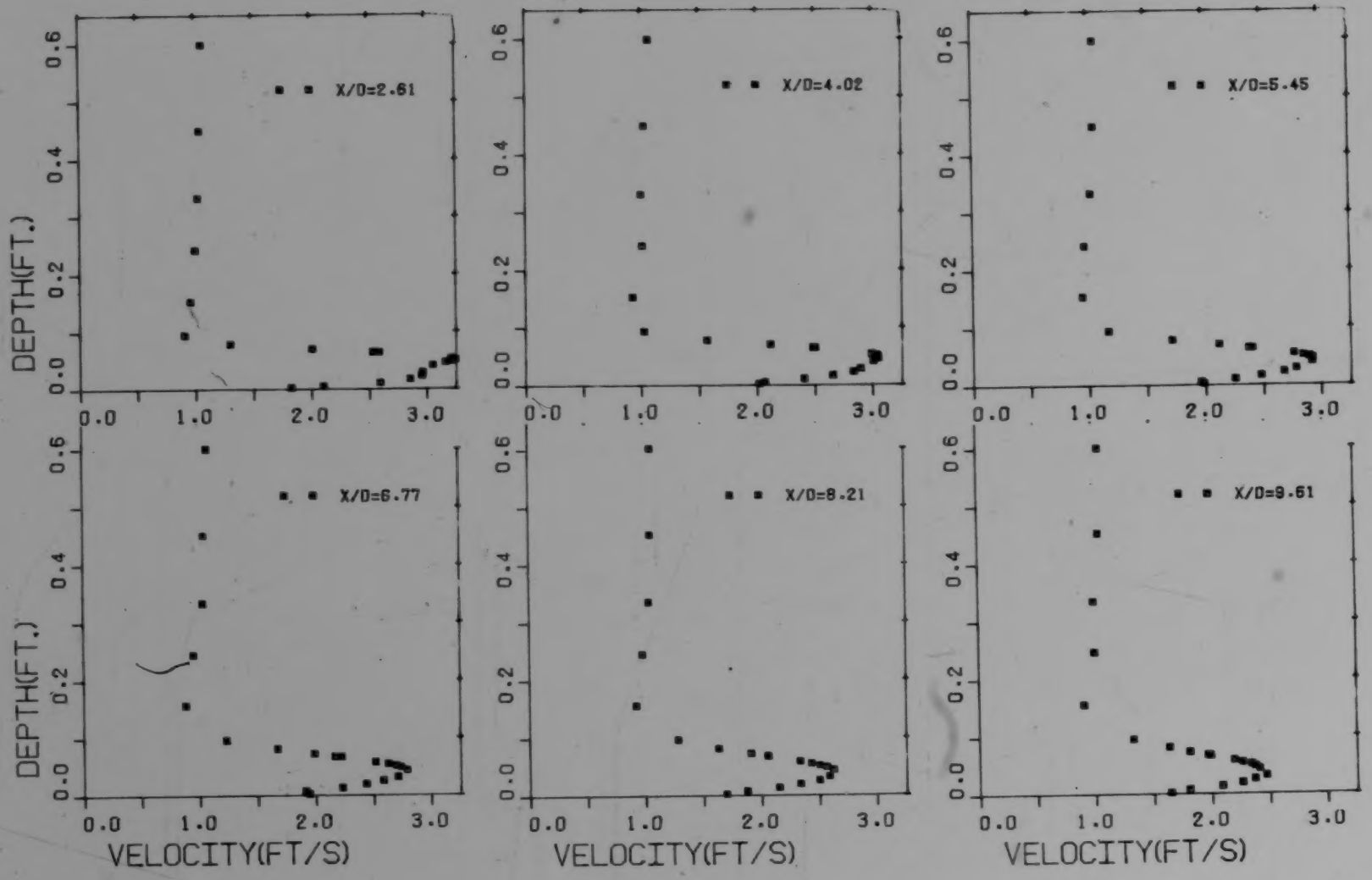

EXPT. 7 ALPHA=3.54:1

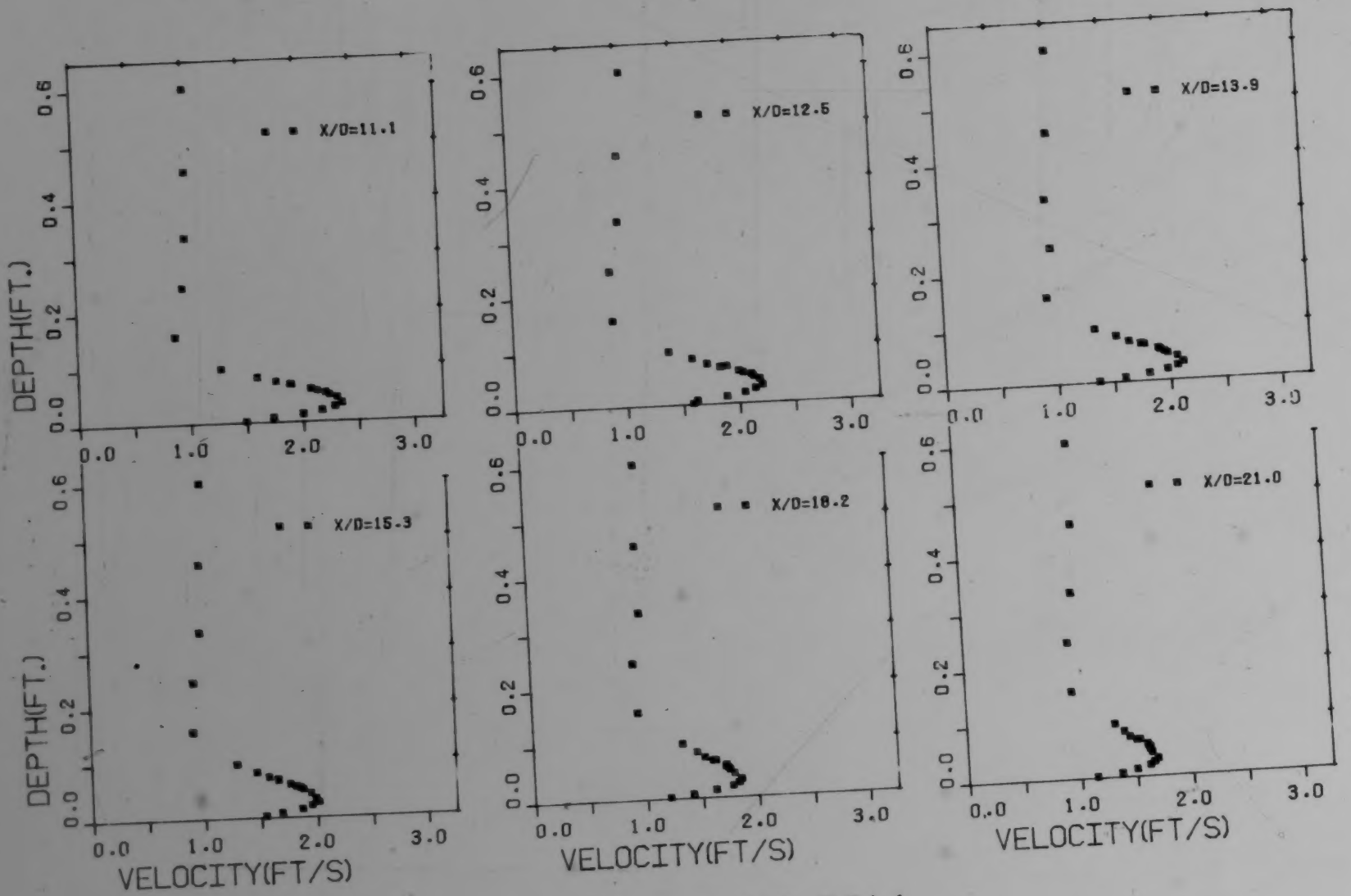

EXPT. 7 ALPHA=3.54:1

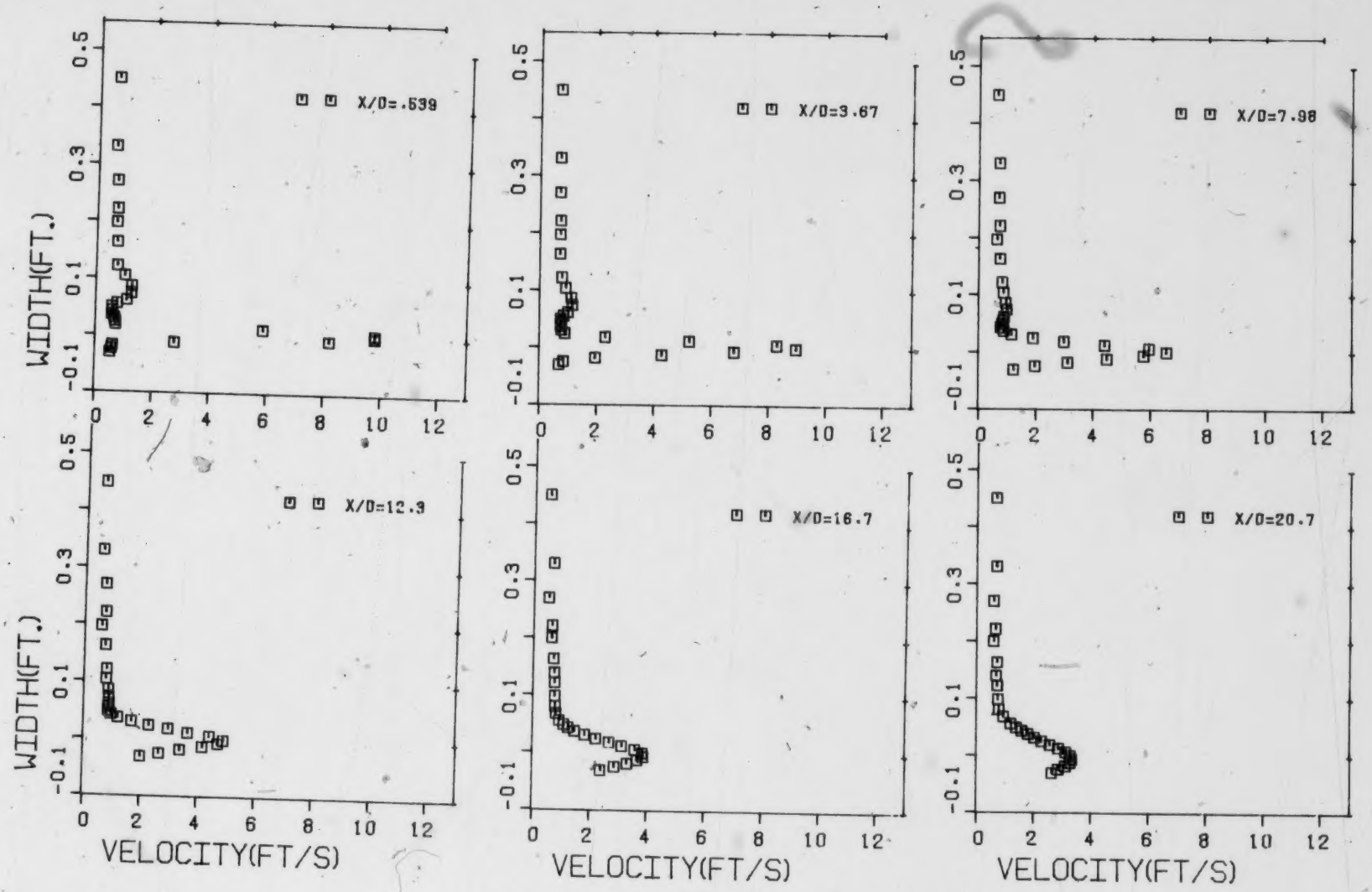

EXPT. 1 ALPHA=12.62:1

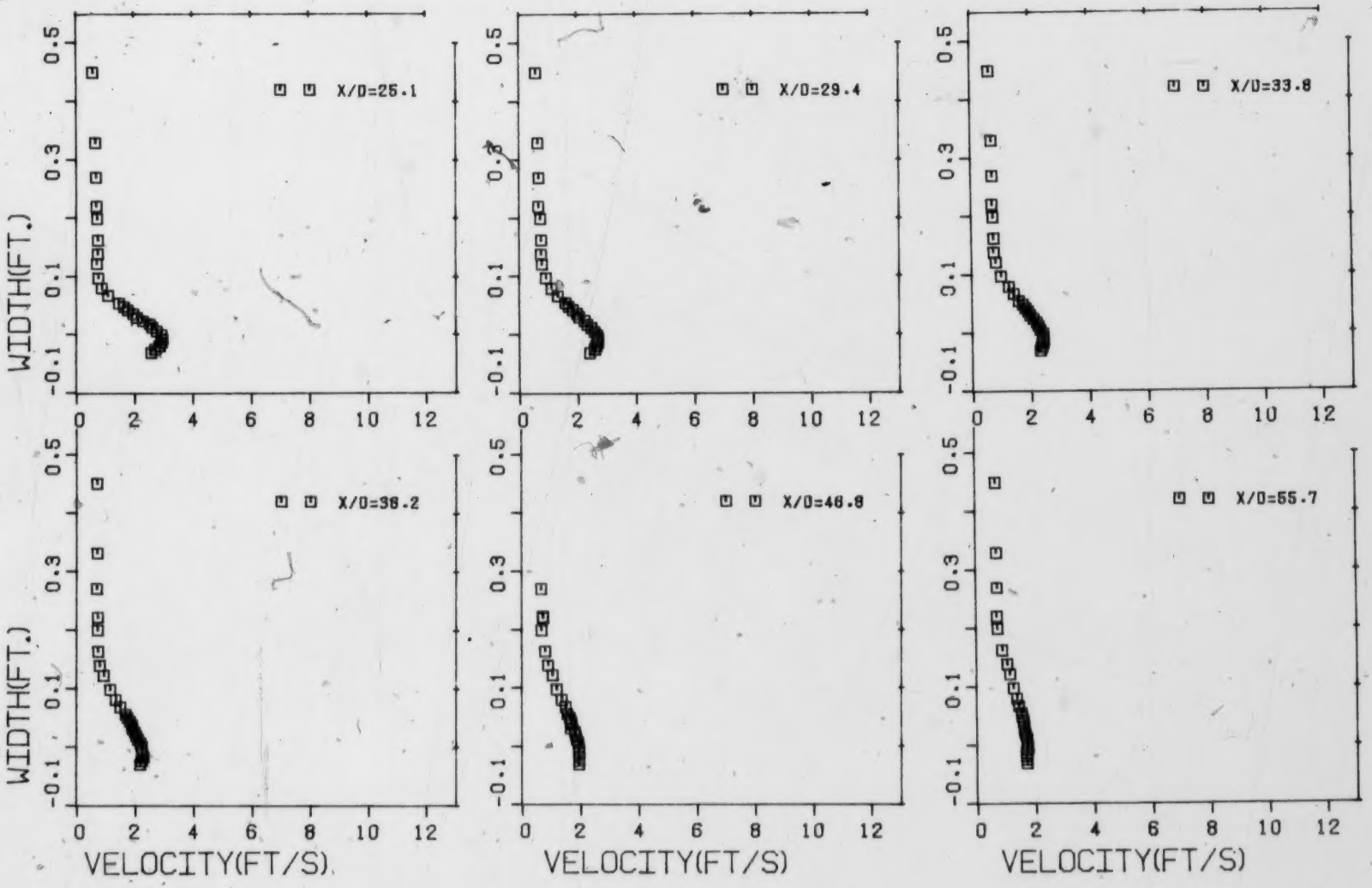

EXPT. 1 ALPHA=12.62:1

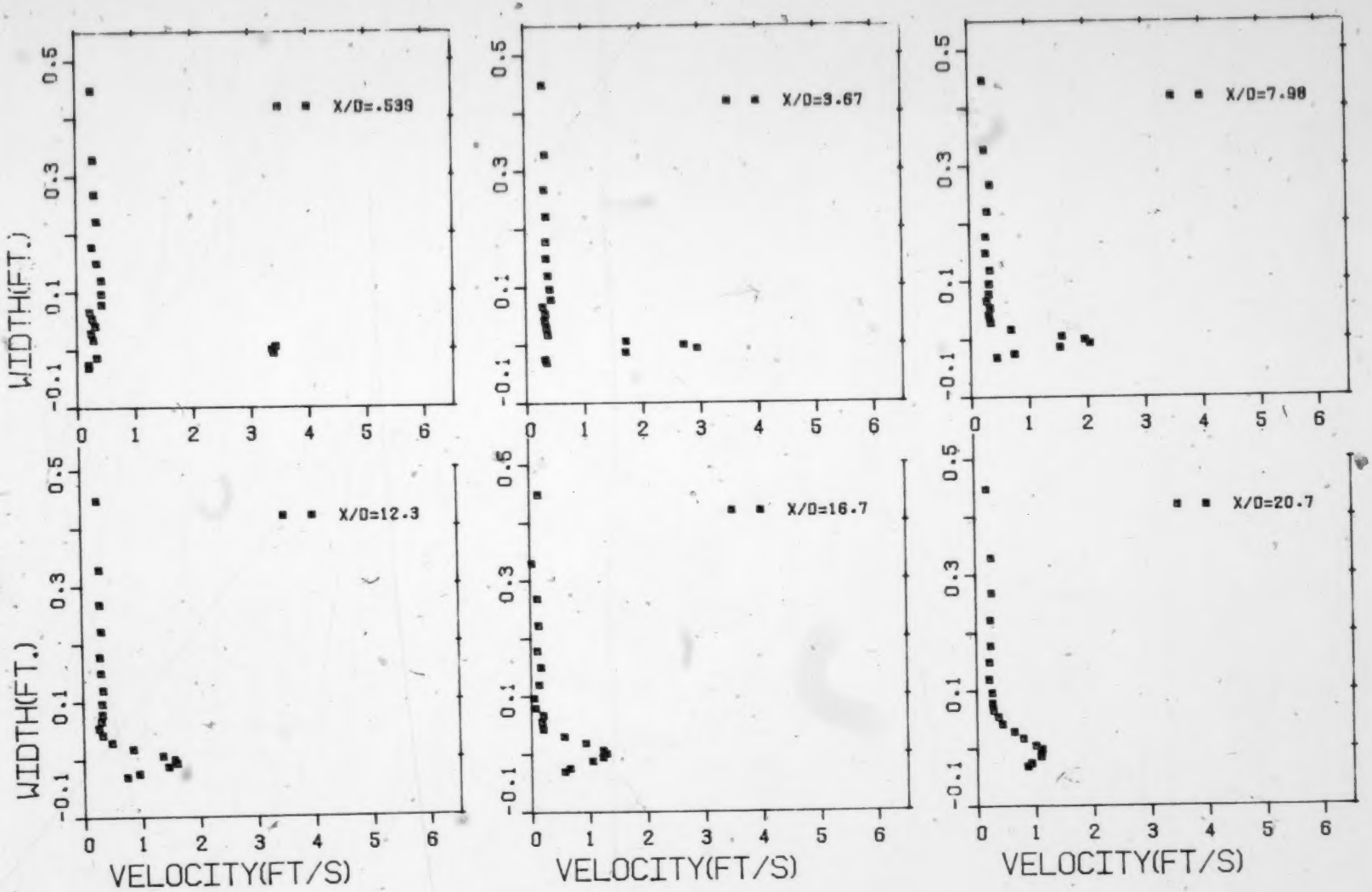

EXPT. 2 ALPHA=4.47:1

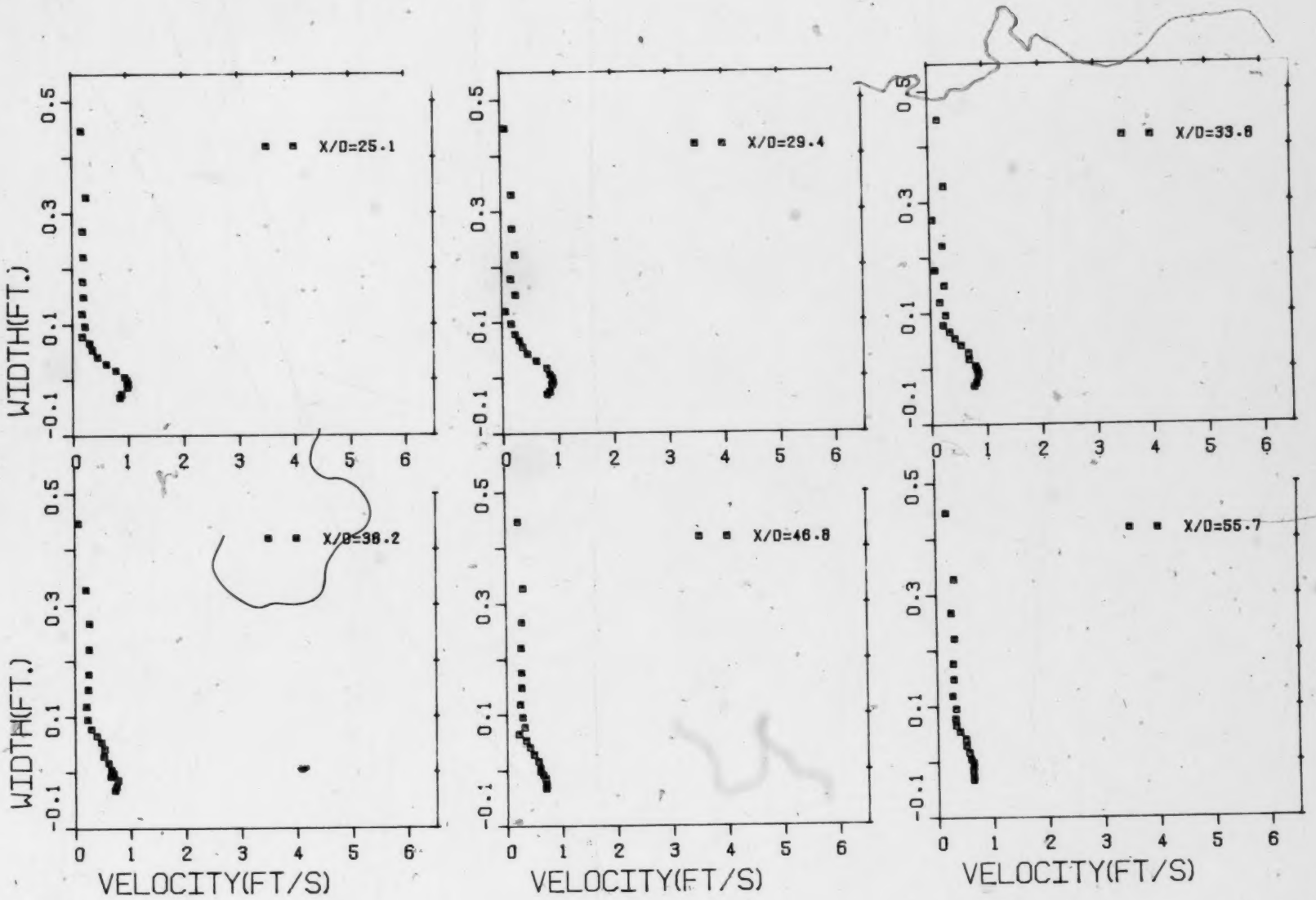

EXPT. 2 ALPHA=4.47:1

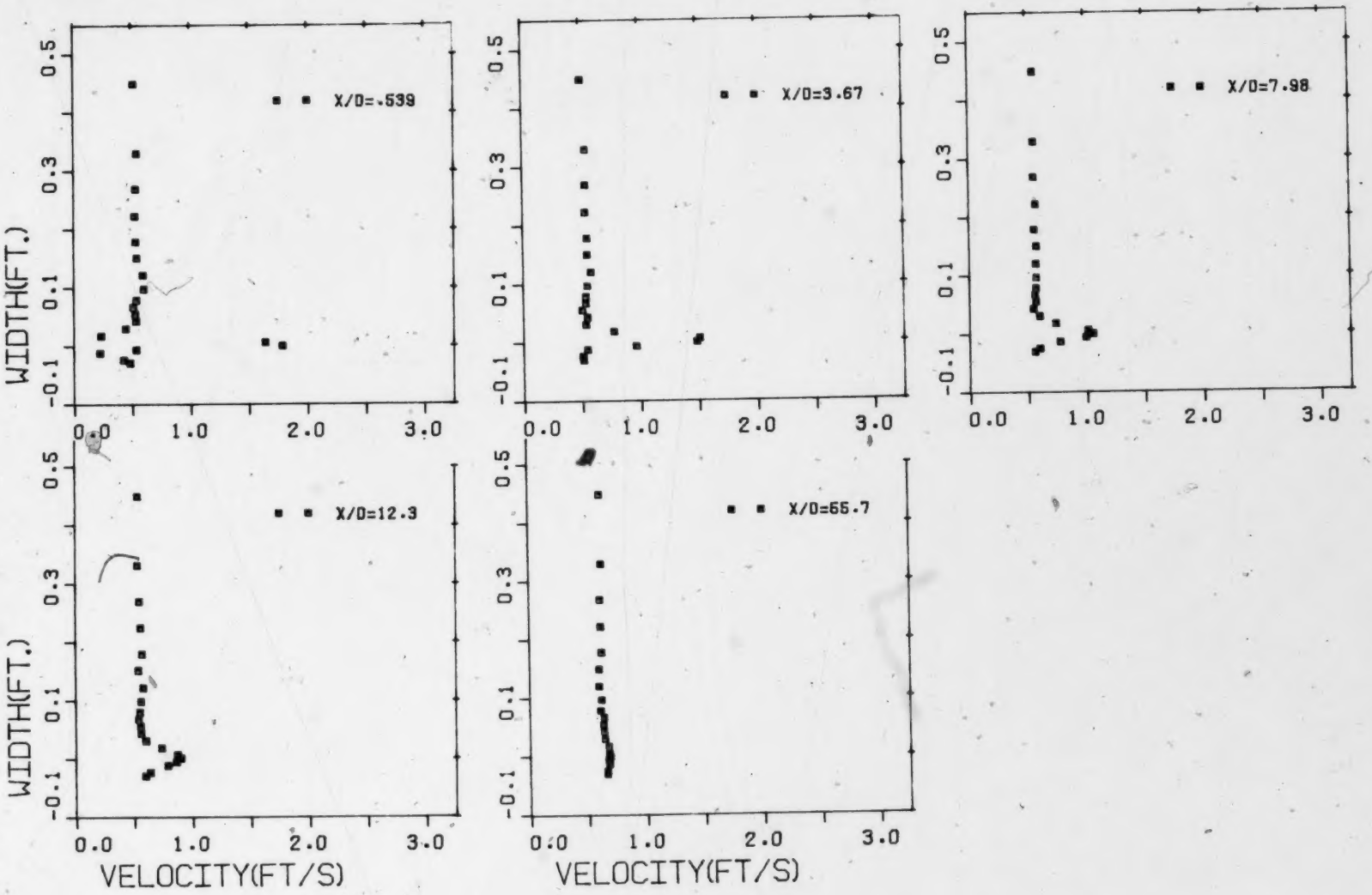

EXPT. 3 ALPHA=2.21:1

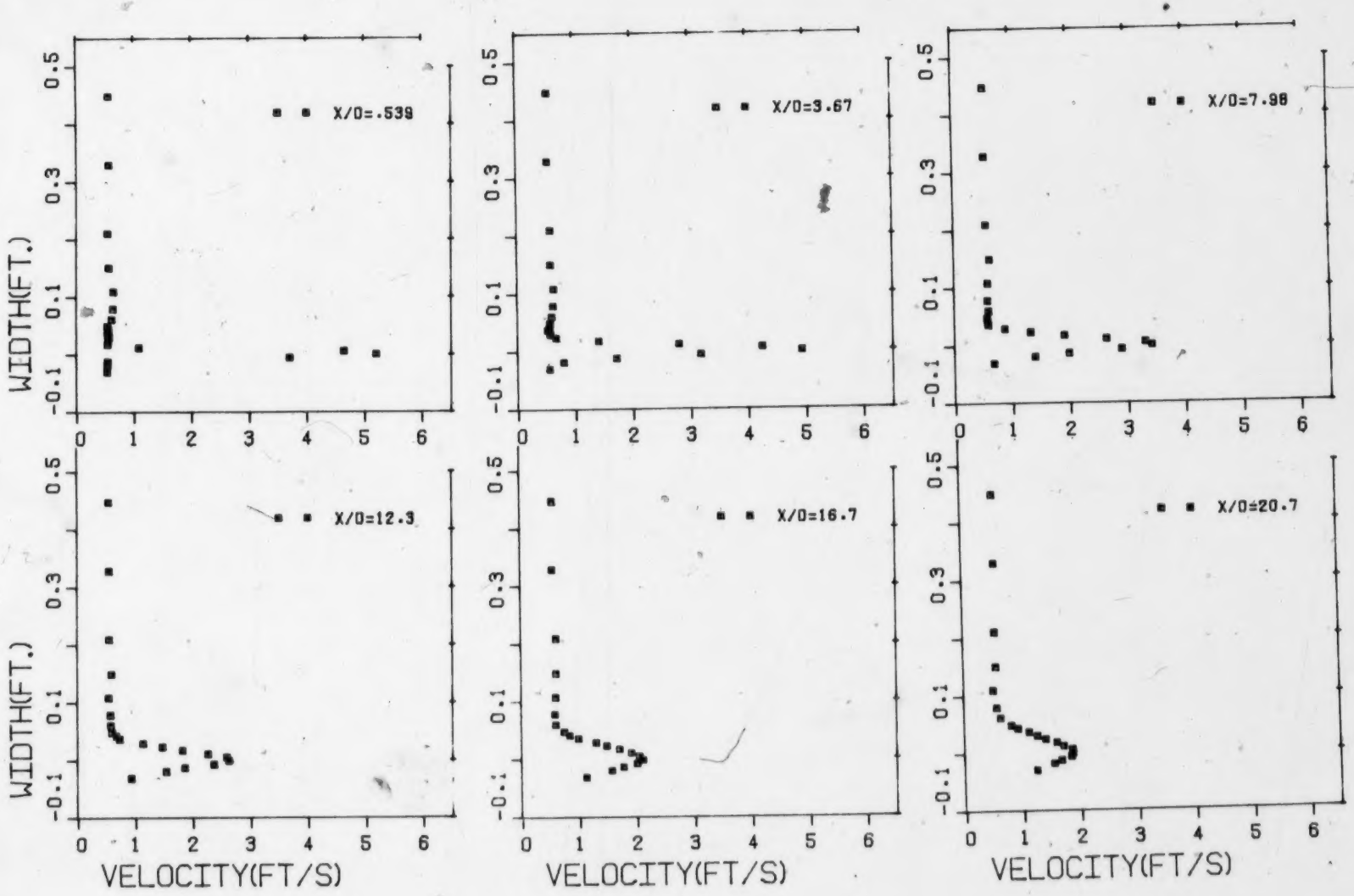

EXPT. 4 ALPHA=7.03:1

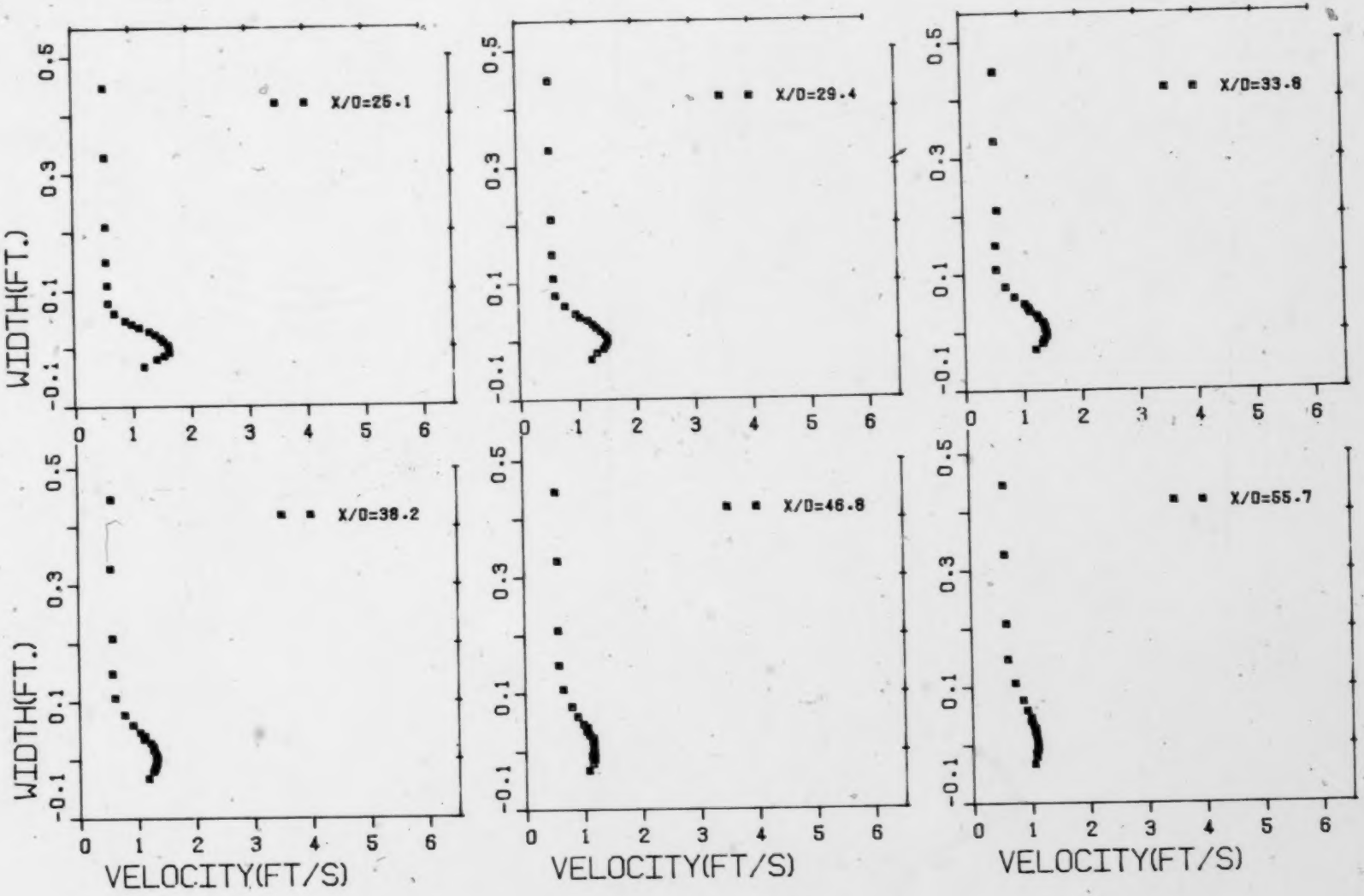

EXPT. 4 ALPHA=7.03:1

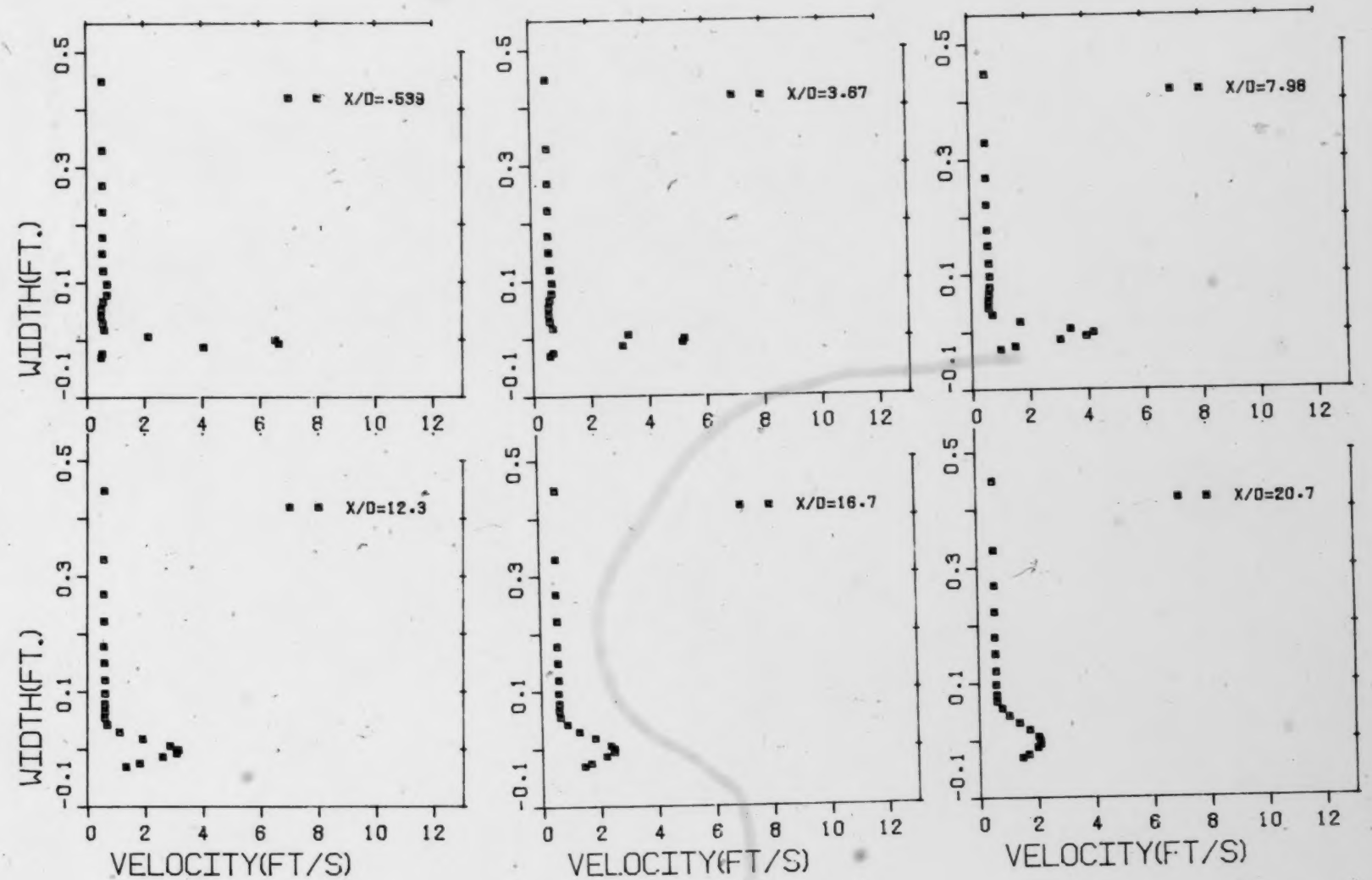

EXPT. 5 ALPHA=21.1:1

B22 98

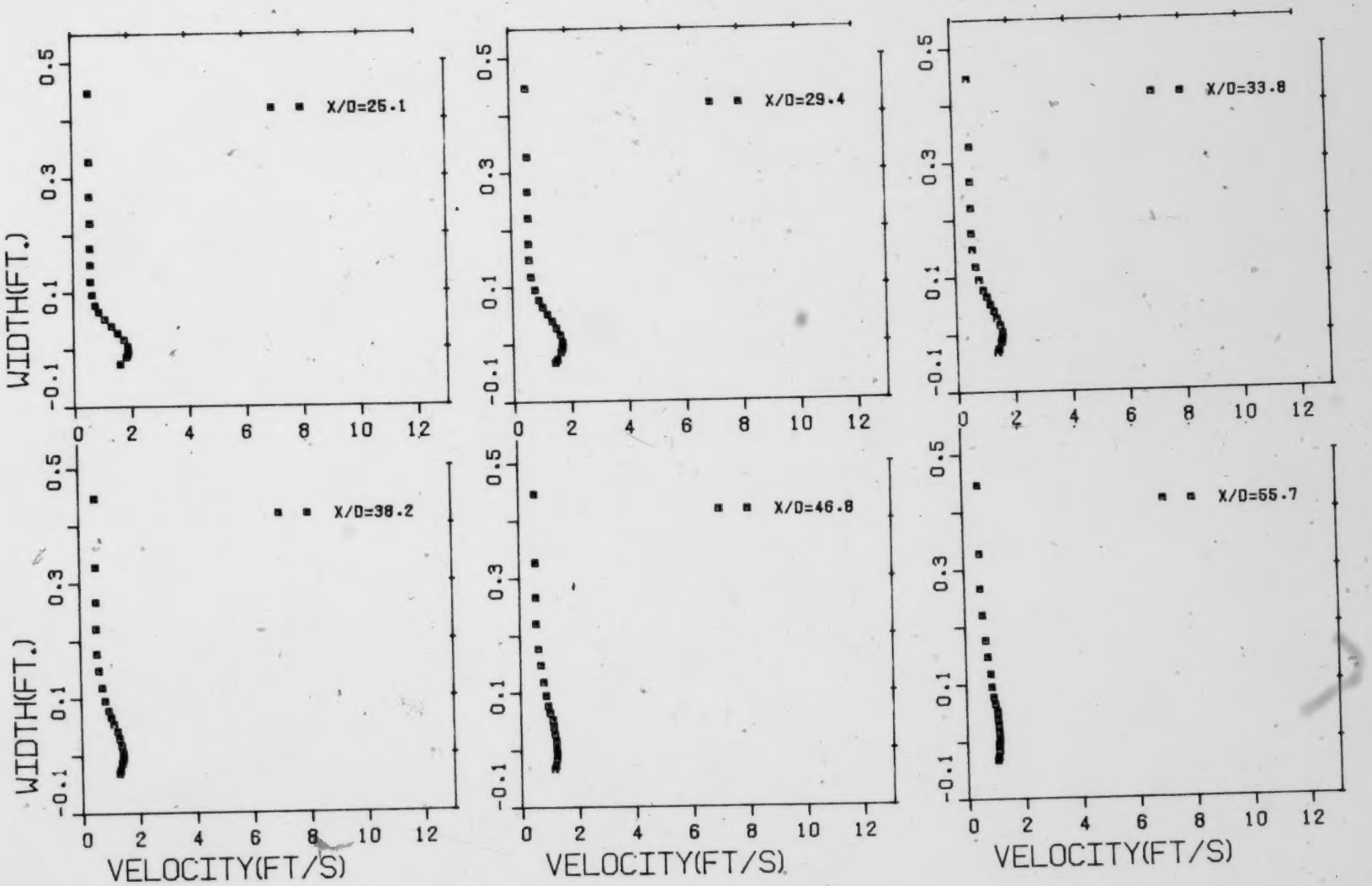

EXPT. 5 ALPHA=21.1:1

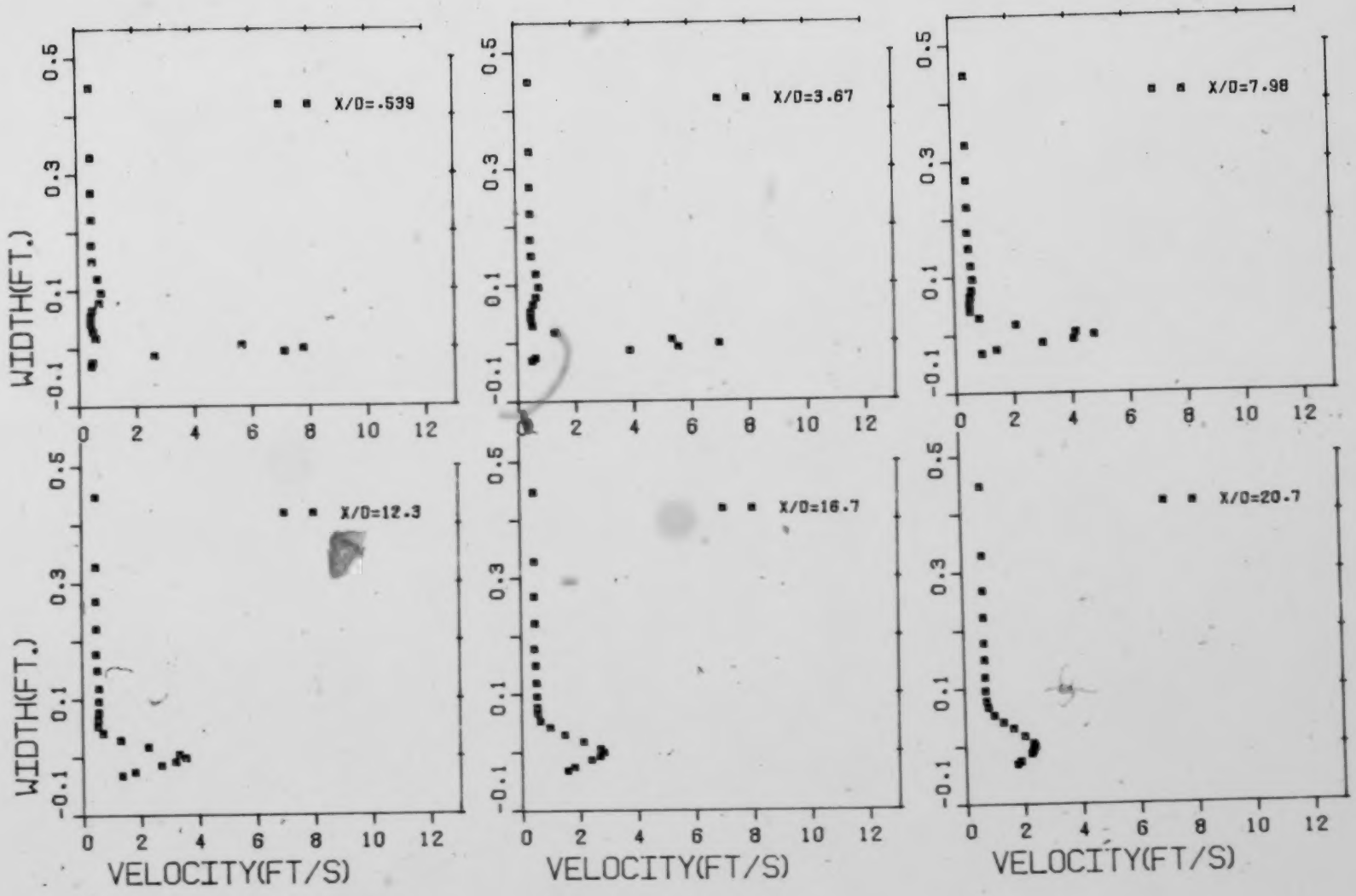

EXPT. 6 ALPHA=31.4:1

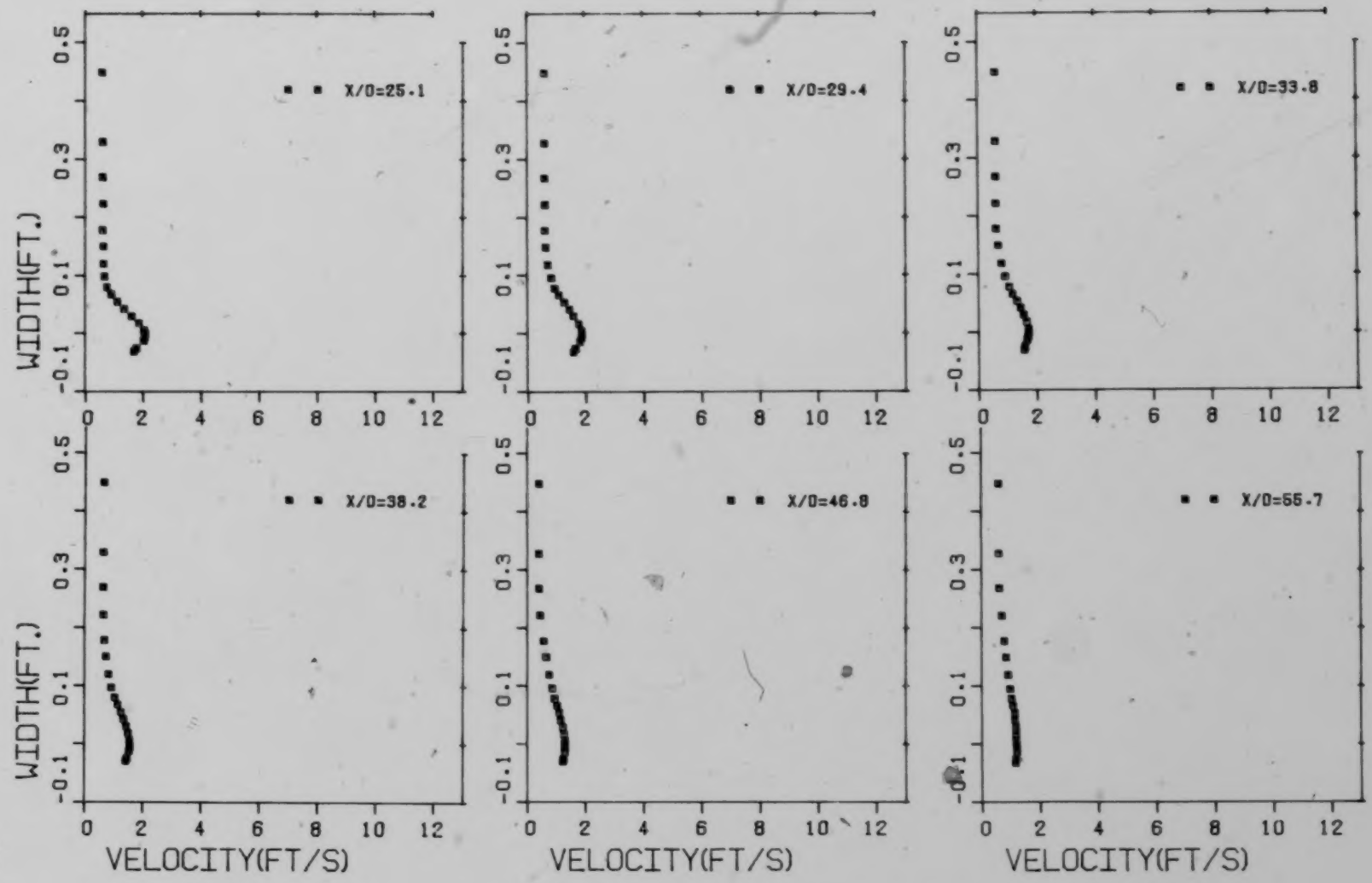

EXPT. 6 ALPHA=31.4:1

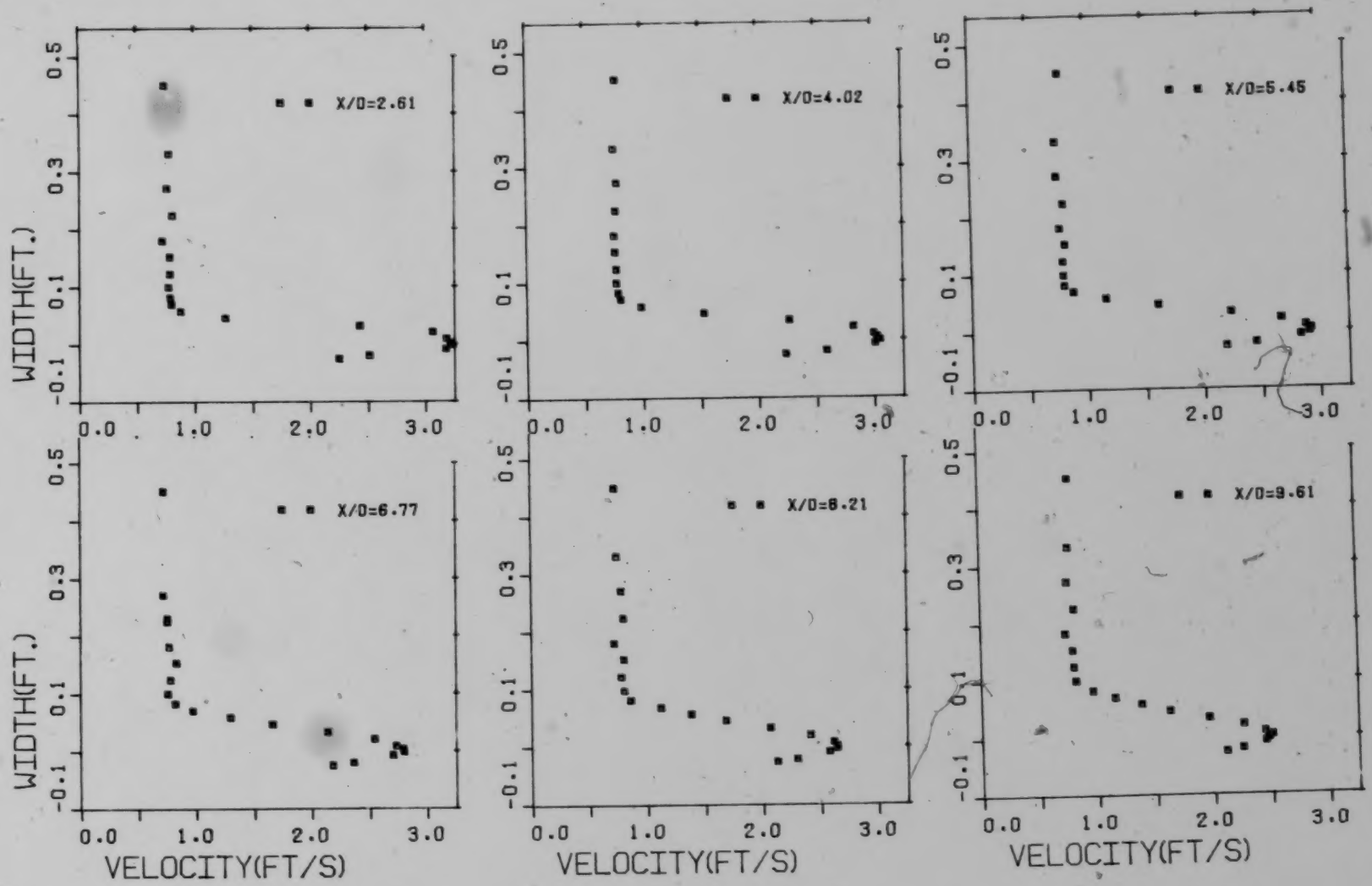

EXPT. 7 ALPHA=3.54:1

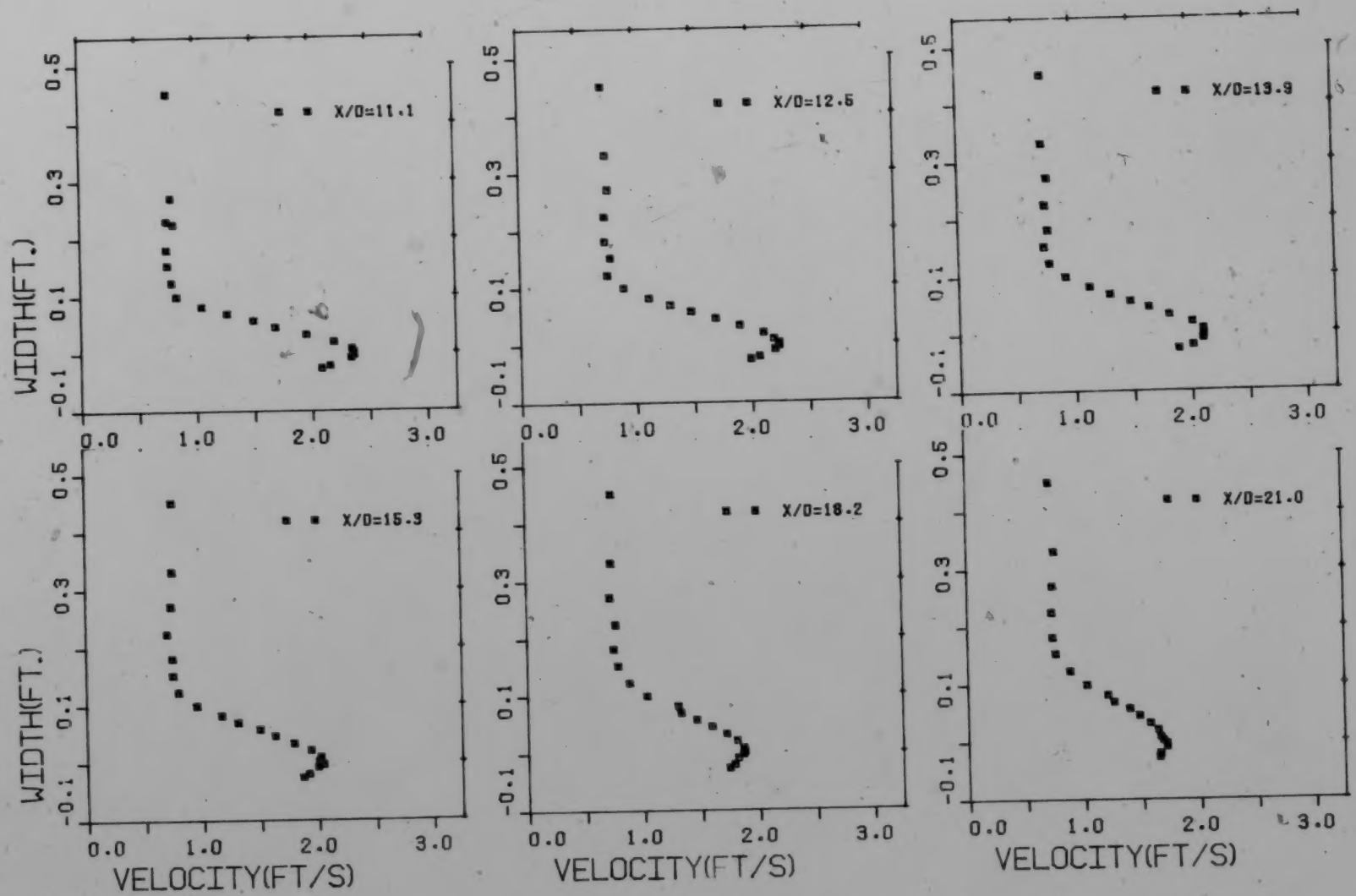

EXPT. 7 ALPHA=3.54:1

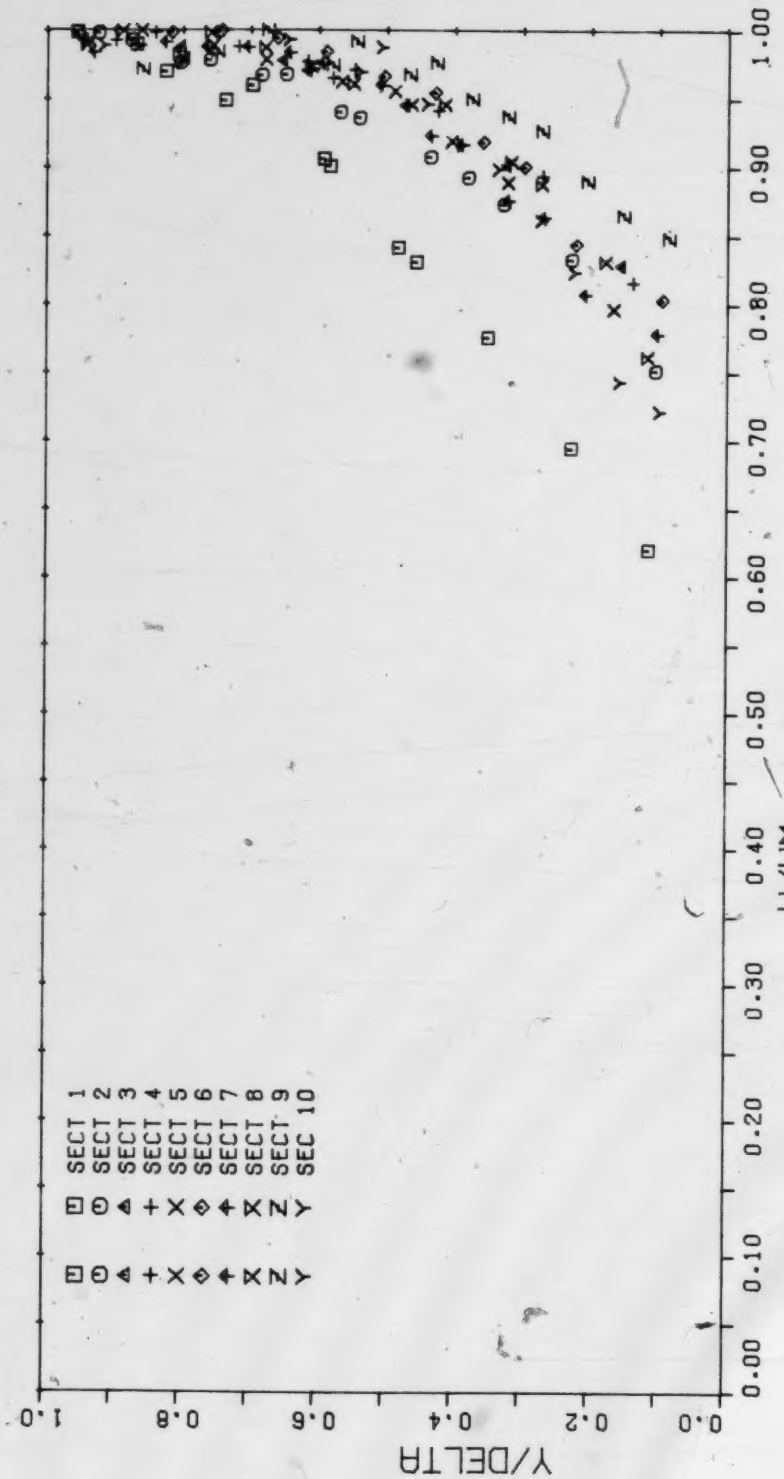

EXPT. 1 ALPHA = 12.62:1

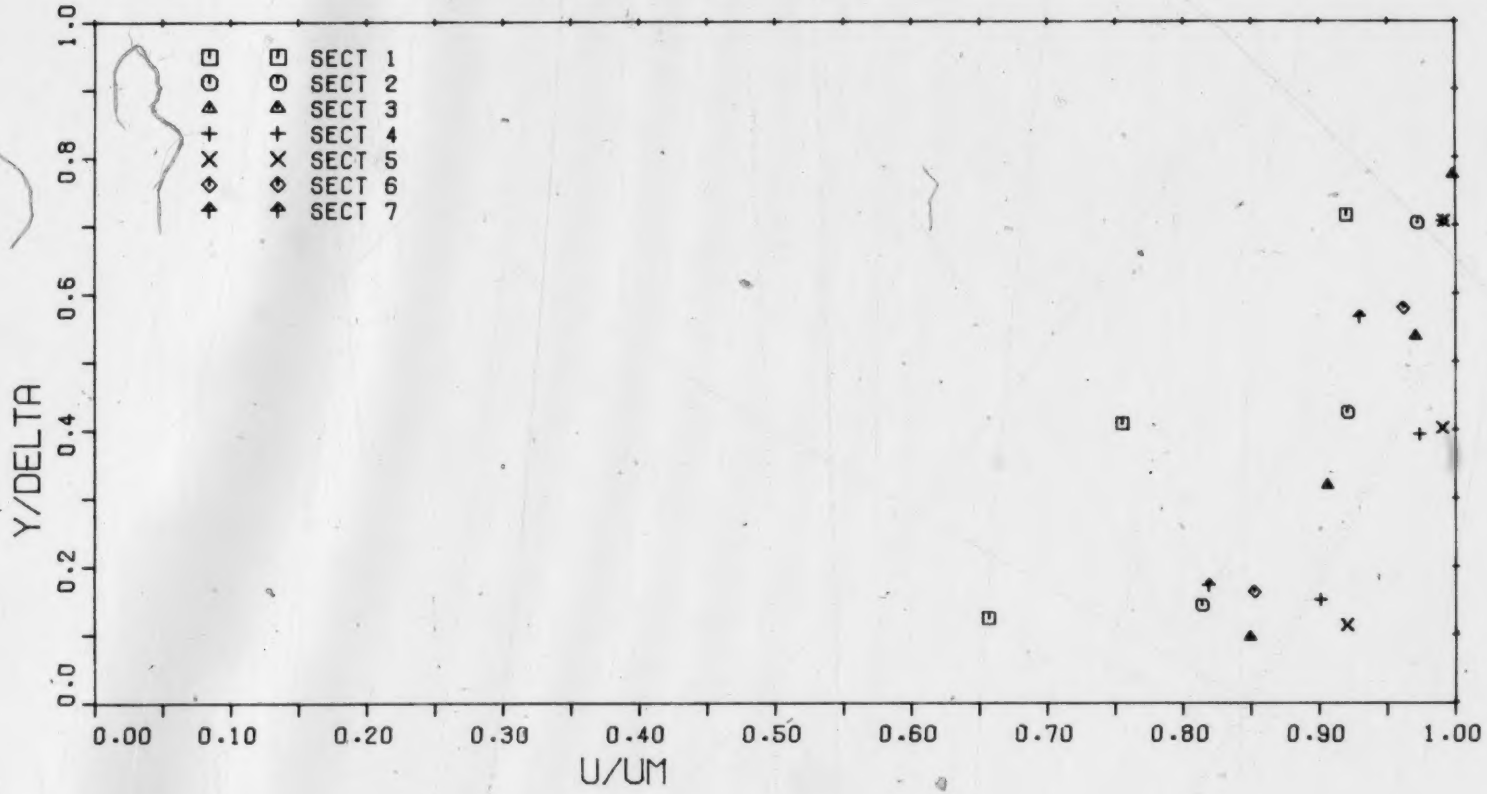

EXPT. 2 ALPHA = 4.47:1

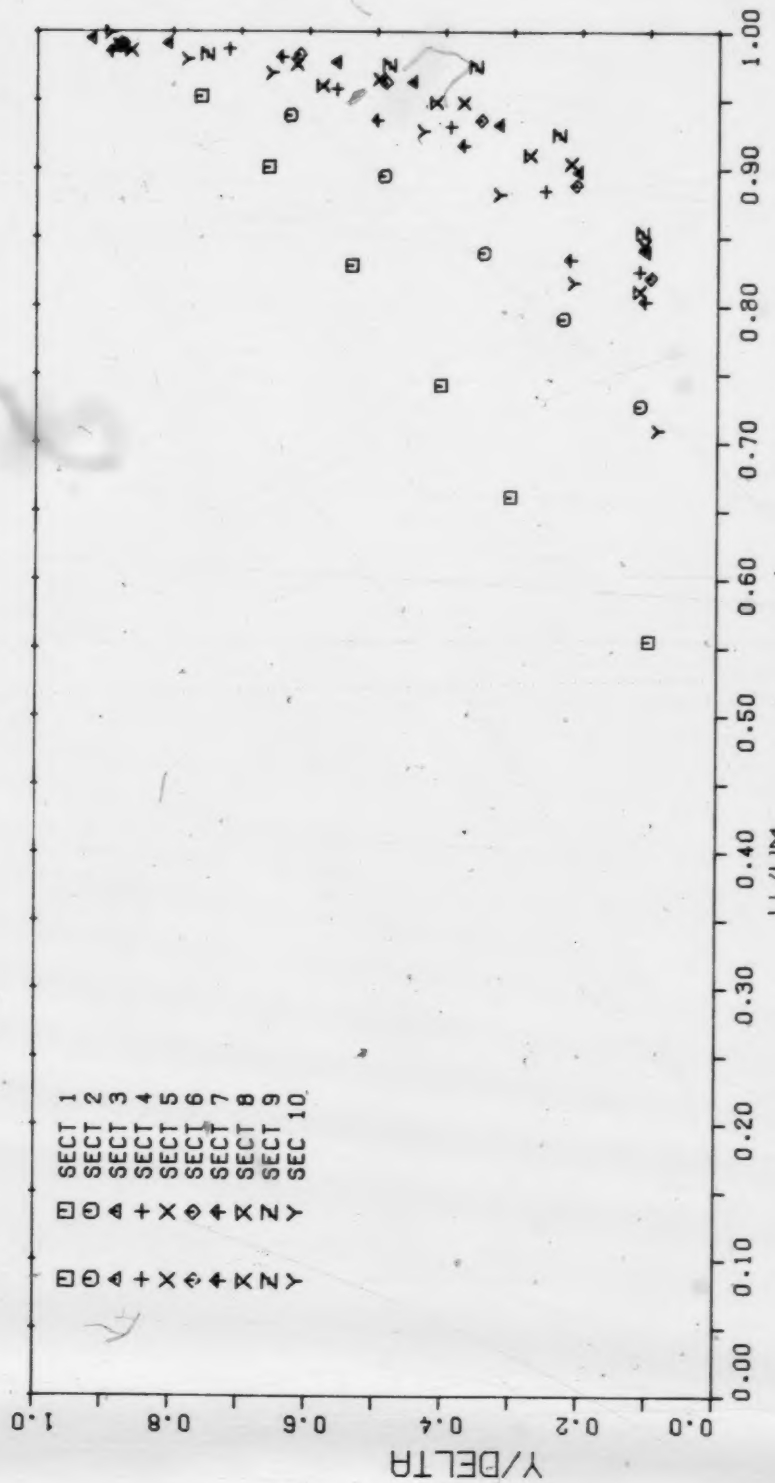

EXPT. 4 ALPHA = 7.03:1

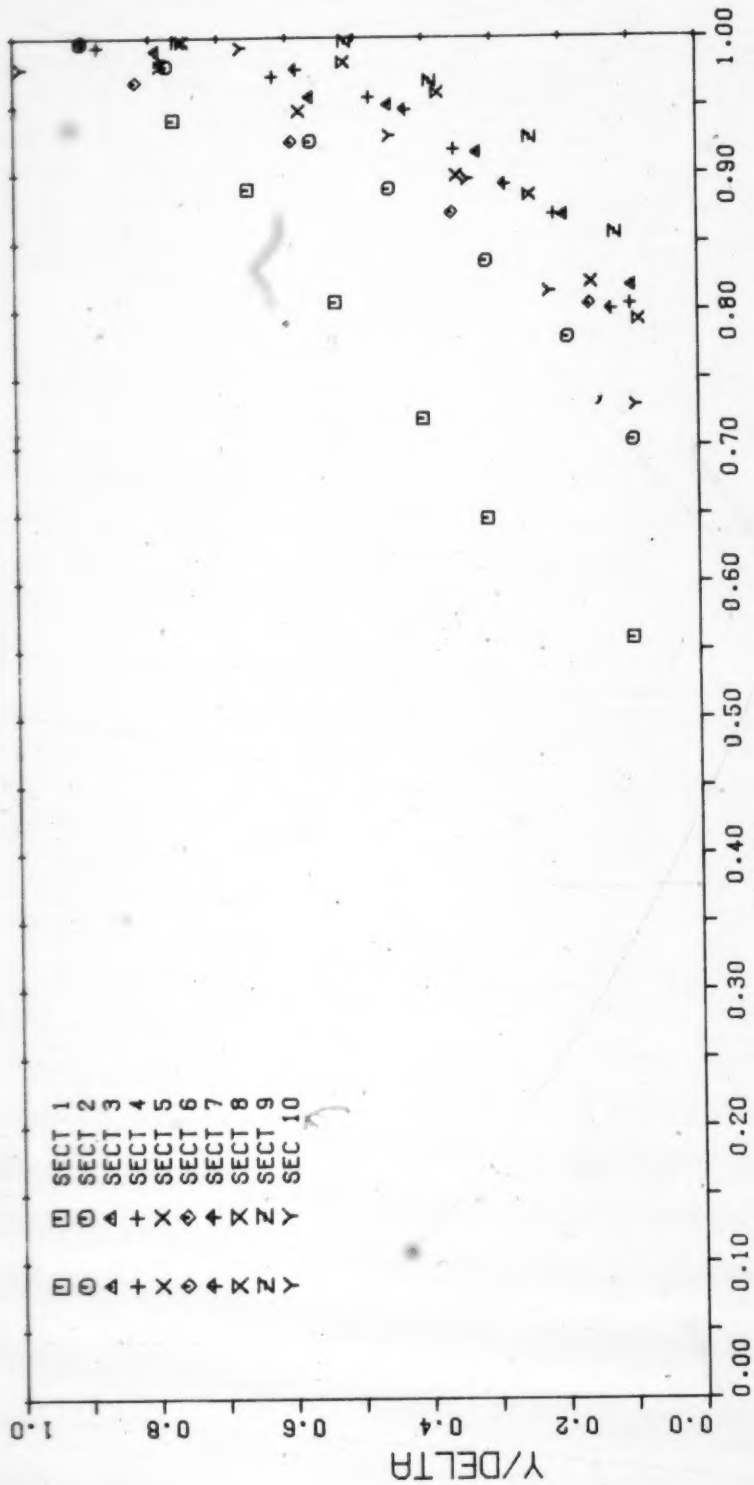

EXPT. 5 ALPHA = 19.89:1

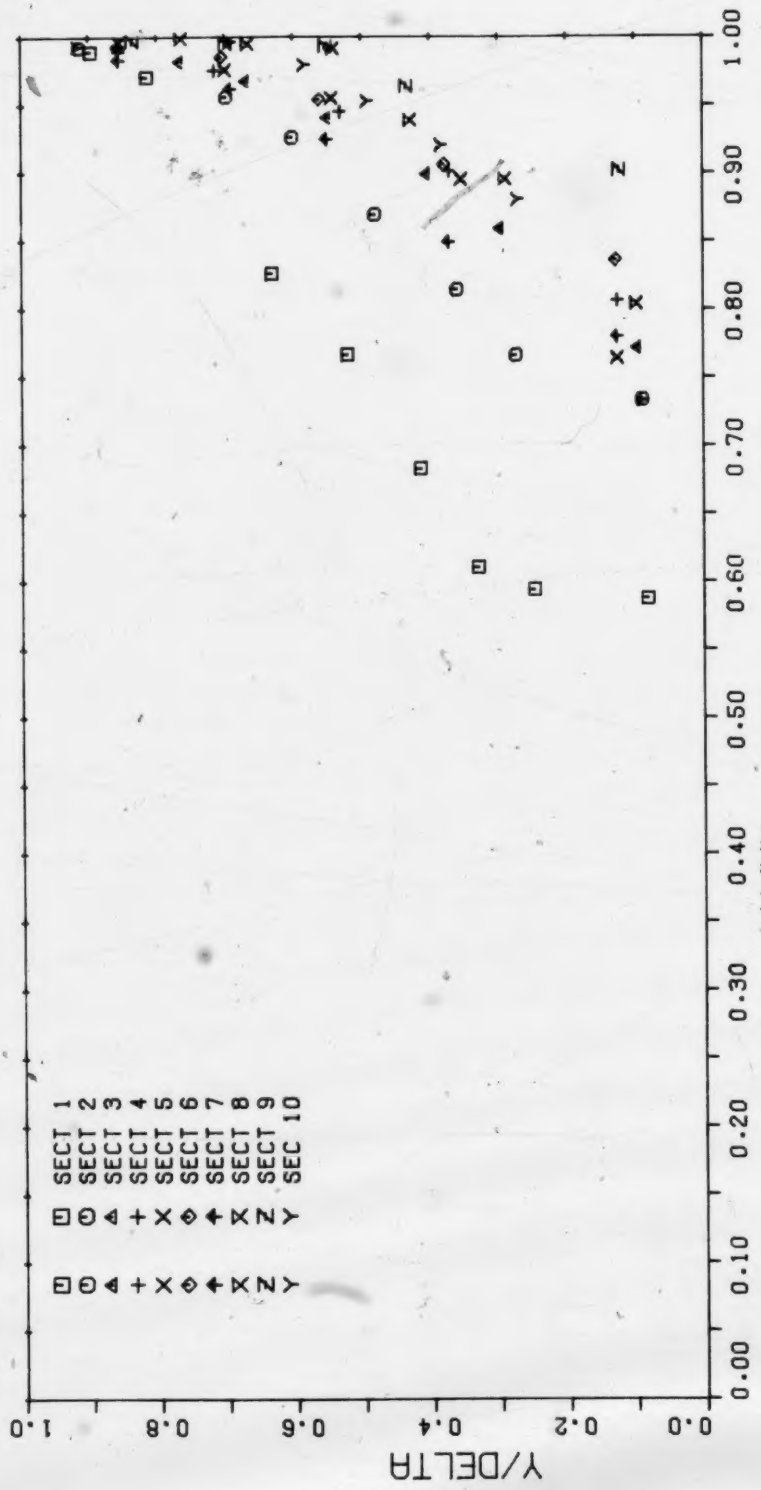

EXPT. 6 ALPHA = 30.64:1

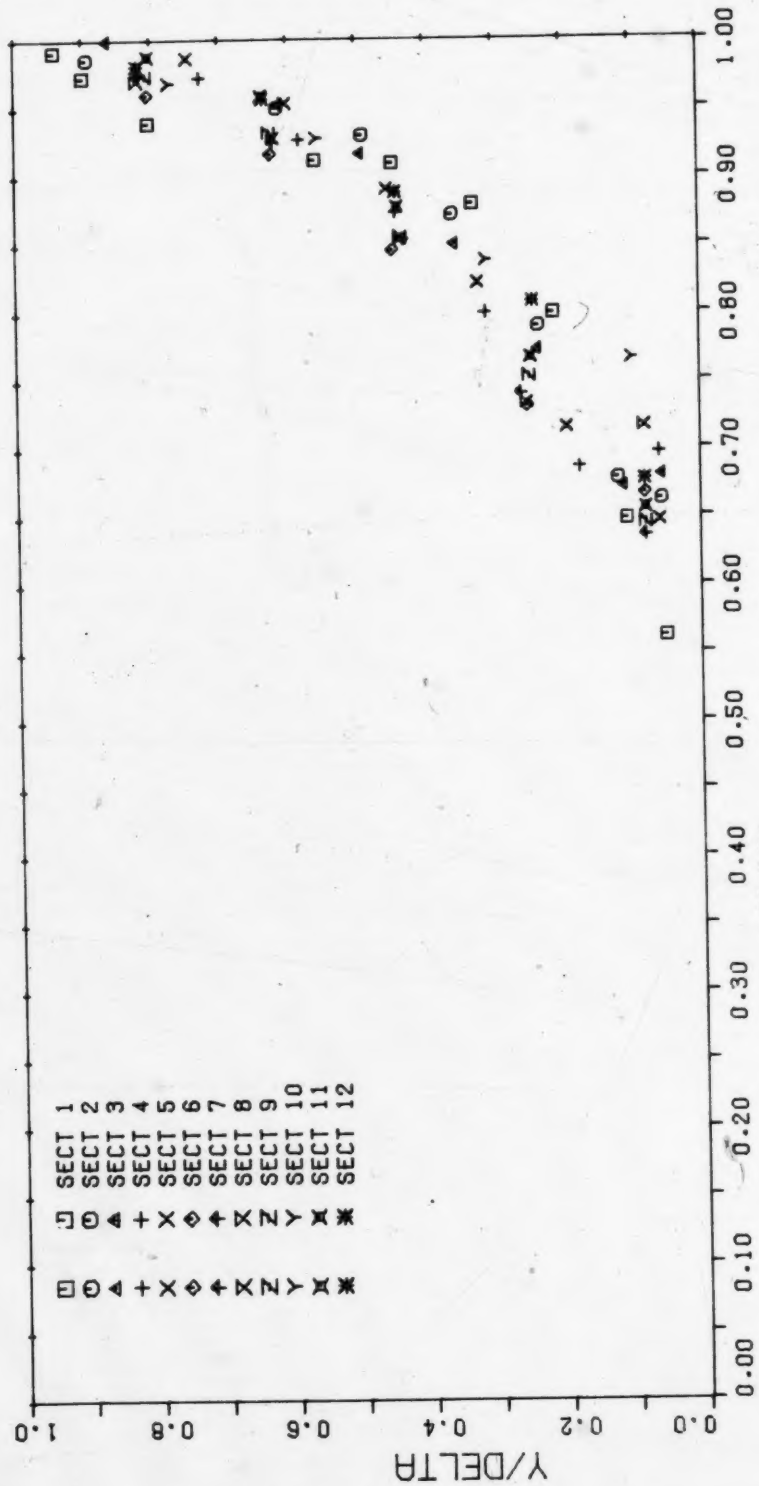

EXPT. 7 ALPHA = 3.54:1

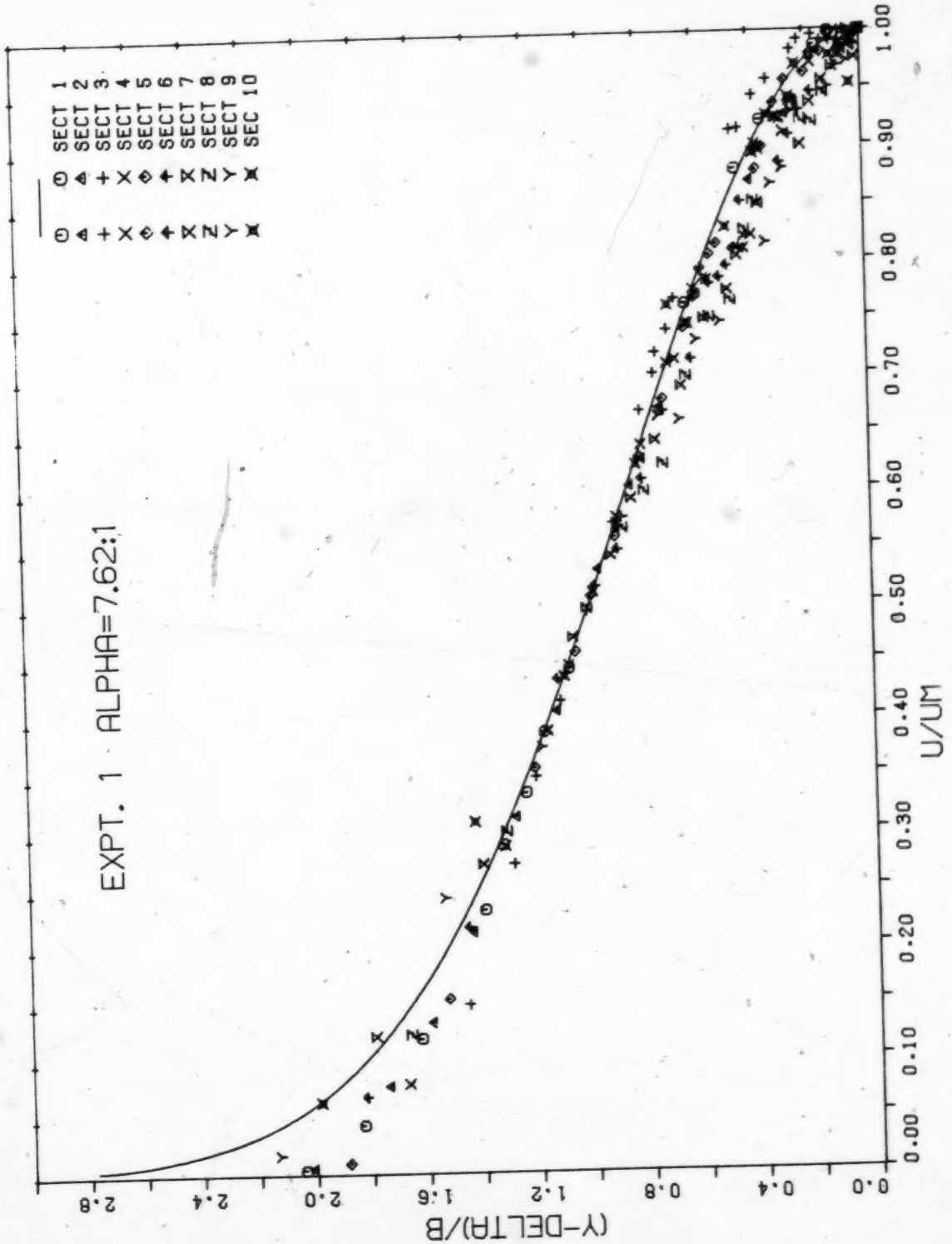
EXPT. 1 ALPHA=7.62:1
SECT 1
SECT 2
SECT 3
SECT 4
SECT 5
SECT 6
SECT 7
SECT 8
SECT 9
SEC 10
(Y-DELTA)/B
U/UM
0.0
0.4
0.8
1.2
1.6
2.0
2.4
2.8
0.00
0.10
0.20
0.30
0.40
0.50
0.60
0.70
0.80
0.90
1.00

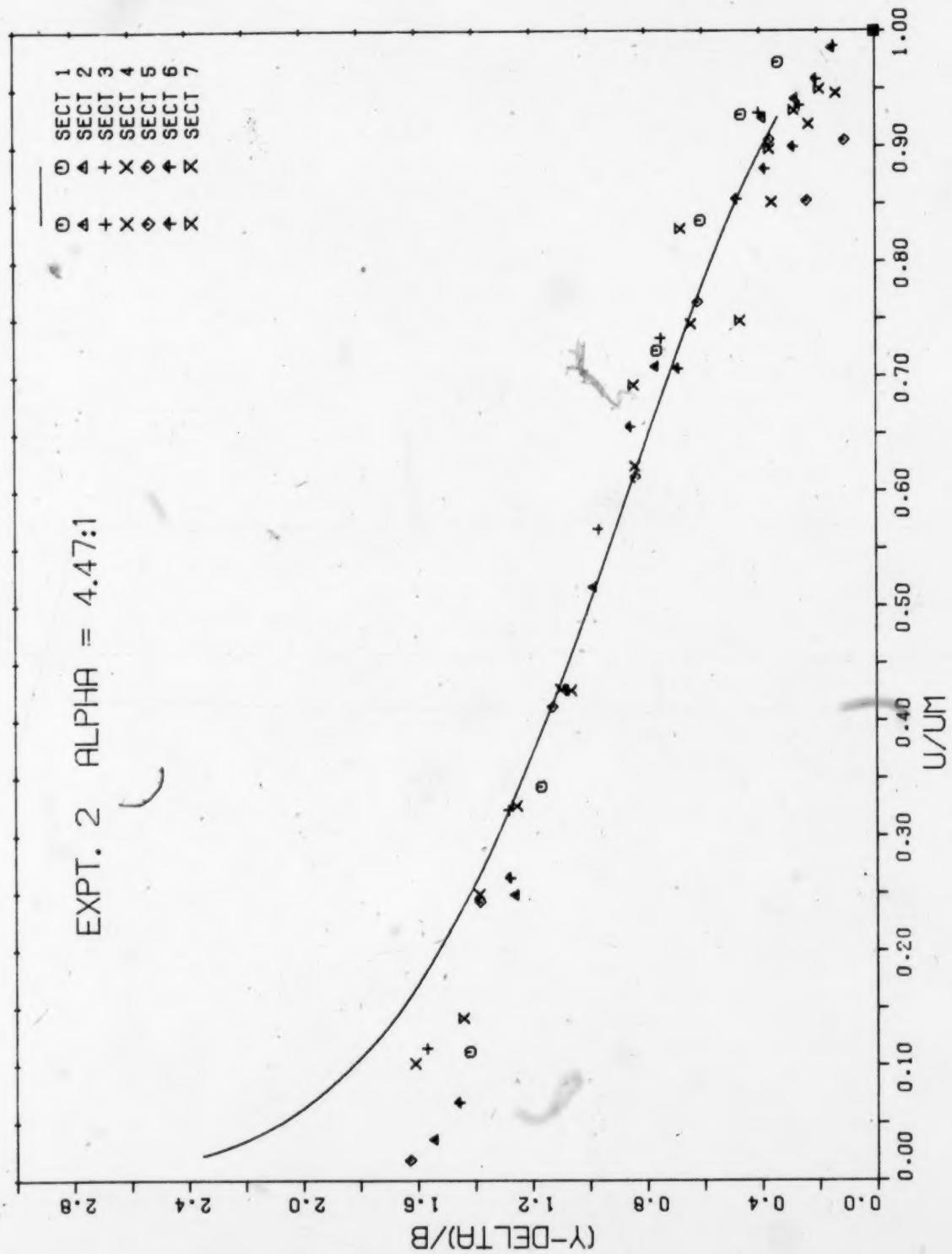
EXPT. 2 ALPHA = 4.47:1
SECT 1
SECT 2
SECT 3
SECT 4
SECT 5
SECT 6
SECT 7
(Y-DELTA)/B
U/UM
0.0
0.4
0.8
1.2
1.6
2.0
2.4
2.8
0.00
0.10
0.20
0.30
0.40
0.50
0.60
0.70
0.80
0.90
1.00

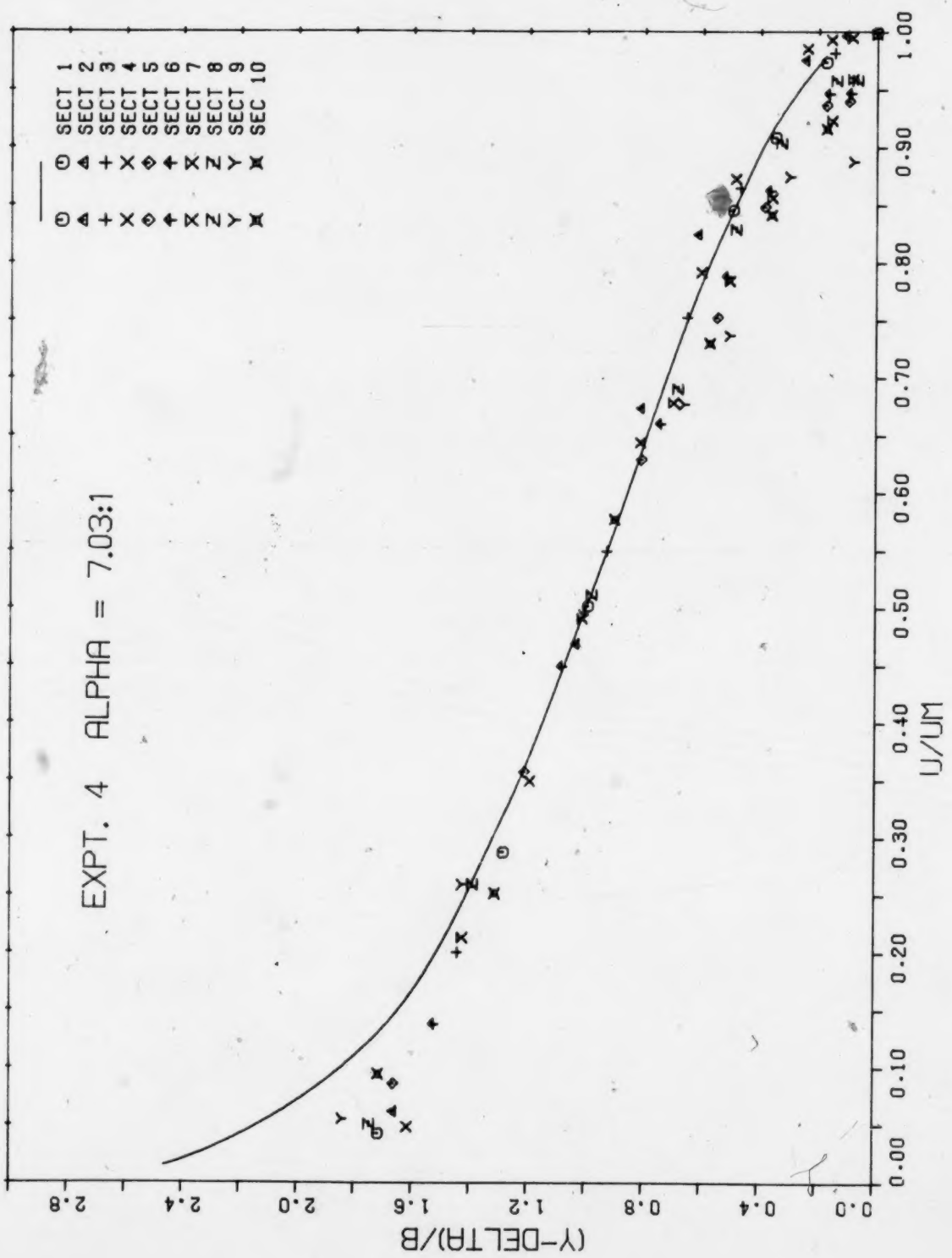
EXPT. 4 ALPHA = 7.03:1
SECT 1
SECT 2
SECT 3
SECT 4
SECT 5
SECT 6
SECT 7
SECT 8
SECT 9
SEC 10
(Y-DELTA)/B
IJ/IJM
0.0
0.4
0.8
1.2
1.6
2.0
2.4
2.8
0.00
0.10
0.20
0.30
0.40
0.50
0.60
0.70
0.80
0.90
1.00

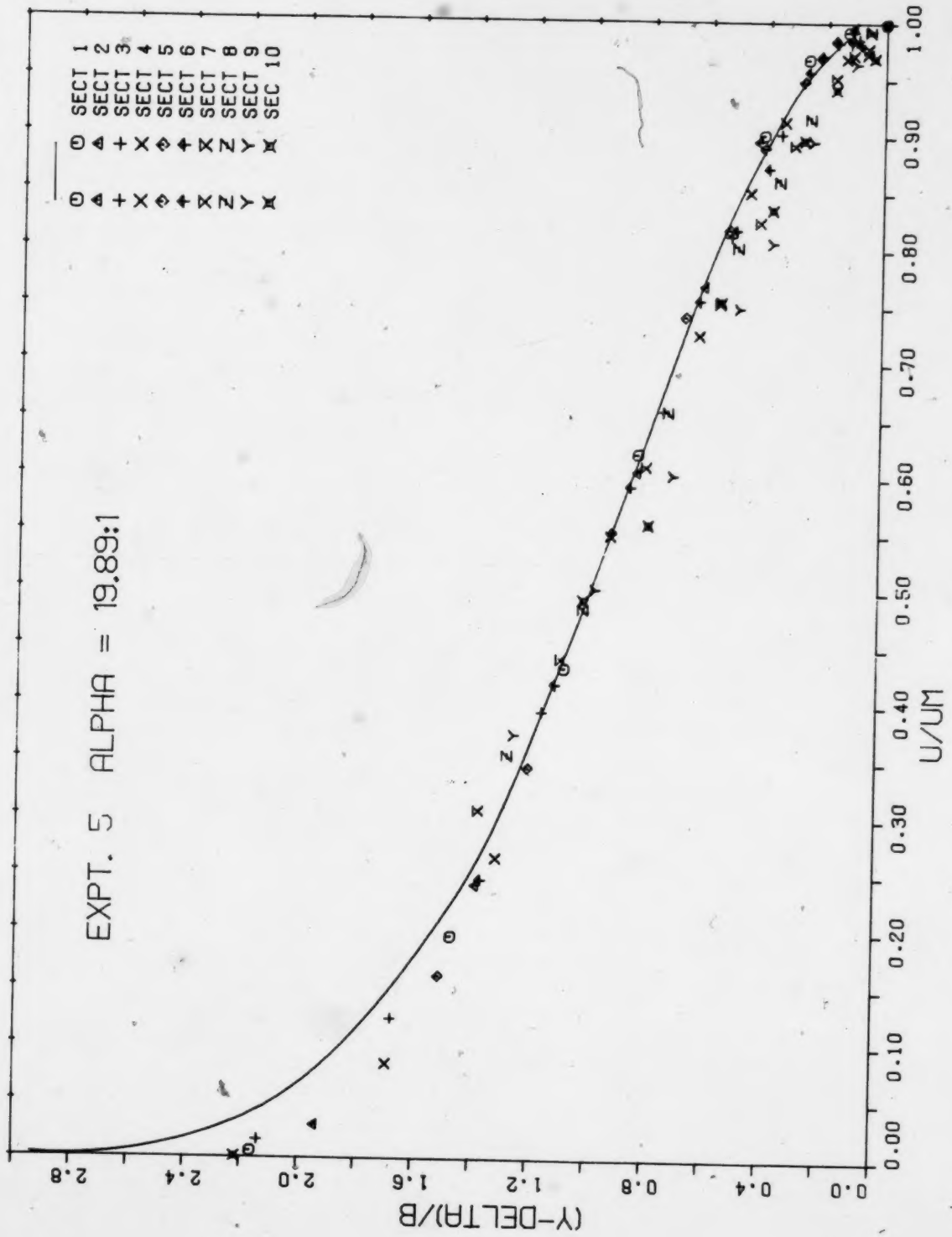
EXPT. 5 ALPHA = 19.89:1
SECT 1
SECT 2
SECT 3
SECT 4
SECT 5
SECT 6
SECT 7
SECT 8
SECT 9
SEC 10
(Y-DELTA)/B
U/UM
0.0
0.4
0.8
1.2
1.6
2.0
2.4
2.8
0.00
0.10
0.20
0.30
0.40
0.50
0.60
0.70
0.80
0.90
1.00

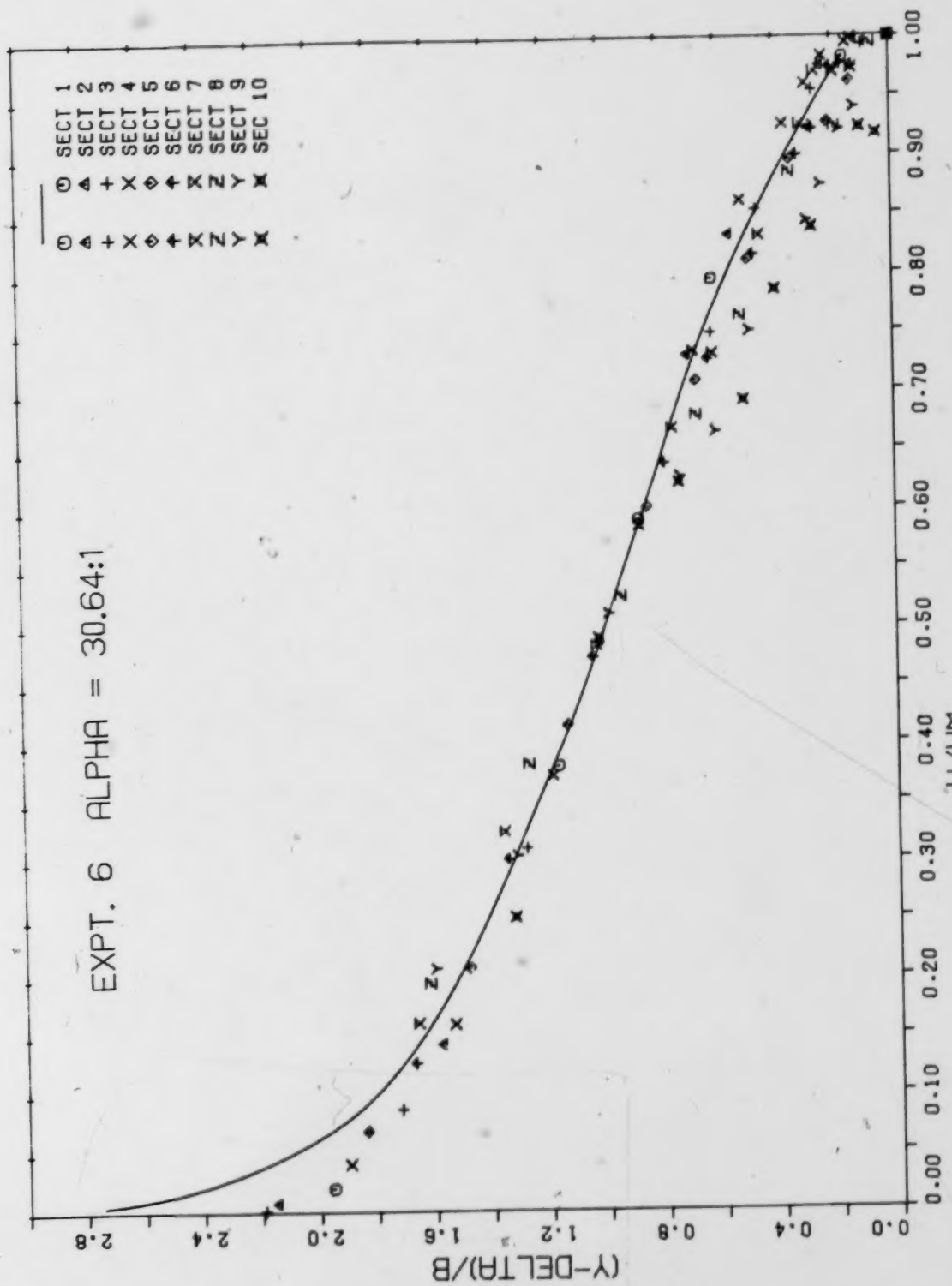
EXPT. 6 ALPHA = 30.64:1
SECT 1
SECT 2
SECT 3
SECT 4
SECT 5
SECT 6
SECT 7
SECT 8
SECT 9
SEC 10
(Y-DELTA)/B
U/UM
0.0
0.4
0.8
1.2
1.6
2.0
2.4
2.8
0.00
0.10
0.20
0.30
0.40
0.50
0.60
0.70
0.80
0.90
1.00

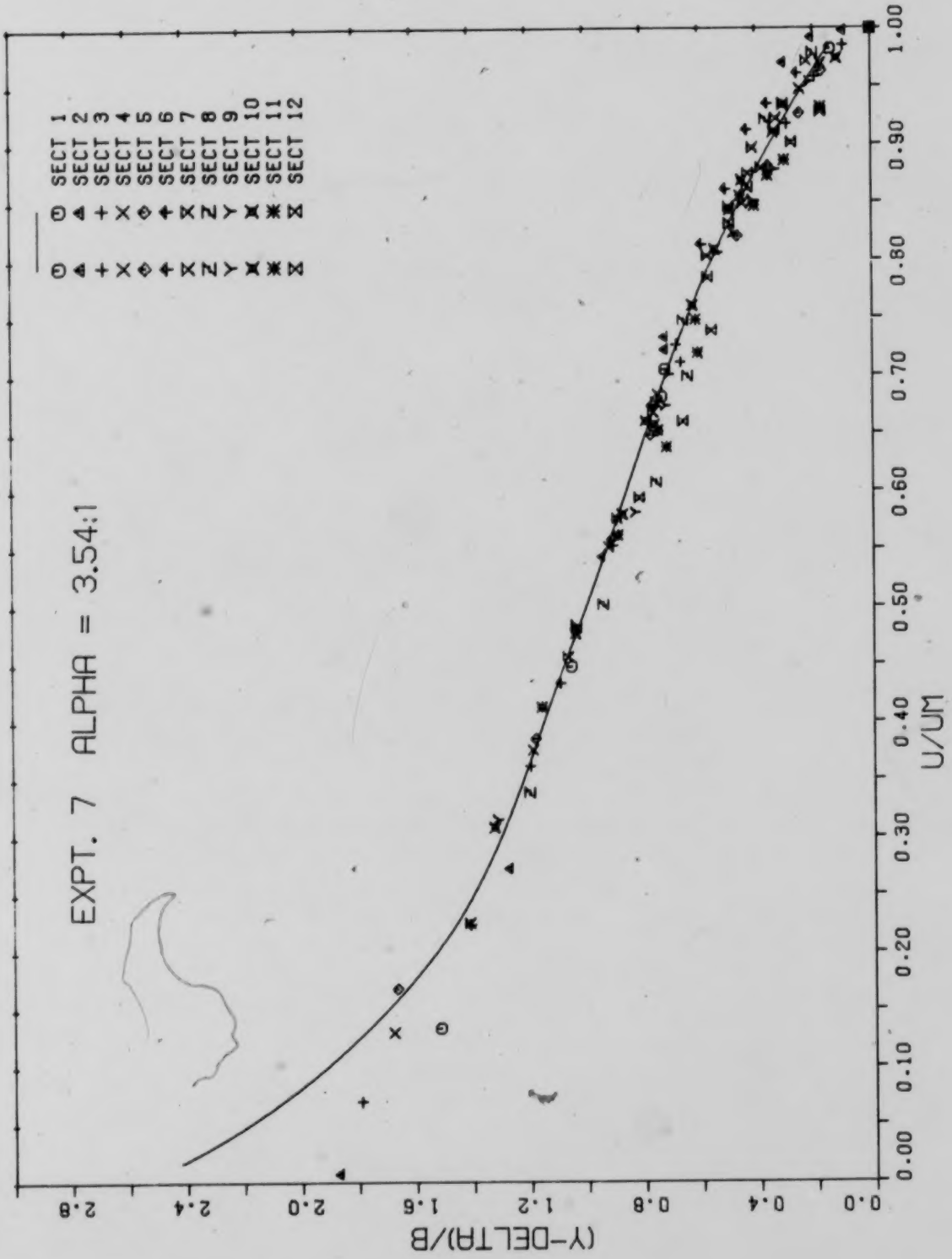
EXPT. 7 ALPHA = 3.54:1
SECT 1
SECT 2
SECT 3
SECT 4
SECT 5
SECT 6
SECT 7
SECT 8
SECT 9
SECT 10
SECT 11
SECT 12
(Y-DELTA)/B
U/UM
0.0
0.4
0.8
1.2
1.6
2.0
2.4
2.8
0.00
0.10
0.20
0.30
0.40
0.50
0.60
0.70
0.80
0.90
1.00

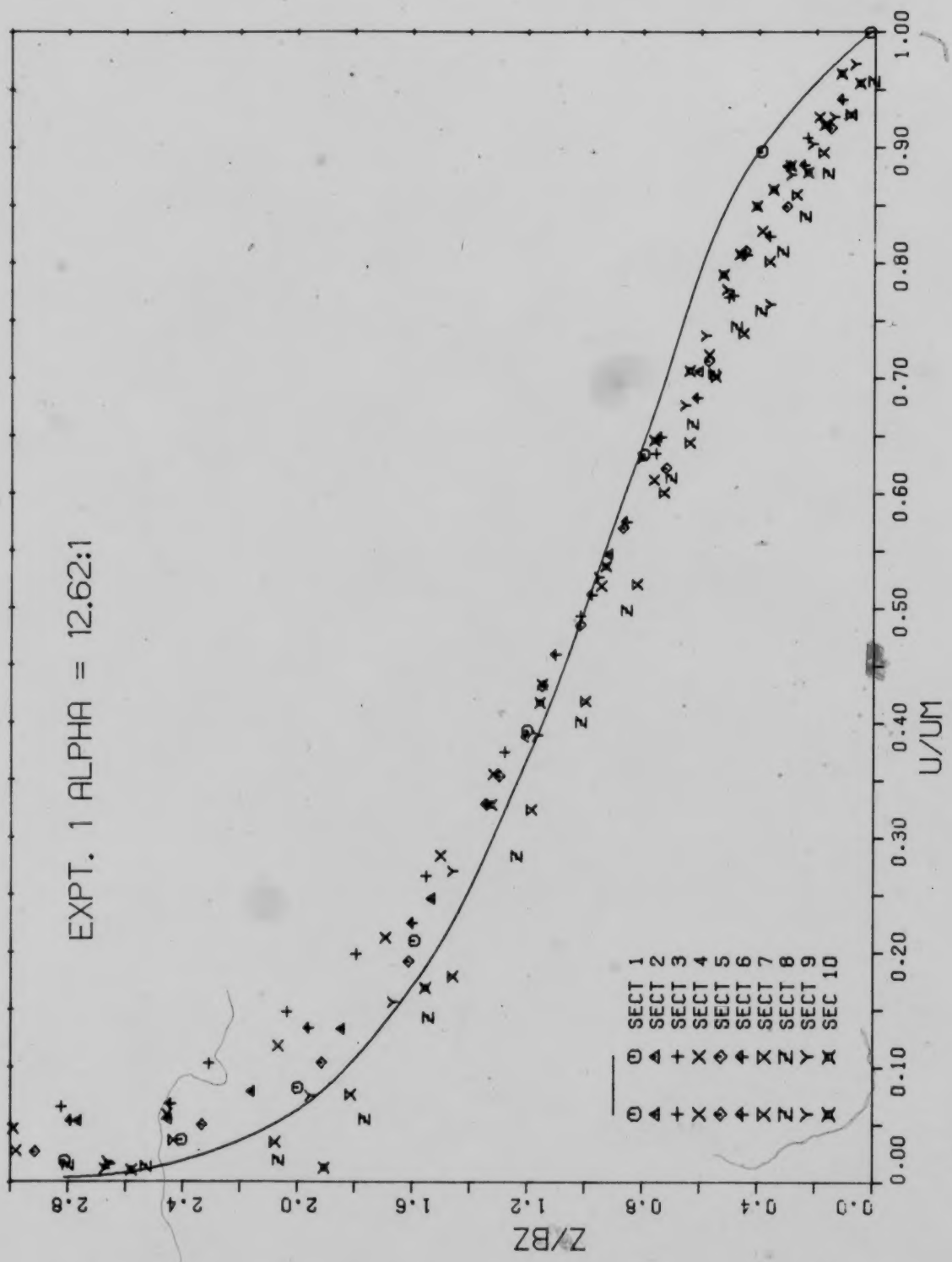
EXPT. 1 ALPHA = 12.62:1
Z/BZ
U/UM
0.0
0.4
0.8
1.2
1.6
2.0
2.4
2.8
0.00
0.10
0.20
0.30
0.40
0.50
0.60
0.70
0.80
0.90
1.00
SECT 1
SECT 2
SECT 3
SECT 4
SECT 5
SECT 6
SECT 7
SECT 8
SECT 9
SEC 10

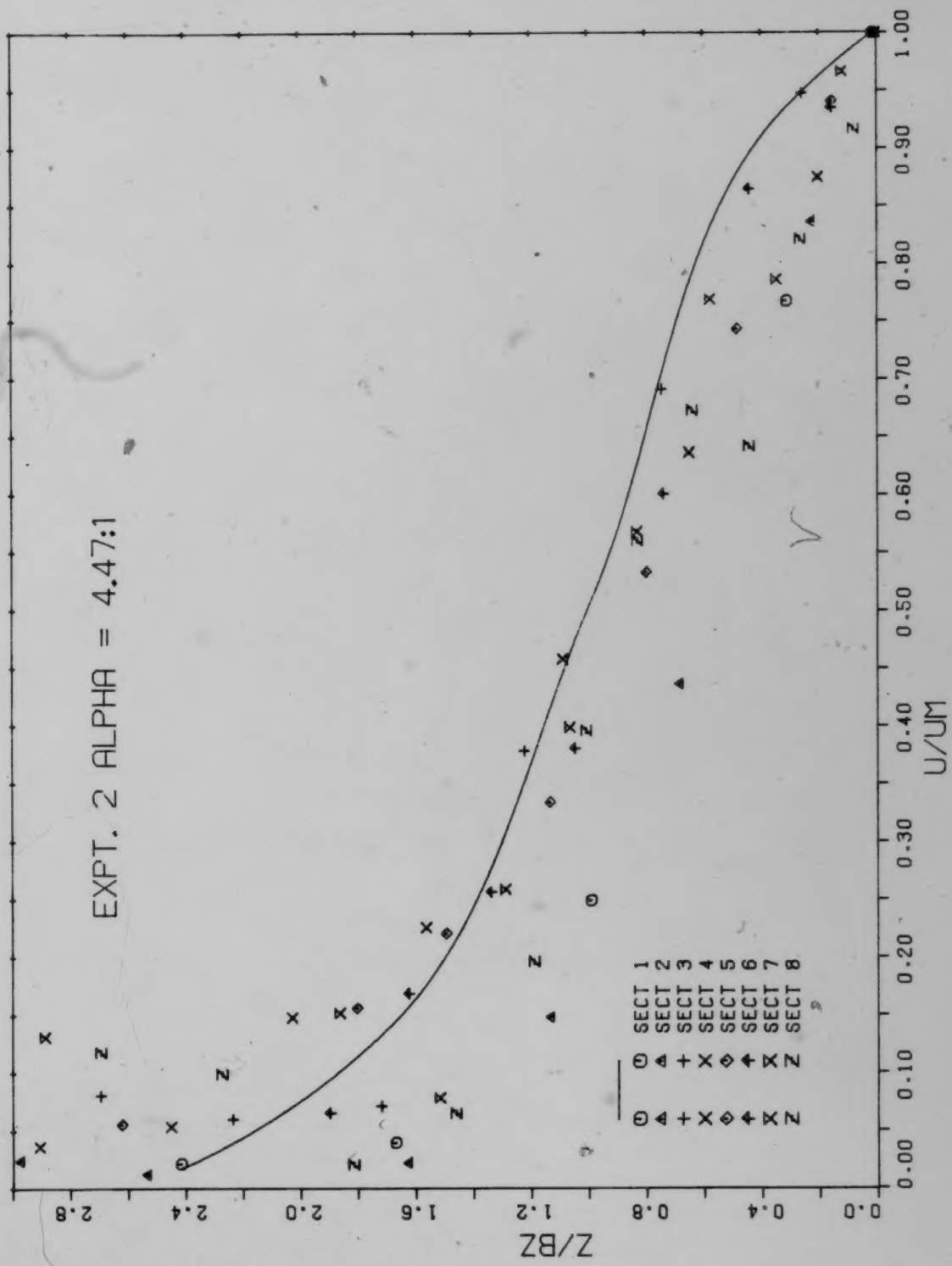
EXPT. 2 ALPHA = 4.47:1
Z/BZ
U/UM
0.0
0.4
0.8
1.2
1.6
2.0
2.4
2.8
0.00
0.10
0.20
0.30
0.40
0.50
0.60
0.70
0.80
0.90
1.00
SECT 1
SECT 2
SECT 3
SECT 4
SECT 5
SECT 6
SECT 7
SECT 8

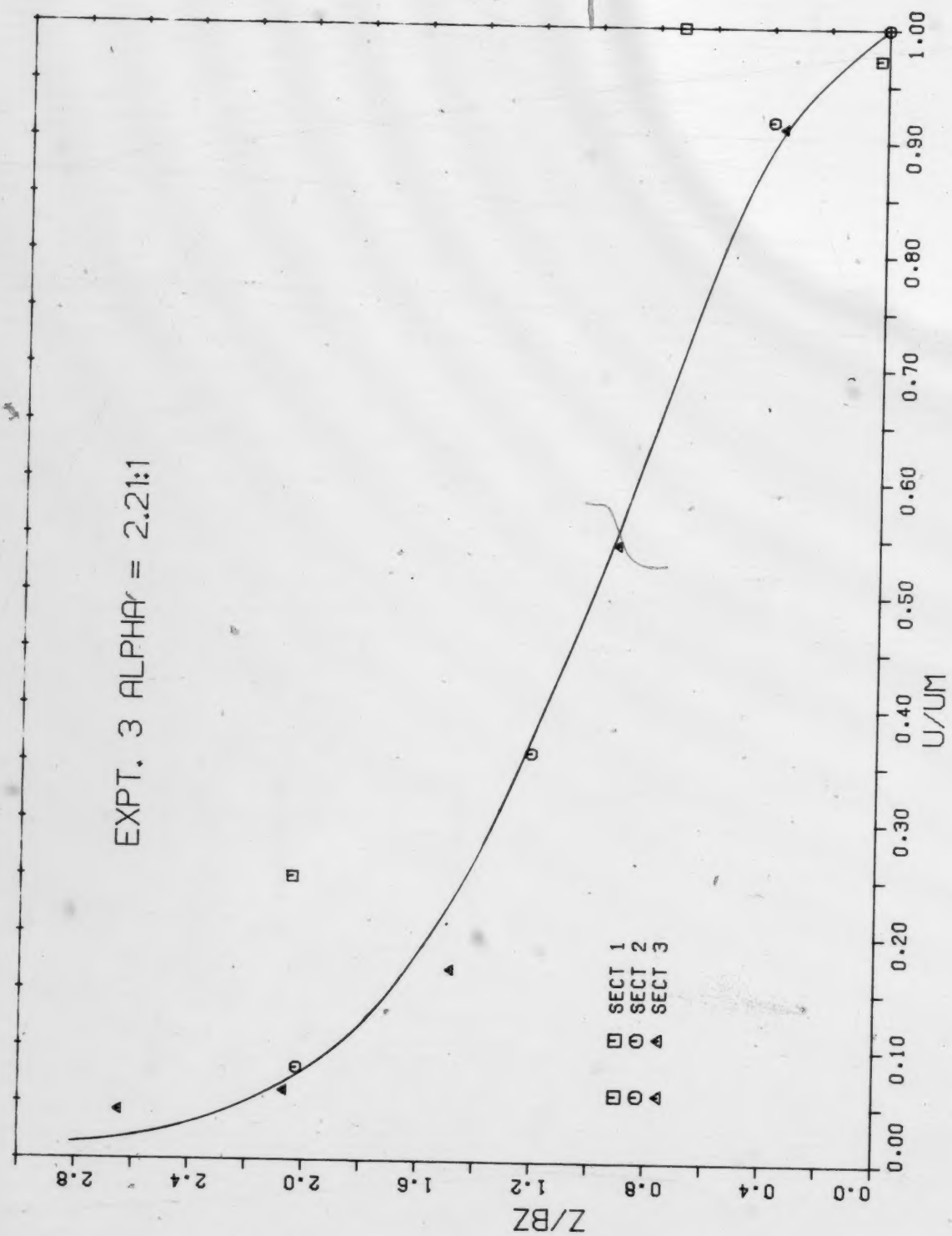
EXPT. 3 ALPHA = 2.21:1
SECT 1
SECT 2
SECT 3
U/UM
Z/BZ
0.00
0.10
0.20
0.30
0.40
0.50
0.60
0.70
0.80
0.90
1.00
0.0
0.4
0.8
1.2
1.6
2.0
2.4
2.8

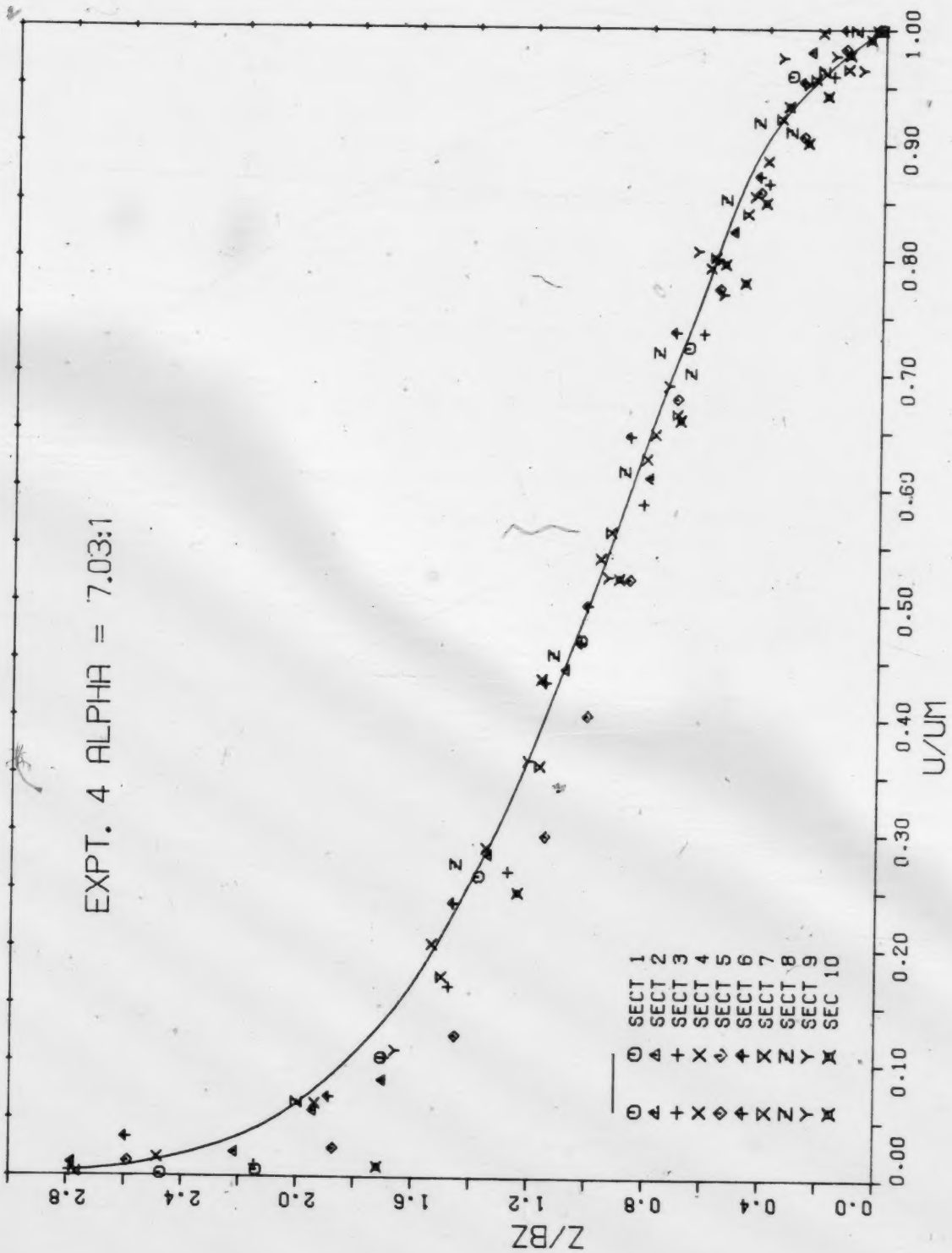
EXPT. 4 ALPHA = 7.03:1
Z/BZ
U/UM
0.0
0.4
0.8
1.2
1.6
2.0
2.4
2.8
0.00
0.10
0.20
0.30
0.40
0.50
0.60
0.70
0.80
0.90
1.00
SECT 1
SECT 2
SECT 3
SECT 4
SECT 5
SECT 6
SECT 7
SECT 8
SECT 9
SEC 10

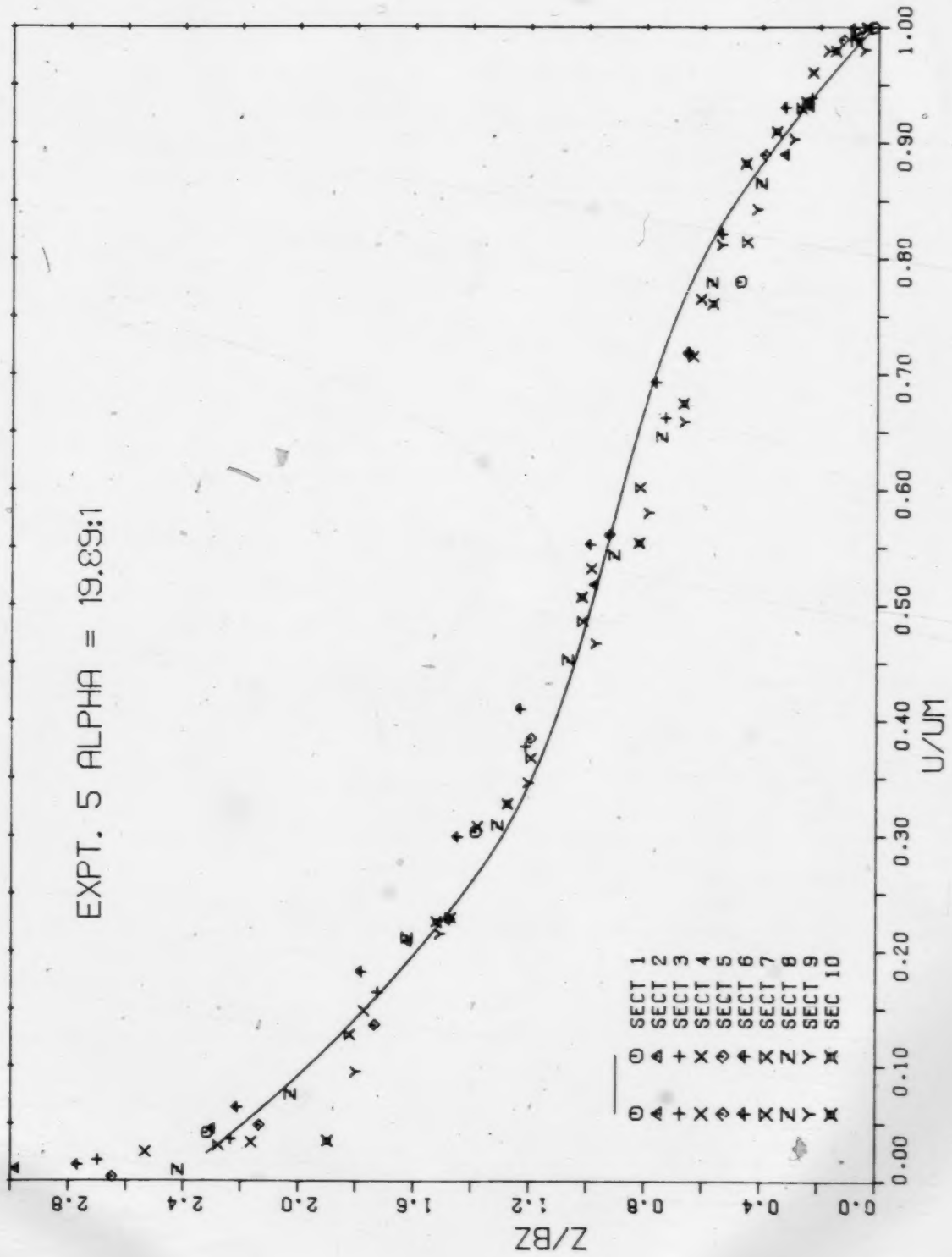
EXPT. 5 ALPHA = 19.89:1
Z/BZ
U/UM
0.0
0.4
0.8
1.2
1.6
2.0
2.4
2.8
0.00
0.10
0.20
0.30
0.40
0.50
0.60
0.70
0.80
0.90
1.00
SECT 1
SECT 2
SECT 3
SECT 4
SECT 5
SECT 6
SECT 7
SECT 8
SECT 9
SEC 10

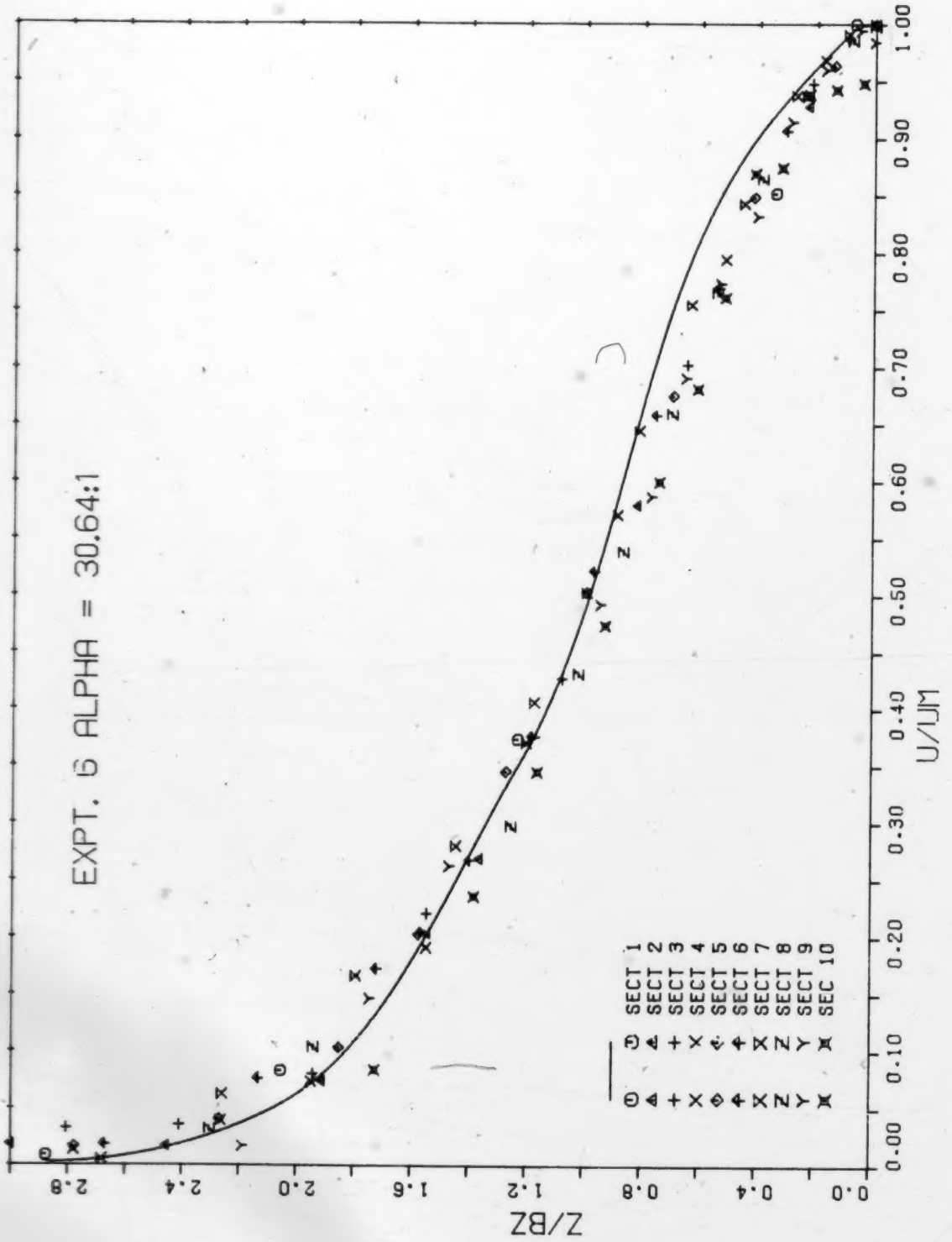
EXPT. 6 ALPHA = 30.64:1
SECT 1
SECT 2
SECT 3
SECT 4
SECT 5
SECT 6
SECT 7
SECT 8
SECT 9
SEC 10
Z/BZ
U/UM
0.0
0.4
0.8
1.2
1.6
2.0
2.4
2.8
0.00
0.10
0.20
0.30
0.40
0.50
0.60
0.70
0.80
0.90
1.00

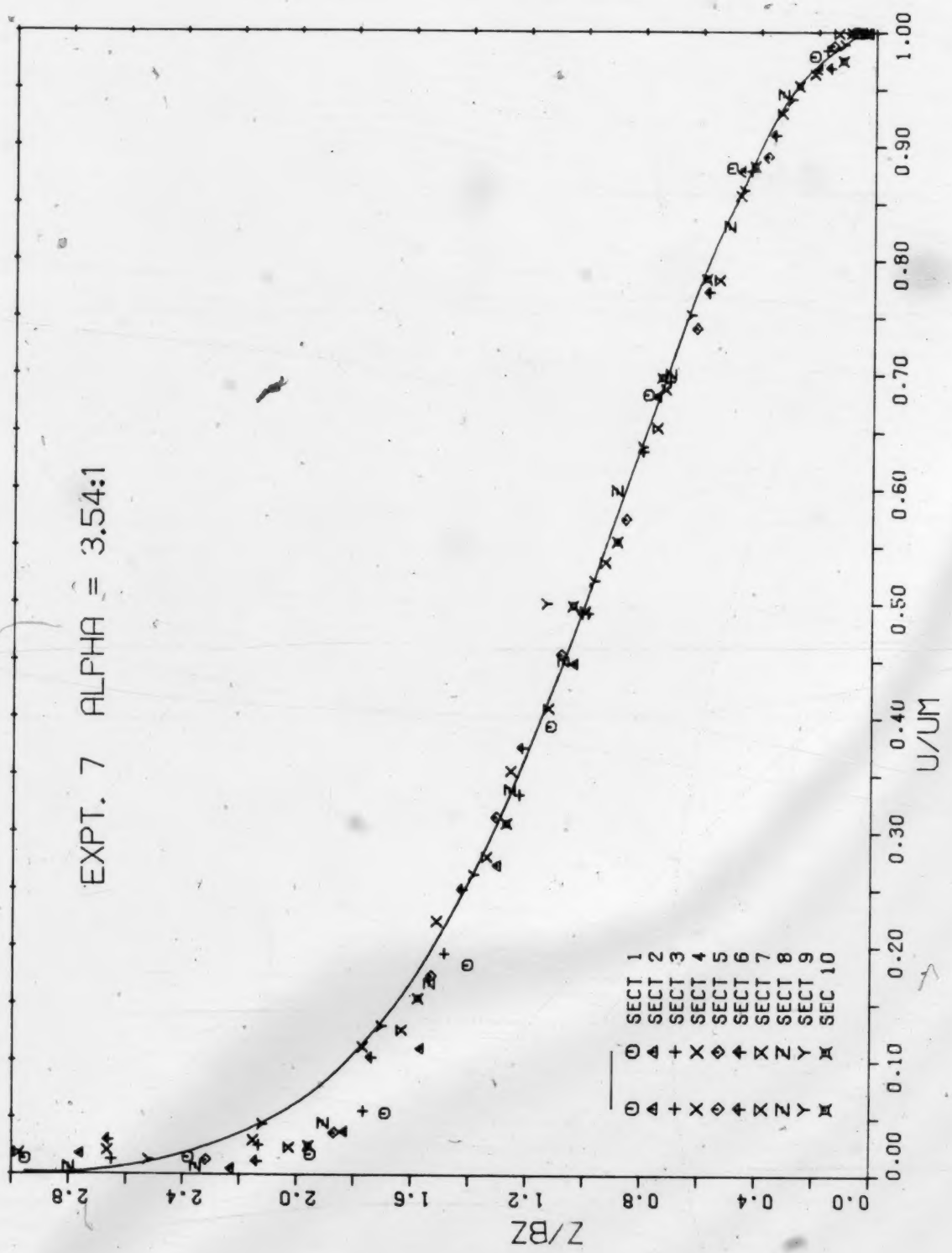
EXPT. 7 ALPHA = 3.54:1
Z/BZ
U/UM
0.0
0.4
0.8
1.2
1.6
2.0
2.4
2.8
0.00
0.10
0.20
0.30
0.40
0.50
0.60
0.70
0.80
0.90
1.00
SECT 1
SECT 2
SECT 3
SECT 4
SECT 5
SECT 6
SECT 7
SECT 8
SECT 9
SEC 10